Ecole Centrale de Nantes

ÉCOLE DOCTORALE

SCIENCES POUR L'INGÉNIEUR, GÉOSCIENCES, ARCHITECTURE

Année 2016 N° B.U. :

Thèse de DOCTORAT

Spécialité : GENIE CIVIL

Présentée et soutenue publiquement par :

YINFU JIN

le ……06-09-2016……..…
à l'Ecole Centrale Nantes

TITRE

IDENTIFICATION LES PARAMÈTRES DES SOLS ET SÉLECTION DE MODÈLES DE COMPORTEMENT EN UTILISANT DES ALGORITHMES GÉNÉTIQUES

JURY

Président :	**OLIVIER MILLET**	Professeur des Universités - Pôle Sciences et Technologie, La Rochelle
Rapporteurs :	**Yujun CUI**	Professeur, École des Ponts ParisTech
	Ali DAOUADJI	Professeur des Universités - INSA Lyon
Examinateur:	**Pierre-Yves HICHER**	Professeur Émérite - Ecole Centrale de Nantes
	Yvon RIOU	Maître de conférences - Ecole Centrale de Nantes
Directeur de thèse:	**Zhenyu YIN**	Maître de conférences et HDR-Ecole Centrale de Nantes
Co-directeur:	**Shuilong SHEN**	Professeur- Université de Jiao Tong de Shanghai, Chine

Acknowledgments

The author would like to express his sincere thanks to all the people who he worked with during this PhD period, without them the research could not be accomplished.

Dr. Zhenyu YIN, as the supervisor of the PhD study as well as the good friend over the past several years, did do a lot of efforts in improving my knowledge and academic ability in the field of geotechnical engineering, providing the chance to study at Shanghai Jiao Tong University and then to study at Ecole centrale de Nantes as well to work at Deltares in Deflt. His excellent academic attitude and kind personality are greatly appreciated.

Prof. Shuilong SHEN in Shanghai Jiao Tong University is also my supervisor of my PhD study. I am greatly indebted to him for his continuous help and strong support throughout this research. His wealth of ideas has enriched this dissertation and is highly appreciated.

The two supervisors of mine provided me with great freedom which allowed me to dive into the sea of research and to think freely. Words are not enough to express my appreciations.

Prof. Pierre-Yves HICHER and Shimu are greatly acknowledged by the author for their charming personalities. During my study in Nantes, Pierre-Yves showed me his patience and strictness, his knowledge and modesty in directing my research and paper writing. Shimu made her effort to help me learn French and English.

I am also extremely grateful to Prof. Yvon RIOU for his assistance in optimization and valuable input to various aspects of this dissertation.

I would also like to acknowledge the valuable inspirations from my good friends in Nantes, especially to Zheng LI for teaching me the professional skills in using the computational software. And to some good friends in Shanghai, the time of our study together is unforgettable throughout my life.

Kisses to my girlfriend Ms. SUN for her great encouragements and supports during my PhD study.

Finally, kisses to my parents and sister for their love and support of my study abroad. Their expectation gave me the motivation to pursue higher academic achievements.

Table contents

Abstract

The subject of this thesis is the identification of soil parameters and the selection of constitutive models using genetic algorithms. First, various optimization methods for identifying soil parameters are studied. Then, a real-coded genetic algorithm (RCGA) has been developed to improve the performance of genetic algorithms (GA) for identifying soil parameters. Subsequently, the RCGA is employed to construct a formula for predicting the compressibility of remolded clays by using an evolutionary polynomial regression (EPR) based on the initial void ratio e_0, the liquid limit w_L and the plastic index I_P. Then, an efficient procedure for identifying the necessary parameters of soft structured clays is proposed by employing the enhanced RCGA coupled with an advanced anisotropic elasto-viscoplastic model. This approach is then validated and several applications are developed to demonstrate that the procedure can be used with a reduction of the testing cost. Finally, an appropriate model of sand with the necessary features based on conventional tests and with an easy way of identifying parameters for geotechnical applications by employing the RCGA and different sand models is selected. A discussion on nonlinear plastic stress-strain hardening, the incorporation of the critical state concept with interlocking effect, test types and numbers, and necessary strain level for the selection and use of sand models concludes the thesis.

Keywords: parameter identification; optimization; constitutive model; sand; clay; genetic algorithm

Résumé

Le sujet de la thèse concerne l'identification des paramètres des sols et sélection de modèles de comportement en utilisant des algorithmes génétiques. Tout d'abord, une étude comparative sur l'identification des paramètres par différentes méthodes d'optimization est effectuée. Ensuite, un algorithme génétique réel codé (RCGA) est conçu pour améliorer la performance d'un algorithme génétique (GA) dans l'identification des paramètres du sol. Par la suite, le RCGA est utilisé pour construire la formulation de la prédiction de la compressibilité des argiles remaniés basée sur la régression polynomiale évolutive (EPR) en utilisant l'indice des vides initial e0, la limite de liquidité wL et l'indice de plasticité IP. Ensuite, une procédure efficace pour identifier les paramètres d'argiles structurées est proposée en employant le RCGA avec un modèle élasto-viscoplastique anisotrope. Une procédure de validation est menée ainsi que des applications démontrant que la procédure est utile pratiquement avec une réduction du coût des essais au laboratoire. Enfin, le choix d'un modèle approprié pour les sables avec les caractéristiques nécessaires en fonction des essais classiques et un moyen facile d'identifier les paramètres pour les applications géotechniques est discuté en utilisant le RCGA et différents modèles de sable. L'écrouissage plastique non-linéaire, l'implémentation de la ligne d'état critique avec l'effet d'enchevêtrement, les types et nombres d'essais et le niveau de déformation nécessaire sont discutés pour la sélection et l'utilisation des modèles de sable.

Mots-clés: Identification des paramètres; optimization; modèle de comportement; sable; argile; algorithme génétique

General introduction

In geotechnical engineering, the identification of soil parameters using intelligent techniques has been increasingly used in the last decades. Among these intelligent techniques, a number of optimization methods has been widely employed to identify soil parameters from laboratory tests, in-situ tests, field tests, and real engineering measurements. However, the performance of these current optimization methods still needs to be improved, and their applications can be extended. Therefore, this thesis addresses the development of the optimization method, applications to the regression of soil properties, parameter identification and model selection. The thesis is divided into seven chapters, and is outlined as follows:

In chapter 1, the optimization techniques for identifying parameters in geotechnical engineering is reviewed. The identification methodology with its three main parts, i.e., error function, search strategy and identification procedure, is first introduced and summarized. Then, current optimization methods are reviewed and classified into three categories with an introduction to their basic principles and applications in geotechnical engineering.

In chapter 2, a comparative study of optimization techniques by using various typical optimization methods, including genetic algorithms (GA), particle swarm optimization (PSO), simulated annealing (SA), differential evolution algorithm (DE) and artificial bee colony algorithm (ABC) for identifying parameters from a synthetic pressuremeter test and an excavation is presented. The performances of these optimization methods are discussed and evaluated.

In chapter 3, an efficient new hybrid real-coded genetic algorithm (RCGA) has been developed for improving the optimization process in identifying soil parameters. This new RCGA, has allowed us to develop a new hybrid strategy by adopting two crossovers with outstanding ability, namely the Simulated Binary Crossover (SBX) and the Simplex Crossover (SPX). In order to increase the convergence speed, a chaotic local search (CLS) technique is used. The performance of the proposed RCGA has first been validated by optimising six mathematical functions, and then evaluated by identifying soil parameters from both laboratory tests and field tests for different soil models.

In chapter 4, a new approach for predicting the compressibility of remolded clays by their physical properties using the evolutionary polynomial regression (EPR) and the developed optimization method is proposed. To highlight the performance of the RCGA in the proposed procedure, three other excellent optimization algorithms has been selected for comparisons.

In chapter 5, the proposed optimization method has been applied to identify the parameters of soft structured clays from a limited number of conventional triaxial tests. A newly developed elastic viscoplastic model accounting for anisotropy, destructuration and creep features of structured clays, and enhanced with the cross-anisotropy of the elastic part has been adopted for test simulations during optimization. Laboratory tests on soft Wenzhou marine clay were selected, with three of them being used as objectives for optimization and the others for validation. The optimization process, using the new RCGA with a uniform sampling initialization method, has been carried out to obtain the soil parameters. A classic genetic algorithm (NSGA-II) based optimization has also been conducted and compared to the RCGA for evaluating the performance of the new RCGA.

Chapter 6 discusses how to select an appropriate model with the necessary features based on conventional tests and an easy way to identify parameters for geotechnical applications. Models with gradually varying features have been selected from numerous sand models as examples for optimization. Conventional triaxial tests on Hostun sand are selected as the objectives in the optimization procedure. Four key points are then discussed in turn: (1) which features are necessary to be accounted for in constitutive modeling of sand; (2) which type of tests (drained and/or undrained) should be selected for an optimal identification of parameters; (3) what is the minimum number of tests that should be selected for parameter identification; and (4) what is the suitable strain level of objective tests for obtaining reliable and reasonable parameters. Finally, a useful guide, based on all comparisons, is provided at the end of the discussion.

Chapter 7 presents the general conclusions and perspectives.

Introduction générale

Dans l'ingénierie géotechnique, l'identification des paramètres de sol en utilisant des techniques intelligentes est devenue de plus en plus populaire dans les dernières décennies. Parmi ces techniques intelligentes, certaines méthodes d'optimization sont largement utilisées pour identifier les paramètres à partir d'essais de laboratoire, d'essais in-situ, d'essais sur le terrain et des mesures sur ouvrages. Cependant, la performance des méthodes d'optimization actuelles doit encore être améliorée, et leur application peut être étendue. Par conséquent, cette thèse porte sur le développement de la méthode d'optimization, les applications à la caractérisation des propriétés du sol, les paramètres d'identification et de sélection du modèle de comportement. La thèse est divisée en sept chapitres, et se présente comme suit.

Dans le chapitre 1, l'état de l'art des techniques d'optimization pour identifier les paramètres de sol dans l'ingénierie géotechnique est présenté. La méthodologie d'identification avec ses trois parties principales, à savoir la fonction d'erreur, la stratégie de recherche et la procédure d'identification, est d'abord présentée et synthétisée. Ensuite, les méthodes d'optimization actuelles sont examinées et classées en trois catégories avec une introduction à leurs principes et applications de base en ingénierie géotechnique.

Dans le chapitre 2, une étude comparative sur les techniques d'optimization pour l'identification des paramètres de sol à partir d'un essai pressiométrique synthétique et une excavation est effectuée en utilisant des méthodes d'optimization classiques, comprenant les algorithmes génétiques (GA), l'optimization par essaims de particules (PSO), le recuit simulé (SA), l'algorithme d'évolution différentielle (DE) et l'algorithme de colonies d'abeilles artificielles (ABC). La performance de ces méthodes d'optimization est évaluée.

Dans le chapitre 3, un nouvel algorithme génétique hybride réel codé (RCGA) est développé pour améliorer la performance de l'optimization dans l'identification des paramètres de sol. Dans ce nouveau RCGA, une nouvelle stratégie hybride est proposée en adoptant deux croisements avec très forte capacité, à savoir le Simulé Binaire Crossover (SBX) et le Simplex Crossover (SPX). Afin d'augmenter la vitesse de convergence, une technique chaotique de recherche locale (CLS) est utilisée. La performance du RCGA proposé est d'abord validée par l'optimization de six fonctions mathématiques. Le RCGA est ensuite évalué en identifiant les paramètres de sol sur la base de deux essais de laboratoire et des essais in-situ pour les différents modèles de sol.

Dans le chapitre 4, une nouvelle approche pour prédire la compressibilité des argiles remaniées à partir de leurs propriétés physiques en utilisant la régression polynomiale évolutive (EPR) et la méthode d'optimization développée est présentée. Pour mettre en évidence la performance du RCGA dans la procédure proposée, trois autres excellents algorithmes d'optimization sont sélectionnés pour les comparaisons.

Dans le chapitre 5, la méthode d'optimization proposée est appliquée pour identifier les paramètres d'argiles molles structurées basée sur des essais triaxiaux conventionnels en nombre limité. Un modèle élastique viscoplastique nouvellement développé comprenant l'anisotropie, la déstructuration et le fluage des argiles structurées est amélioré en prenant en compte l'anisotropie élastique et adopté pour les simulations d'essais lors de l'optimization. Les essais au laboratoire sur l'argile marine de Wenzhou ont été sélectionnés, trois d'entre eux étant utilisés comme objectifs d'optimization et les autres pour la validation. Le processus d'optimization, en utilisant le nouveau RCGA avec un procédé d'initialization d'échantillonnage uniforme est mis en œuvre pour obtenir les paramètres du sol. L'optimization par un algorithme génétique classique NSGA-II est également effectuée et comparée au RCGA pour estimer sa performance.

Dans le chapitre 6, la méthode de sélection d'un modèle approprié avec les caractéristiques nécessaires basées sur des essais classiques et un moyen simple d'identifier les paramètres pour les applications géotechniques sont discutés. Les modèles avec des caractéristiques variables progressivement sont choisis parmi de nombreux modèles de sable comme des exemples d'optimization. Des essais triaxiaux classiques sur le sable de Hostun sont choisis comme objectifs dans l'optimization. Quatre points clés sont ensuite discutés à tour de rôle: (1) les caractéristiques qui sont nécessaires à prendre en compte dans la modélisation du comportement d'un sable; (2) le type d'essais (drainé et/ou non-drainé) qui doit être sélectionné pour une identification optimale des paramètres; (3) le nombre minimum d'essais qui doivent être sélectionnés pour l'identification des paramètres; et (4) le niveau minimum de déformation approprié lors des essais retenus pour obtenir des paramètres fiables et raisonnables. Enfin, un guide utile, sur la base de toutes les comparaisons, est donné à la fin de la discussion.

Dans le chapitre 7, les conclusions générales sont résumées, et les perspectives sont présentées.

Chapter 1 Literature survey

1.1 Introduction

In the geotechnical field, the finite element analysis and the tools based on analytical solution are widely used for pre-design and post-prediction, such as predicting the bearing capacity of foundations (Loukidis and Salgado [1]), calculating the safety factor of slopes (Griffiths and Lane [2]), predicting the ground settlement of embankments (e.g. Shen et al. [3]; Karstunen and Yin [4]) or tunnel (Shen et al.[5]) and predicting the deformation of a retaining wall during excavation (Ou et al. [6]). For these cases, a common requirement is to obtain soil properties or parameters from laboratory or field tests or measurements. Thus it can be seen that the method of parameter identification play an important role in the finite element or the analytical solution based analysis in design and construction project.

Hicher and Shao [7] distinguished three approaches, namely analytical methods, correlation and optimization methods, to determine soil parameters based on soil data. Among these approaches, the inverse analysis by optimization has been successfully used in the geotechnical area [8-11], because it produces a relatively objective determination of the parameters for an adopted soil model, even those that express no physical meaning, and this occurs with any testing procedure and for any constitutive model. For an inverse formulation of parameters identification, the variables are the model parameters. A way to find such parameter values is to simulate several sets of field tests in the laboratory and to minimize the difference between the experimental and numerical values of stresses, strains and other typical data (e.g. void ratio, and excess pore pressures). This type of problem is usually solved by using optimization techniques which can be divided into two categories:: (1) deterministic techniques; and (2) stochastic techniques. However, as the core technique of parameter identification, the advantages and disadvantages of these optimization techniques are rarely systemically summarized and compared in a same geotechnical problem. Therefore, a review and comparative study of those optimization techniques in identifying parameters is necessary for a good understanding of the differences between the various techniques, and for selecting the appropriate optimization method to solve engineering problems.

This chapter reviews the different optimization methods for identifying parameters in geotechnical engineering. The identification methodology is first introduced. Then, the optimization

methods are investigated and classified into three categories with an introduction to the basic principles and an enumeration of different applications in geotechnical engineering.

1.2 Identification methodology

The mathematical procedure of optimization basically consists of two parts: (a) the formulation of an error function measuring the difference between numerical and experimental results, and (b) the selection of an optimization strategy to enable the search for the minimum of this error function.

1.2.1 Formulation of an error function

In the optimization problem to be formulated, the parameters of the constitutive model considered play the role of optimization variables. In general, more reliable model parameters can be obtained if many (qualitatively different) experimental tests form a basis for the optimization.

In order to carry out an inverse analysis, the user must define a function that can evaluate the error between the experimental and numerical results, and then minimize this function. For the optimization to be successful, it is necessary to evaluate the accuracy of the material parameter sets' predictions as accounted for in terms of a fitness function. The material parameter sets with higher fitness should survive to produce new parameters sets. Therefore, it is necessary to devise an error function so that the parameter sets with better predictions result in higher fitness values.

For each test involved in the optimization, the difference between the experimental result and the numerical prediction is measured by a norm value, referred to as an individual norm which forms an error function Error(x),

$$\text{Error}(x) \rightarrow \min \tag{1-1}$$

where x is a vector containing the optimization variables. Bound constraints are introduced on the optimization variables,

$$x_l \leq x \leq x_u \tag{1-1}$$

where x_l and x_u are, respectively, the lower and upper bounds of x.

As the first step in the formulation of an error function, an expression for the individual norm has to be established. In general, the individual norm is based on Euclidean measures between

discrete points, composed of the experimental and the numerical result. The simplest error function can take the absolute expression,

$$\mathrm{Error}(x)=\frac{1}{N}\left(\sum_{i=1}^{N}\left|U_{\exp}^{i}-U_{num}^{i}\right|\right) \tag{1-2}$$

where N is the number of values; $U_{\exp}^{i}$ is the value of the measurement point i; U_{num}^{i} is the value of the calculation at point i.

Another formulation of the error function introduced by Papon et al. [12] is presented as:

$$\mathrm{Error}(x)=\frac{1}{N}\left(\sum_{i=1}^{N}\left(U_{\exp}^{i}-U_{num}^{i}\right)^{k}\right)^{\frac{1}{k}} \tag{1-3}$$

where k is a non-null positive value with k=1 for the sum of error at every point and k=2 for the least square function.

However, Eq.(1-2) and Eq.(1-3) present some disadvantages when they are used for measuring the fitness between simulated and objective curves. For example, if the triaxial tests are selected as the objectives, poor performance of the simulation can result in a small strain level if the same fitness is required at different strain levels, because the value of deviatoric stress is smaller at a small strain level than at a high strain level. Additionally, the number of measured points in different objective curves could also affect the fitness.

In order to make the error independent of the type of test and the number of measurement points, an advanced error function proposed by Levasseur et al. [13] has been adopted. The average difference between the measured and the simulated results is expressed in the form of the least square method,

$$\mathrm{Error}(x)=\sqrt{\frac{1}{N}\sum_{i=1}^{N}\left(\frac{U_{\exp}^{i}-U_{num}^{i}}{U_{\exp}^{i}}\times 100\right)^{2}} \tag{1-4}$$

The scale effects on the fitness between the experimental and the simulated results can be eliminated by this normalized formula. Additionally, the objective error calculated by this function is a dimensionless variable, thus, any difference in error can be avoided for different objectives with

different variables. Due to the stability of Eq.(1-4), it has been adopted by many researchers as the error function to conduct the optimizations [13-16].

Furthermore, another simple error value using the differential area between predicted and observed curves was introduced by Pal et al.[11]. For each stress-strain curve, the error value is defined as the ratio of the area between the predicted curve and the laboratory test curve to the area of the rectangle generated by the maximum and the minimum values of stresses and strains of the laboratory test, (area of rectangle=(maximum stress-minimum stress)×(maximum strain-minimum strain)), as shown in Figure 1.1. Note that the ratio is independent of the scales used for stress and strain. Like Eq.(1-4), this error function has also been widely used by many researchers [12, 17, 18].

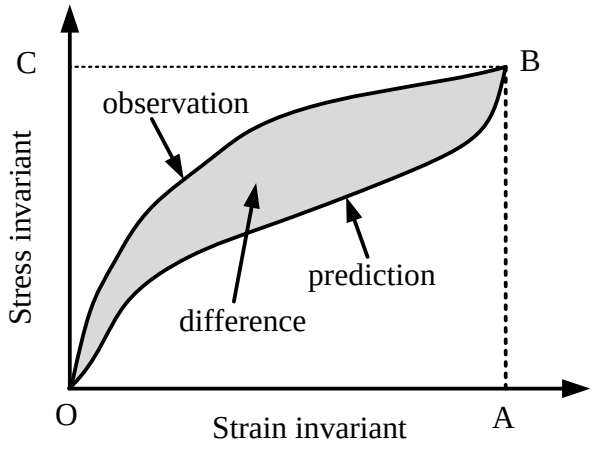

Figure 1.1 Definition of an error function

The next step is to formulate a final norm, a total error function, based on the individual norms computed using the above methods for each experimental test involved in the optimization. Two different final norms have been used in the past and either one can be employed for the total error function. The maximum norm and the combined norm are defined as follows:

$$F_{\max} = \max_{1 \le i \le m} \left(\text{Error}^i \right) \quad \text{and} \quad F_{\text{comb}} = m \cdot F_{\max} + \sum_{i=1}^{m} \left(\text{Error}^i \right) \tag{1-5}$$

where m is the number of experimental tests involved in the optimization, and Error^i is the individual norm value for Test number, i.

Generally, deformation and strength are two extremely important indicators to show the mechanical behavior of soil. For identifying soil parameters, the error function should involve these

two important indicators. Therefore, the generalized individual error function can be expressed as follows,

$$\min\left[\text{Error}(x)\right] = \min\left[\text{Error(stress)},\ \text{Error(deformation)}\right] \tag{1-6}$$

For mono-objective problems, the total error function is expressed as:

$$\text{Error\_total}\left(x\right) = \sum_{i=1}^{Num}\left(l_i \cdot \text{Error}\left(x\right)_i\right) \tag{1-7}$$

where *Num* is the number of the individual errors; $\text{Error}\left(x\right)_i$ is the value of the individual error corresponding to the objective, *i*. l_i is the weight factor with $\sum(l_i) = 1$. Finally, the set of parameters with the minimum error value can be selected as the optimal parameters.

For multi-objective problems, the final error can be expressed as follows,

$$\min\left[\text{Error}(x)\right] = \min\begin{bmatrix}\text{Error(stress)}\\ \text{Error(deformation)}\\ \ldots\end{bmatrix} \tag{1-8}$$

Several sets of parameters on the Pareto frontier can finally be found. The optimal parameters can be determined according to the criterion of selection which was predefined by the user.

1.2.2 Selection of search strategy

After formulating the error function, the selection of the search strategy is the key step of whether the optimized solution can be found or not. The solution to an optimization problem is a vector, x_0 which for any $x_l \leq x \leq x_u$ satisfies the condition, which is a global minimum,

$$F\left(x_0\right) \leq F\left(x\right) \tag{1-9}$$

However, most optimization methods are only capable of searching for a local minimum. For obtaining a more accurate solution, a highly efficient optimization method with the ability to search for a global minimum should be adopted. Different optimizers applied in the geotechnical fields are introduced in Section 1.3.

1.2.3 Procedure of parameter identification

Whether the search strategy used in the optimization is simple or complex, a procedure with a clear structure is necessary and important for the successful identification of parameters. The function of the procedure is to conduct the error function and search strategies together. Therefore, the procedure should be presented before conducting the optimization. Calvello and Finno [19] gave a three step procedure for a general identification of soil parameters, as shown in Figure 1.2; Zentar and Hicher [20] presented a simplified procedure to combine the finite element code CESAR-LCPC and the SiDoLo optimization tool to identify modified Cam-clay (MCC) parameters from pressuremeter tests, as shown in Figure 1.3; Finno and Calvello [18] presented a relatively complex procedure to combine the computer code UCODE and the software tool PLAXIS for identifying Hardening Soil (HS) model parameters from excavation, as shown in Figure 1.4; Obrzud et al. [21] presented a procedure employing a two-level neural network tool to conduct the parameters identification, as shown in Figure 1.5; Zhang et al. [22] presented a procedure involving the MUSEFEM finite element code and particle swarm optimization for identifying the soil parameters of an unsaturated model from pressuremeter tests, as shown in Figure 1.6; Zhao et al. [23] presented an optimization procedure involving a differential evolution algorithm and ABAQUS software for identifying MCC parameters from an excavation, as shown in Figure 1.7.

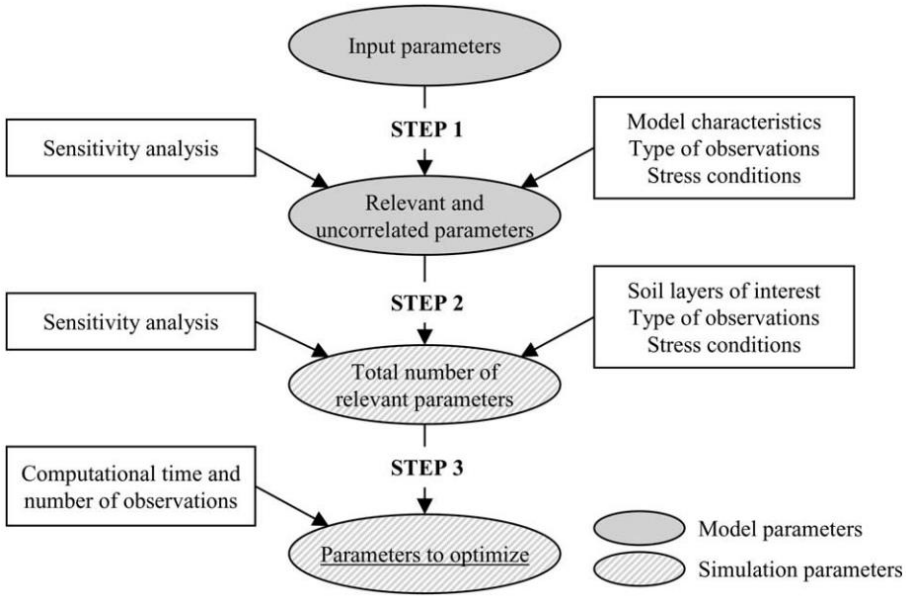

Figure 1.2 Identification of soil parameters to optimize by inverse analysis

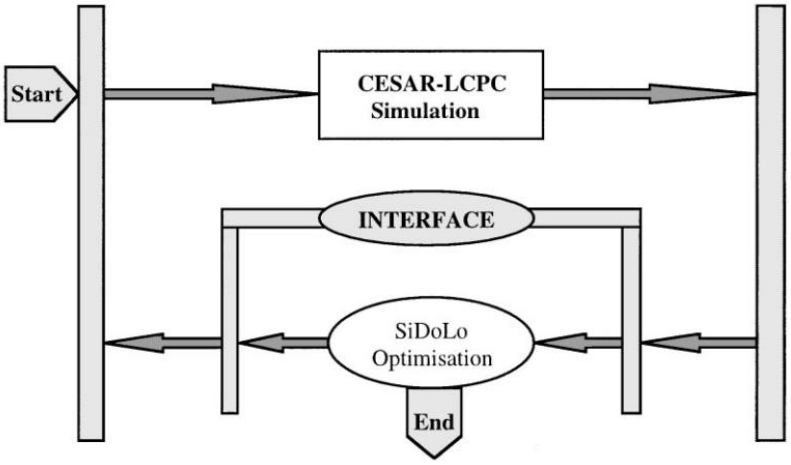

Figure 1.3 Numerical process to identify soil parameters

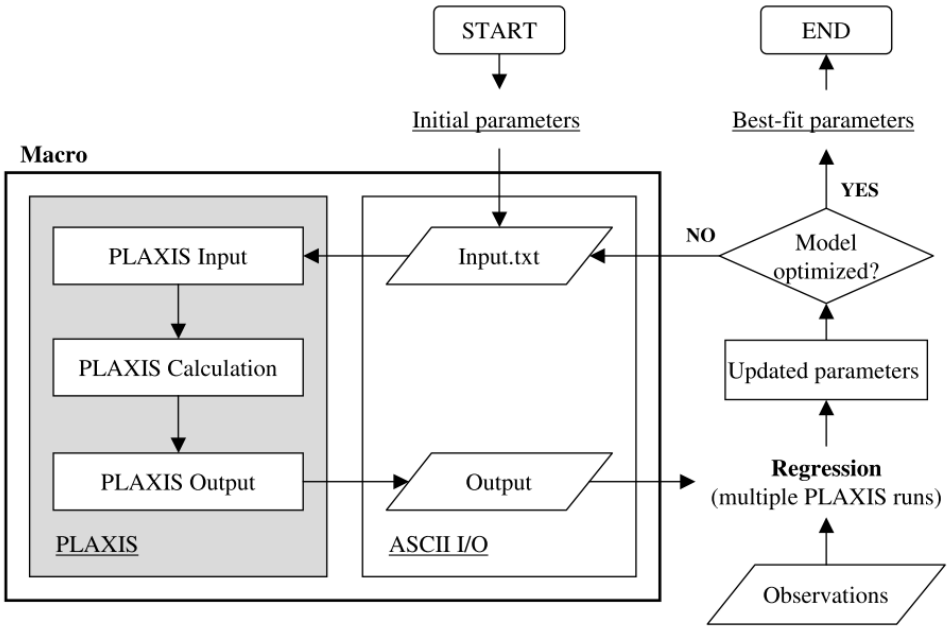

Figure 1.4 Inverse analysis with UCODE and PLAXIS

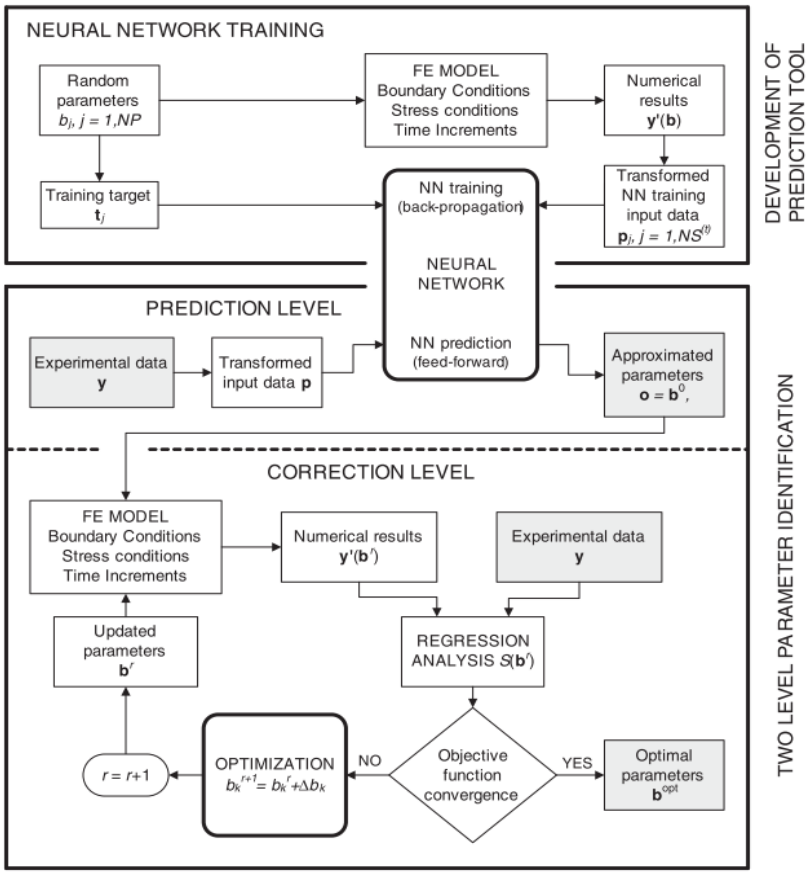

Figure 1.5 Scheme of the two-level parameter identification using neural network tool

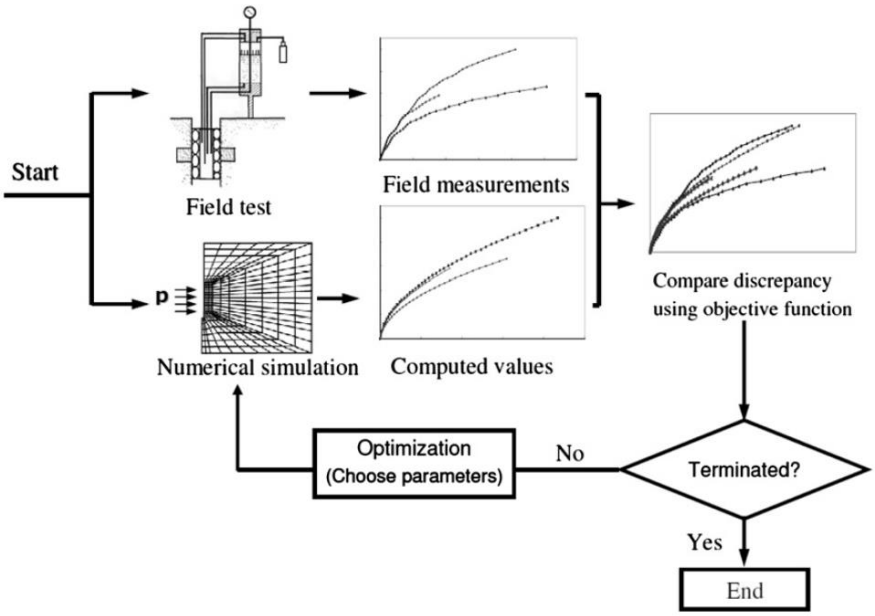

Figure 1.6 Flow chart for identifying soil parameters using particle swarm optimization from pressuremeter tests

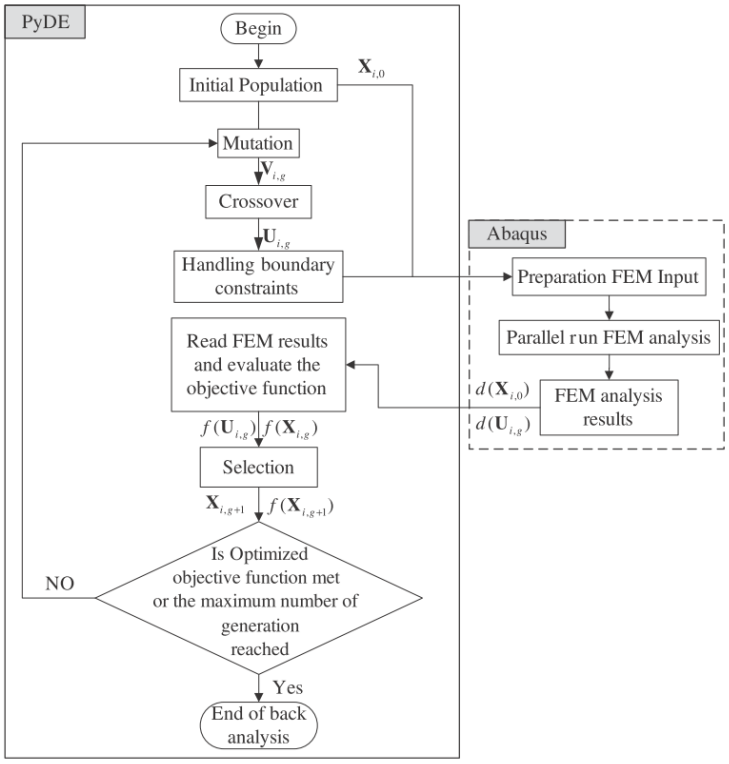

Figure 1.7 Back analysis with an interaction between the differential evolution algorithm and ABAQUS

The procedures presented above, and others which are not presented here, are summarized as Figure 1.8. Most identification procedures are based on two different codes: the FEM code (e.g. PLAXIS [19], FLAC [24] and ABAQUS [23]) or single Gauss point integration of a constitutive model (e.g. Jin et al. [25, 26] and Ye et al. [27]) for the simulation, and the search method code for finding the optimal solution.

For the initialization step shown in Figure 1.8, there are two main methods used for sampling initialization: uniform and random. For uniform sampling, a method introduced by Sobol [28] is usually adopted. The SOBOL method is a deterministic algorithm that imitates the behavior of a random sequence. The aim is to obtain a uniform sampling of the design space. It has been reported to be suitable for problems with up to 20 variables [12, 25-27], and is therefore used in optimising geotechnical engineering problems. For random sampling, a particular method named Latin Hypercube Sampling (ULH), proposed by McKay et al. [29] is usually adopted. ULH is an advanced Random (Monte Carlo) Sampling. Compared to the commonly used Random (Monte Carlo) method,

ULH is better at mapping the marginal probability distributions (i.e., the statistical distribution of each single variable), especially in cases where there is a small number of generated designs.

For objective tests, laboratory tests or field tests can be adopted in the optimization for calibrating model parameters. These test results are usually displayed in the form of a displacement-stress curve, which implies the softening or hardening, the contraction or dilation of soil. In other words, the results of selected tests can provide information to optimize the model parameters, which is the basis of parameter identification with an optimization method. For laboratory tests, the isotropic or anisotropic compression and conventional triaxial tests are usually recommended for use within the industry [17, 18, 25-27, 30]. For field tests, the pressuremeter test [12, 13, 19, 22, 31], cone penetration test [32], excavation [15, 16, 23, 33, 34], and tunnelling [24, 35-37], are usually employed.

Either one of the error functions introduced above can be adopted to calculate the fitness value to the results of the optimization method.

For the optimization algorithms, the deterministic techniques (e.g. gradient-based algorithms, and simplex) or stochastic techniques (e.g., genetic algorithms, particle swarm optimization and differential evolution algorithms) can be employed to minimize the error. The optimization process does not stop until the convergence criterion is attained.

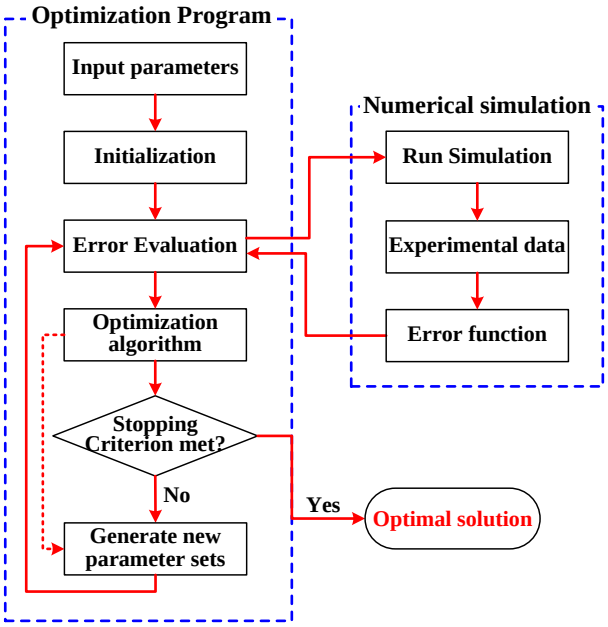

Figure 1.8 General identification procedure

1.3 Review of optimization techniques

Until now, numerous optimization techniques have been applied to solve different problems in geotechnical engineering. In this section, some typical and widely used optimization techniques are reviewed and their basic principles are introduced.

1.3.1 Deterministic optimization techniques

1.3.1.1 Gradient-Based algorithms

The gradient method is probably one of the oldest optimization algorithms, as far back as to 1847 with the initial work of Cauchy. Nowadays, gradient-based methods have attracted a revived and intense interest among researchers both in theoretical optimization and in scientific applications [38]. In optimization, the gradient method is an algorithm used to solve problems, with the search directions defined by the gradient of the function at the current point. Based on the basic principle of gradient, different gradient-based methods have been developed to date, such as the steepest descent method, the conjugate gradient method, the Levenberg-Marquardt method [39, 40], the Newton method and several Quasi-Newton methods. Unlike the steepest descent gradient methods, which only use first order information (the first derivative term in the Taylor series) to obtain a local model of the function, the Newton-based gradient methods use a second-order Taylor series expansion of the function on the current design point. In addition to the above mentioned gradient-based methods, the Davidon-Fletcher-Powell (DFP) method and the Broyden-Fletcher-Goldfarb-Shanno (BFGS) method are also widely used in optimization engineering.

The primary advantage of a gradient-based method is rapid convergence. Clearly, the effective use of gradient information can significantly improve the speed of convergence, unlike a method that does not compute gradients. However, gradient-based methods have some limitations, being strongly dependent on user skill, due to the need to choose the initial trial solutions. Also, they can easily fall to local minimums, mainly when the procedure is applied to multi-objective functions, as is the case with material parameter identification. The requirement of derivative calculation makes these methods non-trivial to implement. Another potential weakness of gradient-based methods is relative intolerant of difficulties such as noisy objective function spaces, inaccurate gradients, categorical variables, and topology optimization.

The gradient-based methods have been used for solving different geotechnical engineering problems, such as identifying the soil model parameters [13, 16, 19, 20, 31, 35, 37, 41-45] or soil permeability [46], optimizing back-analysis for tunneling-induced ground movement [47], and analysis of excavation-induced wall deflection [48]. However, due to their limitations, gradient-based methods cannot be satisfactorily applied to complex nonlinear optimization problems.

1.3.1.2 Nelder-Mead simplex

The simplex algorithm is a nonlinear optimization algorithm developed by Nelder and Mead [49] for minimizing an objective function in a poly-dimensional space, which adopts a direct search strategy. The method uses the concept of a simplex, which is a polytope of N+1vertices in N dimensions, and finds a locally optimal solution to a problem with N variables when the objective function varies smoothly.

The Nelder-Mead simplex can change during iteration in five different ways (Figure 1.9) in two dimensions (Lagarias *et al.*[50]). Apart from the case of a shrink, the worst vertex of the simplex at iteration k (point p_3 in the figure) is replaced at iteration k+1 by one of the reflection, expansion, or contraction points (Nelder and Mead [49]). If this new point is not much better than the previous value, then the algorithm knows it is stepping across a valley, so it will shrink the simplex towards the best point. Based on this description, users feel that they understand how the method functions. The simplex can lead to the best solution using a limited number of calculations. In that sense, it can be fast and efficient.

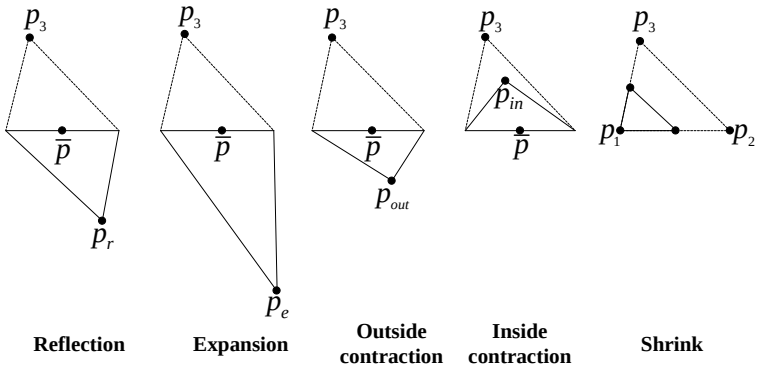

Figure 1.9 Structure of Nelder-Mead simplex algorithm

However, most direct search strategies, such as the gradient-based methods and simplex described above, are only capable of searching for a local minimum. Generally, there is no way to

check whether the local minimum obtained is also the global one. A possible solution to this problem is to start the search from different initial positions and, if the local minima become the same, then this is most probably also the global minimum.

Nevertheless, there are still many applications for the simplex due to its excellent convergence speed, such as identifying the cohesion, and friction angle of an elastoplasticity model and initial stress using a flexible polyhedron (modified simplex) strategy [8]; estimating soil hydraulic properties from field data [51]; identifying parameters of a hardening soil model based on pressuremeter tests [12], and identifying both creep and destructuration related parameters for soft clays [27].

1.3.2 Stochastic optimization techniques

1.3.2.1 Genetic algorithms (GA)

The genetic algorithm (GA) originally developed by Holland [52] is a simulation mechanism of Darwinian natural selection and a genetics computational model of the biological evolutionary process. It is also a process to search for the optimal solution by simulating the natural evolution. In GAs, an encoding scheme is first used to represent a point (individual) in the search of decision variables, and then each individual of the population is assigned a fitness based on certain criteria. In early implementations [53], the decision variables were encoded as strings of binary alphabets using 'zero' and 'one'. The performance of binary GAs are found to be satisfactory on small and moderately sized problems, which do not require as much precision in the solution, but for high dimensional problems in which a higher degree of precision is desired, binary GAs require huge computational time and memory [54]. To overcome these difficulties, real coded GAs, in which decision variables are encoded as real numbers, are now more commonly used. It has been established that real coded GAs are superior to binary coded GAs for continuous optimization problems [55].

The procedure of a general genetic algorithm is presented in Figure 1.10. Once the genetic representation and the fitness function are defined, the GA proceeds by initializing a population of solutions and then improving it through repetitive applications of the selection, crossover, inversion and mutation operators. Genetic algorithms work with a population of solutions, so that they can provide a set of satisfactory solutions. They also do not use any gradient information and they are based on stochastic principles. Therefore, they are considered more robust than the gradient methods.

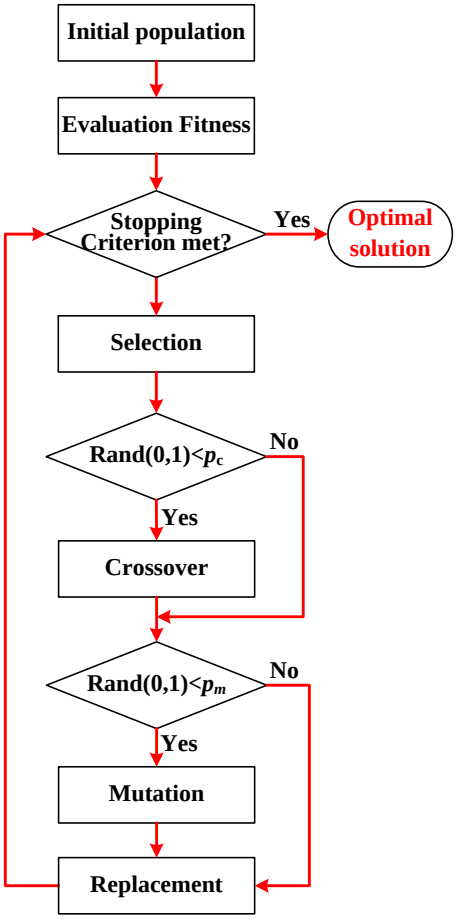

Figure 1.10 General flow chart of GA

In geotechnical fields, GAs have been widely employed to solve various problems such as parameter identification of constitutive models [11-15, 17, 18, 25, 26, 56, 57], prediction of soil hydraulic parameters [58-60], identification of critical slip surfaces in slope stability analysis [61-65], prediction of vertical settlement [66], optimization of pile group design [32, 67], reliability analysis [68], road maintenance [69], and prediction of soil-water characteristic curves [70].

1.3.2.2 Particle swarm optimizations (PSO)

Particle swarm optimization (PSO) is a population-based stochastic global optimization algorithm which was first suggested by Kennedy and Eberhart [71] in an attempt to simulate the graceful choreography of flocks of birds, as part of a socio-cognitive study on the notion of "collective intelligence" in biological populations.

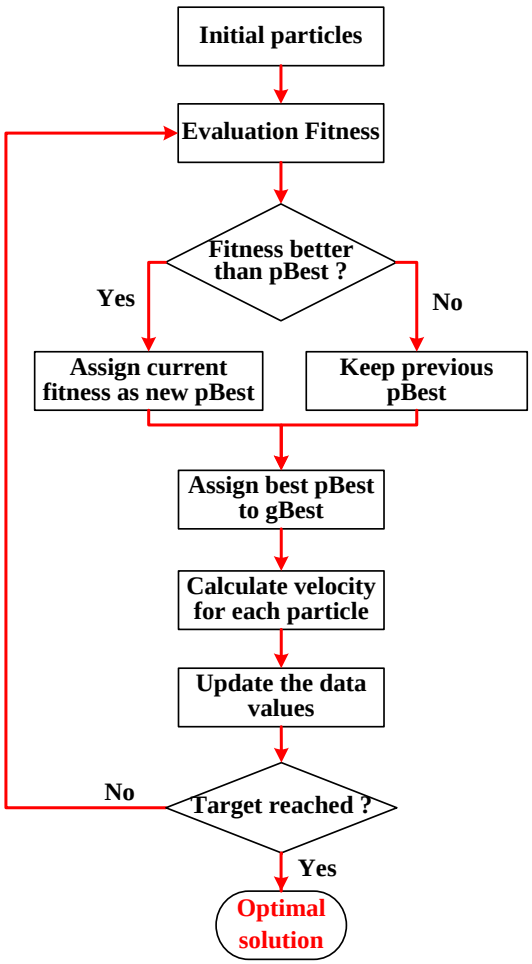

Figure 1.11 General flow chart of PSO

Figure 1.11 shows the procedure of PSO to find the best solution. In PSO, a number of simple entities, the 'particles', are randomly placed in the search space of a given problem or a given function, and each entity evaluates the objective function at a particular location. Each particle then determines its movement through the search space by combining some aspect of the history of its own actual and best (best-fitness) locations with those of one or more members of the swarm, with some random perturbations, as shown in Figure 1.12. The new position $\boldsymbol{x}_i(t)$ of the *i*th particle can be defined as,

$$\boldsymbol{x}_i(t) = \boldsymbol{x}_i(t-1) + \boldsymbol{V}_i(t), \quad i = 1,\ 2,\ \ldots,\ N_p \tag{1-10}$$

where N_{p} is the total number of particles. The new velocity $\boldsymbol{V}_i(t)$ of the *i*th particle is calculated by,

$$\boldsymbol{V}_i(t) = w(t)\boldsymbol{V}_i(t-1) + c_1 r_1\left(pBest_i - \boldsymbol{x}_i(t-1)\right) + c_2 r_2\left(gBest - \boldsymbol{x}_i(t-1)\right) \tag{1-11}$$

where r_1 and r_2 are random numbers between 0 and 1; $pBest_i$ is the local best position (the best among all previous positions at time (t-1)); $gBest$ is the global best position (the best particle position among all known particle positions within the whole swarm); $w(t)$ is the inertia weight used to control the impact of the previous particle velocities on the current velocity and it is usually taken as slightly less than 1 [30]. The learning factors c_1 (cognitive weight) and c_2 (social weight) are positive constants, which determine how much the particle is directed towards the good positions and are usually adapted to the individual task to be solved by manual variation, but usually are set as equal to 2 [30]. The local best position for the ith particle is updated, if

$$F\left(\boldsymbol{x}_i\right) < F\left(pBest_i\right) \tag{1-12}$$

and the global best position is updated, if

$$F\left(\boldsymbol{x}_i\right) < F\left(gBest\right) \tag{1-13}$$

The next iteration takes place after all particles have been moved. Eventually, the swarm as a whole, like a flock of birds collectively foraging for food, is likely to move close to an optimum of the fitness function.

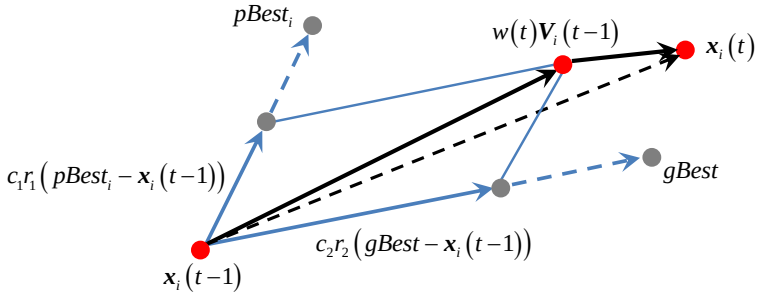

Figure 1.12 Schematic diagram of the method of the PSO

Unlike in GA with its binary encoding, in PSO, the design variables can take any value, even outside their constraint, based on their actual position in the design space and the calculated velocity vector. PSO also has no evolution operator such as crossover or mutation, which makes it ideal for asynchronous parallel implementation. However both algorithms have similar functions for finding the best solution. The comparison between GA and PSO has already been investigated in terms of computational effectiveness and efficiency by several researchers [72, 73]. Each algorithm has its unique advantages for solving different types of problems.

PSO has been shown to provide valuable results in various inverse geotechnical problems, such as parameter identification of constitutive models [22, 30, 74-80], identification of hydraulic

parameters for unsaturated soils [81], parameter identification in soil-structure interaction [82], location of the critical non-circular failure surface in slope stability analysis [83], and parameter estimation of laboratory through-diffusion transport of contaminants [84].

1.3.2.3 Simulated annealing (SA)

Simulated annealing (SA) is a random-search technique which exploits an analogy between the way in which a metal cools and freezes into a minimum energy crystalline structure (the annealing process) and the search for a minimum in a more general system [85]. Classical simulated annealing (CSA) was proposed by Kirkpatrick et al. [86]. Due to the inherent statistical nature of simulated annealing, in principle local minima can be hopped over more easily than in gradient-based methods [87].

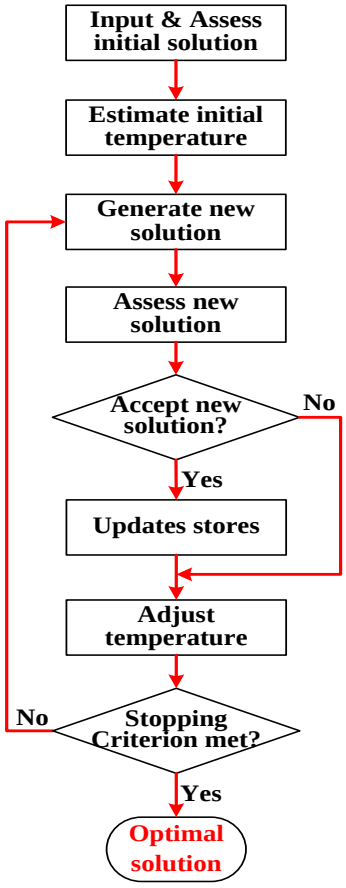

Figure 1.13 General structure of SA algorithm

Figure 1.13 shows a general structure of simulated annealing algorithm. A simple form of local search (a descent algorithm) starts with an initial solution. A neighbor of this solution is then

generated by some suitable mechanism and the change in cost can be calculated. If a reduction in cost is found, the current solution can be replaced by the generated neighbor; otherwise the current solution is retained. The process is repeated until no further improvement can be found in the neighborhood of the current solution and so, the descent algorithm terminates at a local minimum.

Further details about the strengths, and weaknesses of simulated annealing, and a comparison with other methods, can be found in Busetti [85]. For simulated annealing, there are few applications in geotechnical field, one example is to determine a safety factor for slope stability [88].

1.3.2.4 Differential evolution algorithm (DE)

The differential evolution (DE) algorithm, proposed by Price and Storn [89, 90] is a simple, yet powerful population-based stochastic search technique, which is an efficient and effective global optimizer in the continuous search domain. Like other population-based optimization algorithms, DE also involves two phases: initialization and evolution. In the initialization phase, the DE population is generated randomly if nothing is known about the problem. In the evolution phase, individuals from the population traverse mutation, crossover, and selection processes repeatedly until the termination criterion is met. The DE algorithm was sometimes considered as a variant of a GA because it had the same optimization process. The main difference in constructing better solutions is that a GA mainly relies on crossovers whereas DE relies mainly on a mutation operation. The DE uses a mutation operation as a search mechanism and a selection operation based on the differences in randomly sampled pairs of solutions in the population,

$$\begin{aligned} &\boldsymbol{x}_i = \boldsymbol{x}_{r3} + F^k\left(\boldsymbol{x}_{r2} - \boldsymbol{x}_{r1}\right), \\ &r1,\ r2,\ r3 \in \left\{1,\ 2,\ ...,\ N_p\right\},\ k \in \left\{1,\ 2\right\},\ F^k \in \left[0,\ 1\right] \end{aligned} \tag{1-14}$$

where F^k is a scaling factor which is closely related to the convergence speed. k indicates the number of difference vectors taking part in the mutation operation; $\boldsymbol{x}_{r1}$, $\boldsymbol{x}_{r2}$ and $\boldsymbol{x}_{r3}$ are selected individuals from the population which are different from the running individual $\boldsymbol{x}_i$.

Furthermore, the DE algorithm also uses a non-uniform crossover that can take child vector parameters from one parent more often than it does from others. Selecting the DE algorithm takes the competition mechanism. Each new solution produced competes with a mutant vector and the better one wins the competition.

As evolution proceeds, the population of DE may move through different regions in the search space, within which certain strategies associated with specific parameter settings may be more effective than others (Qin et al. [91]). However, the performance of the conventional DE algorithm depends highly on the chosen trial vector generation strategy and associated parameter values used. DE does not guarantee the convergence to the global optimum. It is easily trapped into local optima resulting in a low optimizing precision or even a failure (Jia et al. [92]).

In geotechnical engineering, the DE has been applied to cope with different optimization problems, such as parameter identification of constitutive models [23, 93, 94], and back analysis of tunneling [24].

1.3.2.5 Artificial bee colony (ABC)

The artificial bee colony (ABC) algorithm originally developed by Karaboga [95] in 2005 is an optimization algorithm simulating the intelligent foraging behavior of honey bee swarms. It is a very simple, and robust population-based stochastic optimization algorithm.

The ABC algorithm describes the foraging, learning, memorizing and information sharing behavior of honeybees. A basic model of the foraging behavior of honeybee swarms consists of two essential components, and defines two leading modes of behavior. The artificial bee colony consists of three groups of bees: employed bees, onlookers, and scout bees.

The colony of the artificial bees is divided into two groups: the first half of the colony consists of the employed artificial bees, and the second half of the onlooker bees. Scout bees are the employed bees whose food source has been abandoned. In the ABC algorithm, the position of a food source represents a possible solution to the optimization problem (value of design variables) and the nectar value of a food source corresponds to the quality of the associated solution (fitness value). The number of employed bees is equal to the number of onlookers, and is also equal to the number of food sources. Any food sources that cannot be improved further in certain cycles will be replaced with a new food source by a scout bee.

Following Karaboga and Akay [96], the flow chart of the algorithm is shown in Figure 1.14. Further details of the ABC algorithm, can be found in Karaboga and Basturk [97].

However, as in other evolutionary algorithms, the ABC algorithm also faces some challenging problems [98]. For example, the convergence speed of an ABC algorithm is typically slower than those of representative population-based algorithms (e.g., DE and PSO) when handling these unimodal problems [96]. In addition, an ABC algorithm can become easily trapped in the local optima when solving complex multimodal problems.

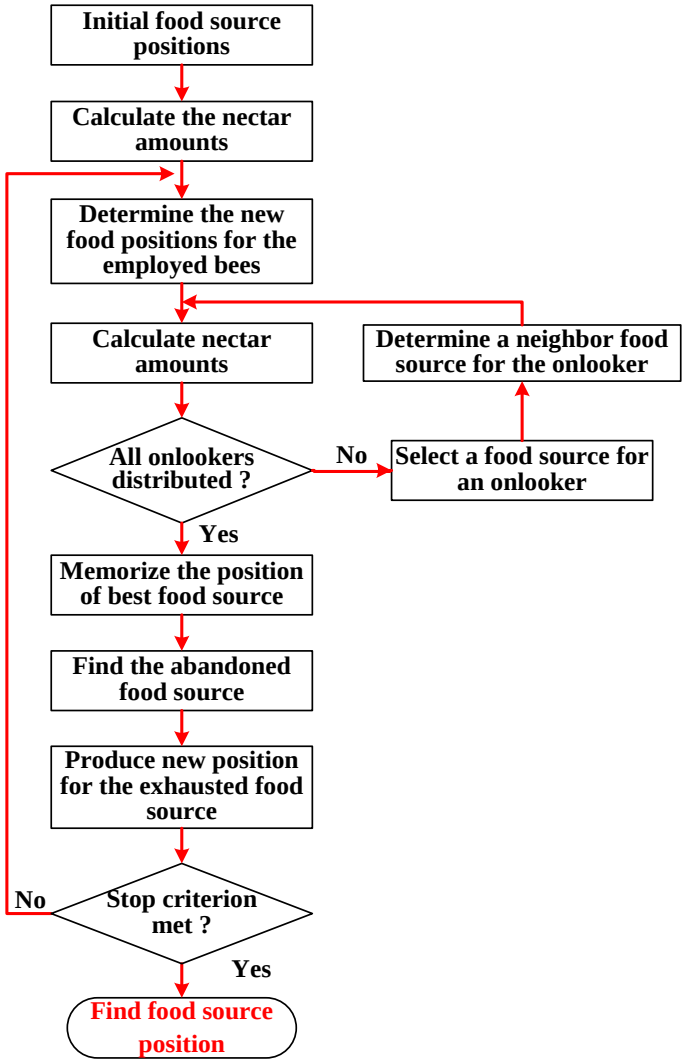

Figure 1.14 Flow chart of the ABC algorithm

The applications of ABC algorithms in geotechnical engineering vary for different problems. The ABC algorithm has been employed to locate the critical slip surface of a slope [99, 100]; to predict the uplift capacity of suction caissons [101]; and to analyze the reliability of geotechnical engineering solutions [102, 103].

1.3.2.6 Others

Apart from the previously mentioned optimization methods, some other algorithms, initially developed by modeling the behavior of social insects such as ants and bees, have been developed for the purpose of solving some certain optimization problems. Among them, Ant Colony Optimization (ACO), a metaheuristic for solving difficult combinatorial optimization problems, was introduced by Dorigo et al. [104, 105] as a novel nature-inspired metaheuristic for solving of hard combinatorial optimization (CO) problems. The inspiration behind ACO is the trail laying of pheromone and following behavior of real ants, who use pheromones as a communication medium. More information about ACO can be found in Dorigo [106]. In the geotechnical field, ACO has initially attracted more attention, as applications include estimating unsaturated soil hydraulic parameters [107] and determining the critical failure surface for slope stability analysis [108].

Similar way to ACO, the Honey-bee mating algorithm (HBMO) [109], the Bacterial Foraging Optimization Algorithm (BFOA) [110] and the Krill herd (KH) algorithm [111] are also considered as typical bio-based approaches to optimization. However, their applications in geotechnical engineering have not been presented to date.

1.4 Hybrid optimization techniques

Conventional optimization methods usually suffer from the local optimality problem and slow convergence speed, which limits the application of these traditional methods to a small range of real word problems, even sometimes causing a failure optimziation at times. In order to enhance the optimizing performance of these traditional algorithms, an efficient method is to combine the advantages of each approach with a hybrid strategy (e.g. Tsai et al. [112] and Shi et al. [113]). The hybrid strategies can generally be divided into three groups: (1) hybrids of different operators (e.g. different crossovers in GAs [114]); (2) hybrids with a local search (e.g. GA or PSO with simplex [115], GA, and GA, PSO or DE with chaotic [92, 116, 117]); and (3) hybrids of different optimization techniques (e.g. GA and PSO [118, 119], GA and DE [24], PSO and ABC [120], and PSO and ACO [121]). In geotechnical engineering, due to the high performance, hybrid optimization algorithms, have become more used and have been applied to many optimization problems, such as optimization of pile groups [67], the identification of geomechanical parameters [122], slope reliability analysis [123], and prediction of the uplift capacity of suction caissons [101]. In the future, other geotechnical problem are likely to be solved with these hybrid optimization techniques.

1.5 Conclusions

A review of optimization techniques in identifying parameters has been presented. First, the methodology of parameter identification was reviewed. Different kinds of error functions for measuring the difference between experimental and numerical results and different optimization procedures were reviewed.

The widely used optimization techniques in geotechnical engineering including: (1) deterministic techniques (gradient-based methods and Nelder-Mead simplex); (2) stochastic techniques (GA, PSO, SA, DE, ABC and other similar techniques); and (3) hybrid optimization methods have been presented with an introduction to their basic principles and applications,.

Chapter 2 Comparative study of currently used typical optimization techniques

2.1 Introduction

Generally, each optimization technique has its advantages and drawbacks, which means that not all the optimization problems can be solved effectively by one optimization method. For any given optimization problem, it is necessary to evaluate the optimizing performance of different methods and then to select the most appropriate method for conducting the optimization procedure. In order to evaluate the search ability and convergence speed of optimization techniques in identifying parameters, different optimization techniques need to be applied to the same optimization problem.

The deterministic optimization methods have significant discrepancies of search ability ensuring only the local minimization reported by many researchers, and therefore they have not been repeated for comparative study. The stochastic methods have generally good search ability, and are usually adopted for combining hybrid methods. Therefore, stochastic methods are more basic than hybrid methods, and five of the mostly used stochastic methods in geotechnical field (i.e., GA, PSO, SA, DE and ABC) were thus adopted for comparisons. Two typical cases, i.e. identification of parameters from pressuremeter tests and excavation measurements respectively were adopted for optimization process.

2.2 Case 1: Pressuremeter test

2.2.1 Simulation of Pressuremeter test

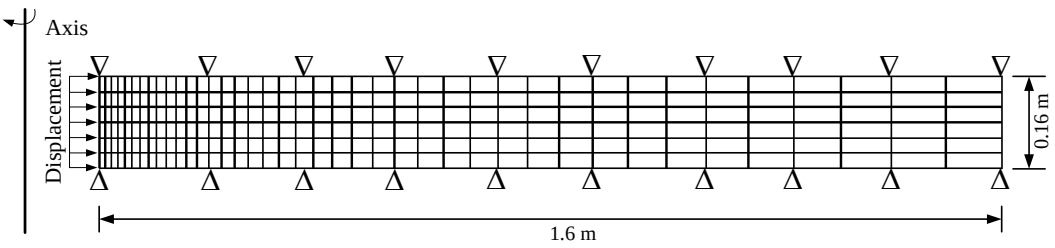

Figure 2.1 Geometry model of PMT test in ABAQUS

In order to conduct the comparative study, a parameter identification using the Mohr-Coulomb (MC) model for a pressuremeter test (PMT) was selected. For a fair comparison and absolute

evaluation of selected intelligent computing techniques, a synthetic objective pressuremeter test was generated in the FEM code with the same set of parameters as that used in the MC model. For generating the stress-displacement curve of PMT, a 2D finite element model with an axisymmetric condition in ABAQUS was created, as shown in Figure 2.1. A total of 240, 4-node reduced-integration elements (CAX4R) was used to simulate the soil. For reproducing the in-situ conditions, the initial stress state of the soil was set to the K_0 condition. The initial vertical stress and horizontal stress were respectively set to 31 kPa and 22 kPa, consistent with field tests [12]. The same displacement as in the field test was applied, and at each step, the same displacement increment was applied.

Using a typical set of MC parameters (elastic modulus E=30000 kPa, Poisson's ratio=0.30, friction angle ϕ=35°, cohesion c=5 kPa and dilatancy angle ψ=5°), a synthetic result from a pressuremeter test was generated and the results are shown in Figure 2.2, and these are employed as the objective in the optimization procedure.

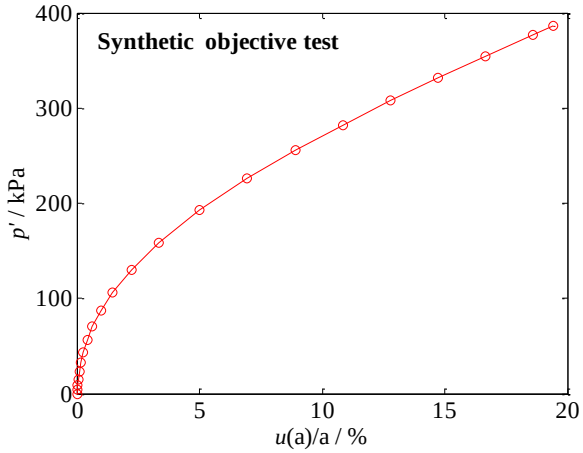

Figure 2.2 Result of synthetic objective test

2.2.2 Sensitivity analysis

To evaluate the relative importance of each model parameter on the pressuremeter test, a sensitivity analysis should be performed prior to the optimization procedure [19, 43, 124, 125]. In this study, the stress-displacement result from a synthetic objective test was selected as the observation and the composite scaled sensitivity (CSS_j) analysis proposed by Hill [126] was adopted to conduct the sensitivity analysis. The composite scaled sensitivity analysis indicates the amount of information provided by the i-th observations for the estimation of the j-th parameter and is defined as:

$$CSS_j^i = \sqrt{\left(\frac{1}{N} \sum_{i=1}^{N} \left(\left(\frac{\partial y_i}{\partial x_j} \right) \cdot x_j \sqrt{\omega_i} \right)^2 \right)} \tag{2-1}$$

where y_i is the ith simulated value; x_j is the jth estimated parameter; $\partial y_i / \partial x_j$ is the sensitivity of the ith simulated value with respect to the jth parameter; N is the number of observations. ω_i is the weight factor, which is related to the ith observation and can be evaluated based on the statistics (i.e. variance, or standard deviation, or coefficient of variation of the error of the observations). See Calvello and Finno [19] for more details concerning ω for the laboratory data.

The composite scaled sensitivities indicate the total amount of information provided by the observations for the estimation of parameter j, and measure the relative importance of the input parameters being simultaneously estimated. Low values of CSS_j indicate a high uncertainty in the parameter estimation and can be considered to be poorly identified from the observations.

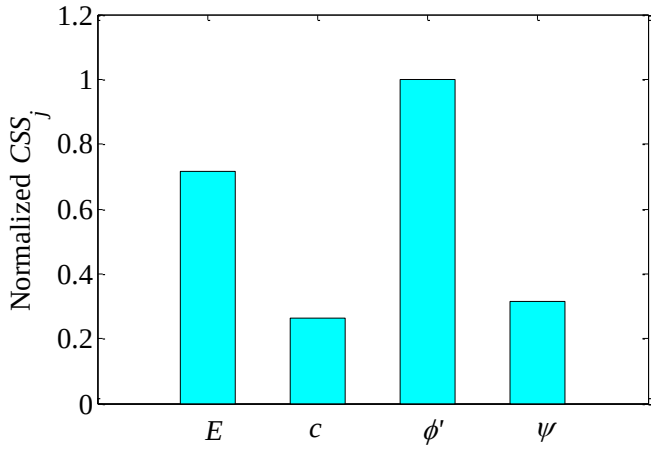

Figure 2.3 Composite scaled sensitivity (CSS_j) of MC model parameters on PMT

Apart from the Poisson's ratio ν, the rest of the MC parameters were selected to evaluate the sensitivity on PMT test. Figure 2.3 shows the normalized composite scaled sensitivity (CSS_j) of the selected parameters. It can be seen that the friction angle, ϕ, and Young's modulus, E, have significant effects on the simulation of PMT, which indicates that more attention should be paid to these parameters. The dilatancy angle, ψ , and the cohesion , c, have relatively minor effects on simulated PMTs, which demonstrates that a large step size for these parameters can be given in the optimization.

Table 2.1 Search domain for MC parameters in the optimization

MC Parameters	ν	E	ϕ'	ψ	c
Lower bound	- (0.1)	10000 (10000)	20 (20)	0 (-)	0 (0)
Upper bound	- (0.4)	50000 (50000)	50 (50)	20 (-)	20 (20)
Step size	- (0.02)	1000 (1000)	0.1 (0.1)	0.5 (-)	0.5 (1.0)

Remark: ν=0.25 is fixed for PMT; values in ( ) is for excavation.

Thus, based on the sensitivity results shown in Figure 2.3, the intervals of the selected parameters are given in Table 2.1, and these are much larger than those corresponding to their typical values.

2.2.3 Optimization results and discussion

The error function shown in Chapter 1 was used to measure the error between the objective test results and its simulation. For all the selected methods used in the optimization procedure, the number of initial individuals and the maximum evaluations were set at 30 and at 3000. All the initial individuals (or populations) were generated by SOBOL. For the GA, the RCGA proposed by Jin et al. [25] was adopted, and the probabilities of crossover were set at 0.8, and the probability of mutation was set at 0.05; for PSO, the learning factors c_1 and c_2 were set at 2.0; for DE, the mutation factor was set at 0.8 and the probability of crossover was set at 1.

Following the procedure shown in Chapter 1, the optimizations using selected optimization methods were conducted. The results of optimal parameters with objective errors and the number of evaluations corresponding to convergence are summarized in Table 2.2. It can be seen that the GA has the fastest convergence speed, and the ABC has the slowest convergence speed. The DE has the strongest search ability but slower convergence speed. In all the selected methods, however, it is difficult to find the preset parameters with 3000 evaluations. To find the reason leading to failure optimization, several sets of parameters with objective errors less than 0.5% and 0.1% were selected and can be plotted in Figure 2.4. Note that all the parameters shown in Figure 2.4 are normalized through $(x\text{-}x_{\min})/(x_{\max}\text{-}x_{\min})$ using the upper and lower bound. For those sets of parameters with an error less than 0.5%, it can be seen that a bigger ϕ' with a smaller c or a smaller ϕ' with a bigger c can result in similar objective errors, which indicates that a coupling effect exists among the parameters apart from E. With a decrease in the value of the error, each parameter varies within a small range, which indicates the weak variability of each parameter. Thus, the identification of MC for PMTs can

be considered to be a multimodal optimization problem, as illustrated in Figure 2.5. Many existing local minima with similar objective errors would show a deceptive search direction, which could lead to a failure of the optimization process. The failure of the optimization process also demonstrates that the search ability of each selected algorithm is not satisfactory for solving conventional geotechnical optimization problems.

Table 2.2 Optimal parameters for different optimization methods with objective error and number of evaluations corresponding to convergence

Methods	E /kPa	ϕ' / °	ψ / °	c / kPa	Objective error /%	Number of evaluations to convergence
GA	29000	35.2	4.5	5.5	0.084	1381
PSO	29000	35.0	5.0	5.5	0.114	2716
SA	31000	39.0	2.0	3.0	0.145	1730
DE	29000	32.5	7.0	6.5	0.055	2041
ABC	30000	28.5	9.5	8.0	0.157	-

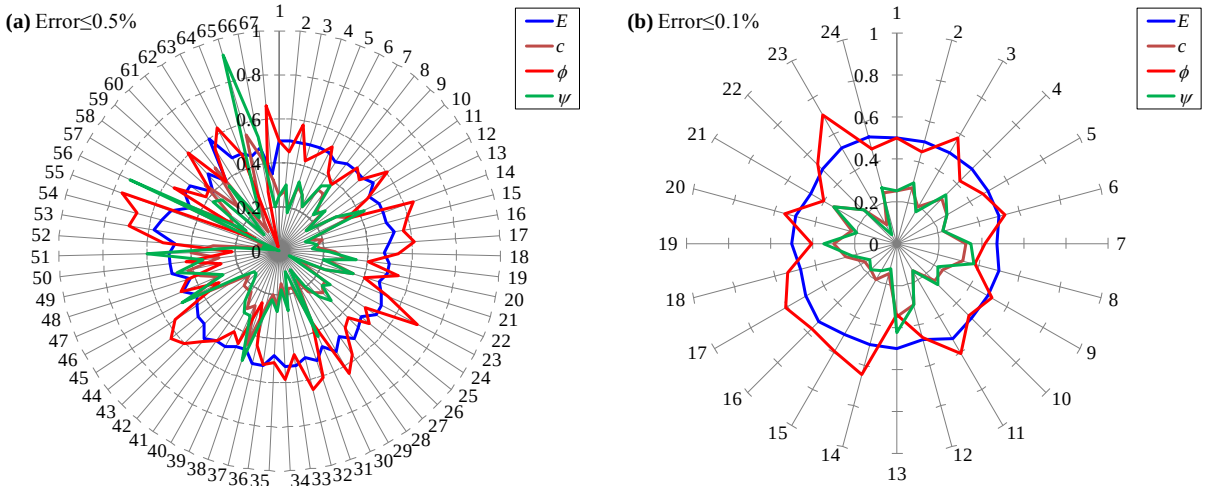

Figure 2.4 Relationship between each parameter for similar simulation (a) error≤0.5%; (b) error≤0.1%

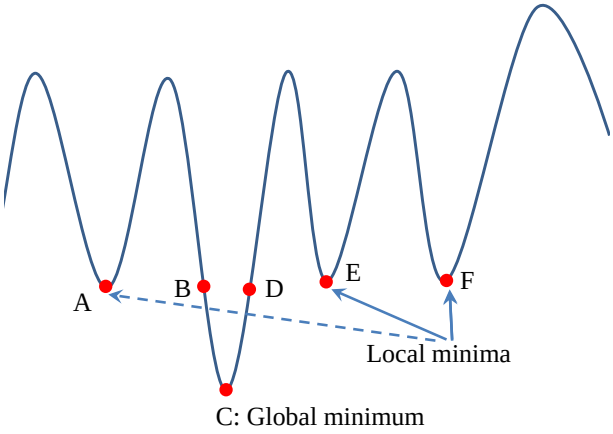

Figure 2.5 Illustration of a multimodal optimization problem

When solving a real engineering problem, h owever, the characteristics of the problem are usually unknown. Consequently, it is difficult to choose the most appropriate optimization method in advance. Therefore, an enhanced optimization algorithm responsible for finding a global minimum with a faster convergence speed is the first choice for solving real engineering problems.

2.3 Case 2: Excavation

In order to compare further the performance of the above optimization algorithms, a new optimization for identifying MC parameters was conducted on a synthetic excavation. The same preset parameters used in the PMT case were again adopted to generate objective tests. Figure 2.6(a) shows the geometry and finite element mesh of the synthetic excavation. In the simulation, because of the geometric symmetry, only half of the excavation was modeled under a plain strain condition. The overall model size is 100 m long and 45 m high, which is considered large enough to avoid boundary constraints. The excavation was conducted in three steps with 3m for each step. A strut is then installed at the level of the ground surface to support the retaining wall. The MC model is adopted for modeling soil in the excavation. The retaining structure, including the retaining wall and the strut, are assumed to be linear-elastic. The element type for the soil is a four-node bilinear rectangular element. A spring element and a two-node linear beam element were adopted for the strut and the retaining wall, respectively. The displacement of the retaining wall after the third step is shown in Figure 2.6(b), and this one has been adopted as the objective test in the optimization.

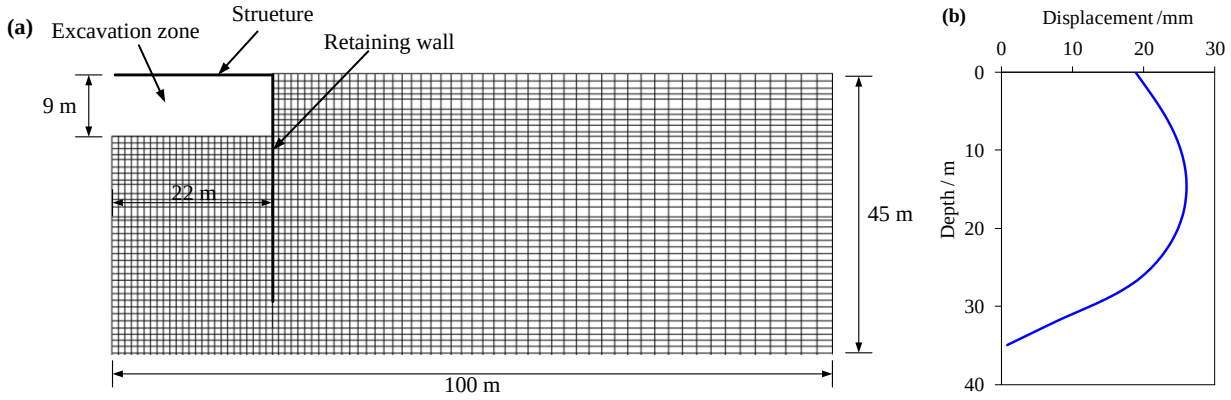

Figure 2.6 (a) Geometry and finite element mesh of the synthetic excavation case in ABAQUS; (b) Displacement of retaining wall in synthetic excavation

Prior to the optimization, a sensitivity analysis using composite scaled sensitivity was also conducted. Figure 2.7 shows the normalized value of CSS_j of the MC parameters on the excavation. The significant influence of Poisson's ration on the wall deflection of the excavation was found, and was then followed by E, ϕ', c and ψ. The effect of ψ is too slight, and so it can be ignored in the optimization. Thus, the intervals of the MC parameters on the excavation were determined according to the sensitivity analysis and are shown in Figure 2.7. The settings for each selected optimization algorithm are the same as those used in the PMT case.

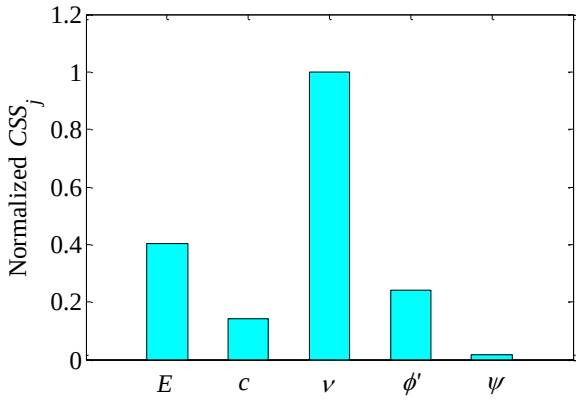

Figure 2.7 Composite scaled sensitivity (CSS_j) of MC model parameters on excavation

The optimal parameters and the number of evaluations to convergence for all selected optimization algorithms are shown in Table 2.3. It can be seen that the PSO and DE can eventually obtain the preset parameters, while the DE has a faster convergence speed than the PSO. In terms of

convergence speed, the ABC has the fastest convergence speed and the SA has the slowest convergence speed among all selected methods for this excavation.

Table 2.3 Optimal parameters for different optimization methods with objective error and number of evaluations corresponding to convergence

Methods	E /kPa	ϕ' / °	ν	c / kPa	Objective error /%	Number of evaluations to convergence
GA	30000	28.0	0.3	8.0	0.033	1681
PSO	30000	34.9	0.3	5.0	0.0287	1714
SA	30000	22.6	0.3	11.0	0.16	-
DE	30000	35.0	0.3	5.0	0.0	1259
ABC	30000	32.5	0.3	6.0	0.045	845

Overall, for comparison, Figure 2.8 shows the minimization process with increasing generation numbers, for all selected optimization methods. All the results demonstrate that the DE performs well in identifying parameters.

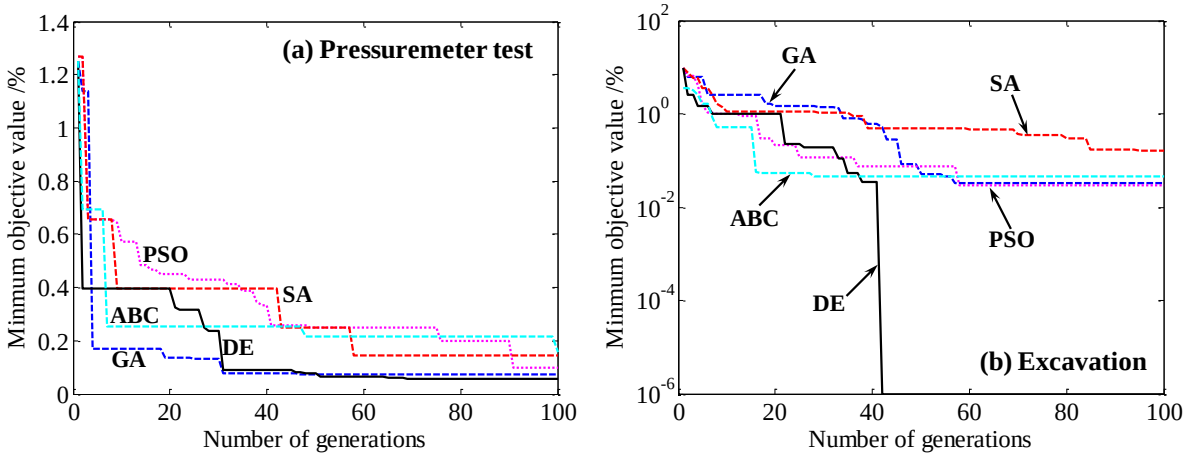

Figure 2.8 Minimization process with increasing generation numbers

2.4 Conclusions

A comparative study was performed for identifying Mohr-Coulomb parameters from a synthetic PMT and excavation. The GA, PSO, SA, DE and ABC were selected to conduct the optimizations. All the comparisons demonstrate that the DE has the strongest search ability with the smallest objective error, but a weaker convergence speed.

In the future, the proposed algorithm will be applied to many more geotechnical engineering problems.

Chapter 3 Development of new hybrid RCGA

3.1 Introduction

In recent years, optimization methods have been extensively developed and applied to various problems. Many fields of study have adopted this effective and intelligent method to solve different types of sophisticated problems. Many successful cases have demonstrated that optimization techniques are remarkably able to solve problems, providing optimum solutions. The existing optimization techniques can be divided into two categories: (1) deterministic optimization techniques; and (2) stochastic optimization techniques. Deterministic optimization techniques, such as Gradient-Based algorithms and Simplex [31, 49], work with a single solution and are local minimiser in nature because they begin the search procedure with a guess solution (often chosen randomly in the search space), and if this guess solution is not close enough to the global minimum solution, it is likely to be trapped in the local minimum solution. Most of the deterministic optimization techniques are designed to solve a particular class of optimization problem. On the other hand, stochastic optimization techniques such as evolutionary algorithms [127], simulated annealing [128] and particle swarm optimization [129] rely heavily on computational power. Among these, evolutionary algorithms are found to be very promising global optimizers. Evolutionary algorithms include three population based heuristic methodologies: genetic algorithms, evolutionary programming, and evolutionary strategies. Of these, genetic algorithms (GA) are perhaps the most frequently used evolutionary algorithms [130].

The genetic algorithm (GA) originally developed by Holland [52] is a simulation mechanism of Darwinian natural selection and a genetics computational model based on the biological evolutionary process. It is a process which involves searching for the optimal solution by simulating natural evolution. In GAs, an encoding scheme is first used to represent a point (individual) in the search of decision variables, and then each individual of the population is assigned a fitness based on certain criteria. In early implementations [53], the decision variables were encoded as strings of binary alphabets using ‘zero’ and ‘one’. The performance of binary GAs are found to be satisfactory on small and moderately sized problems requiring less precision in the solution, but for high dimensional problems in which a higher degree of precision is desired, binary GAs require huge computational time and memory [54]. To overcome these difficulties, real coded GAs, in which

decision variables are encoded as real numbers, are now widely used. It has been established that real coded GAs are superior to binary coded GAs for continuous optimization problems [55].

In geotechnical fields, optimizations combined with GA have been widely used to deal with different problems [17, 26, 58, 59, 131, 132]. Among these applications, the identification of soil parameters by GA has received the most attention [12, 13, 18, 133]. Numerous constitutive models have been developed with an increasing number of parameters. However, using these models could result in difficulties in parameter determination, although they can give a relatively accurate description of soil behavior. The determination of parameters has currently become a critical issue, as it can plays an important role in possible applications of a newly developed model. However, there is not much published literature related to the application of a real-coded GA to determine soil model parameters. Therefore, applying a real-coded GA to identify parameters may be appropriate and worth further investigation.

The aim of this Chapter has been to develop a new hybrid real-coded genetic algorithm (RCGA) to identify soil parameters under the framework of a classical GA by combining two recently developed and efficient crossover operators with a hybrid strategy. A dynamic random mutation has been incorporated into the new RCGA to maintain the diversity of the population. Additionally, in order to improve the convergence speed, a chaotic local search (CLS) has been adopted. The performance of the proposed RCGA was first evaluated and compared with other RCGAs in finding the minimum solution of six mathematical benchmark functions. The search ability and efficiency of the new hybrid RCGA was then further estimated by identifying soil parameters based on both laboratory tests and field tests. Finally, an effective and efficient optimization procedure using the new hybrid RCGA for the identification of parameters has been proposed.

3.2 New hybrid RCGA

3.2.1 Scope of the proposed RCGA

In this section, a new hybrid RCGA is proposed. A flow chart showing the new hybrid RCGA is plotted in Figure 3.1. where p_C, p_M and p_S are the probabilities at which ‘offspring’ are produced by ‘crossover1’, ‘mutation’ and ‘crossover2’, respectively.

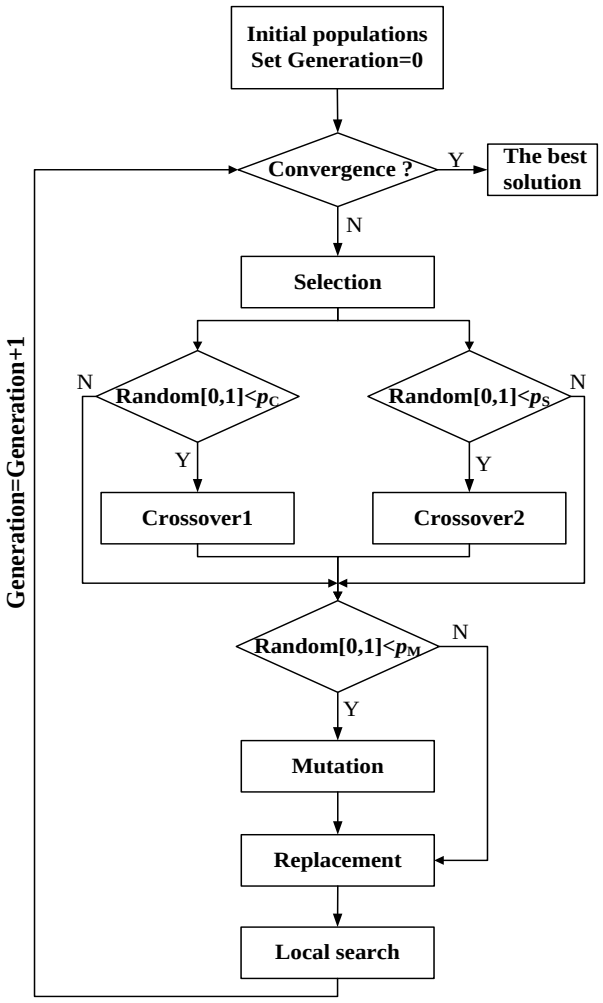

Figure 3.1 Flow chart of the proposed RCGA

First, the evolution process starts with a set of initial individuals which are randomly generated. Then the individuals are selected from the parent population using a tournament selection to perform the crossover and mutation, which is critical for maintaining the diversity of the population. The tournament selection is implemented for selecting the individuals to enter the mating pool, which has been demonstrated to perform well in RCGAs [134, 135]. In order to prevent the loss of diversity of the population, the chosen tournament size is two in the proposed algorithm.

In the new hybrid RCGA, a newly proposed hybrid strategy with two crossover operators is adopted to generate offspring. The selected crossover is determined by the probability of the crossover (p_C or p_S). In this hybrid RCGA, the Simulated Binary crossover (SBX) proposed by Deb and Agrawal [136] and the Simplex crossover (SPX) developed by Da Ronco and Benini [137] is adopted. The SBX is a conventional outstanding operator, with an ability that has been highlighted by Deb and Agrawal [136] and other researchers in the optimization fields. According to Da Ronco

and Benini [137], the experimental results with test functions used in their studies showed that SPX performed well on functions having multimodality and/or epistasis. Therefore, the search ability of the new RCGA can be improved by combining the advantages of each crossover operator.

In order to prevent the population to converge to a suboptimal solution, a newly developed mutation operator, the Dynamic Random Mutation (DRM), proposed by Chuang et al. [138], was adopted to enlarge population diversity in the new RCGA. The DRM mutation is a self-adaptive operator, which can improve the search efficiency of the proposed genetic algorithm.

Since the population size is kept constant, the selection of survivor from both parent and offspring populations is critical to preserve the current best found solution for subsequent evolution. Thus, the elitism strategy in NSGA-II proposed by Deb et al. [139] was implemented to perform the replacement process, which allows the parent and the offspring to compete after the crossover and mutation processes, ensuring better solutions.

Additionally, in order to increase the convergence speed, a chaotic local search (CLS) with a 'shrinking strategy' proposed by Jia et al. [92] was adopted. At the beginning of the evolution process, the diversity of the population is rich, so that the convergence speed can be accelerated easily if the CLS is applied. As the generation number increases, the population converges to an optimal solution more gradually, so it is more difficult to make the population progress to the optimal solution. Therefore, in order to save computational time, only 1/3 of the total number of generations from the beginning was used in the CLS.

The pseudo code of new hybrid RCGA is given below:

1. Begin
2. Set number of generation gen=0
3. Initialization, generating the initial population P (gen)
4. Evaluate the fitness of P (gen)
5. Check the criterion of convergence. If yes, stop; if no, continue.
6. Select m individuals from the P (gen) using tournament selection to perform crossover
7. If (rand<p_C), apply SBX crossover; else if, (rand <p_S), apply SPX crossover
9. Apply DRM mutation on population generated after crossover according to probability p_M and get the new children P'(gen)
10. Put P(gen) and P'(gen) to survive with elitism strategy, get new population P''(gen)

11. Apply the CLS conditionally on P''(gen), and update the best individual

12. Gen=gen+1, and P(gen+1)= P''(gen)

13. Back to step 5.

3.2.2 Main operators in the new hybrid RCGA

3.2.2.1 Simulated binary crossover (SBX)

This operator simulates the behavior of the single-point crossover operator on binary strings in the sense that common interval schemata between the parents are repeated in the offspring. It works for generating the components of the offspring as follows:

$$\begin{aligned} \xi_i &= 0.5\left[\left(1+\beta_i\right)x_i^1+\left(1-\beta_i\right)x_i^2\right] \\ \eta_i &= 0.5\left[\left(1-\beta_i\right)x_i^1+\left(1+\beta_i\right)x_i^2\right] \end{aligned} \tag{3-1}$$

with,

$$\beta_i=\begin{cases}\left(2u\right)^{\frac{1}{\eta+1}} & if\ u\le 0.5\\ \left(\dfrac{1}{2\left(1-u\right)}\right)^{\frac{1}{\eta+1}} & if\ u>0.5\end{cases} \tag{3-2}$$

where ξ_i and η_i are two offspring generated by SBX; β_i is spread factor; u is a uniformly distributed random variable within [0,1]; and x_i^1 and x_i^2 are two parents selected by the tournament to create the offspring. In this case, the value of η is set to 20, as recommended by Deb et al. [139]and Zitzler and Thiele [140].

3.2.2.2 Simplex crossover (SPX)

The offspring vector is formed as follows:

$$\xi_i=\left(1+Refl\right)\cdot \mathrm{M}-Refl\cdot x_i^2 \tag{3-3}$$

where M is the centroid of x_i^1, which can be calculated in the following manner:

$$\mathrm{M}=\left(\frac{1}{n}\right)\cdot x_i^1 \tag{3-4}$$

where x_i^1 and x_i^2 are two parents selected by the tournament to create the offspring. It is assumed that x_i^1 is the best fitness individual among the two chosen parents to form the offspring. The *Refl* coefficient is set as equal to a random number [0, 1], *n* is the number of the remaining individuals, after the worst one is excluded, and *n*=2 is employed, in this study, according to the test results conducted by Da Ronco and Benini [137].

3.2.2.3 Mutation operator

The DRM applies the mutation rule of,

$$x_i^* = x_i + s_m \Phi_0 \left(x_i^U - x_i^L \right) \tag{3-5}$$

where x_i^* is the offspring after the mutation; s_m is the mutation step size; and x_i^L and x_i^U are the lower and upper bounds of the variable in the chromosome. Φ_0 is a random perturbation vector in the *n*-dimensional cube $[-\phi_0,+\phi_0]^n$ of which ϕ_0 is a user-specified number chosen within the interval [0,1].

The step size was dynamically adjusted by the following update rule,

$$s_m = \left(1 - k / k_{\max}\right)^b \tag{3-6}$$

where the parameter $b>0$ is used to control the decay rate of s_m; and k and $k_{\max}$ denote the current generation number and the maximum number of generations, respectively. In this study, Φ_0=0.25 and *b*=2 are employed.

3.2.2.4 Chaotic Local Search (CLS)

The chaotic local search (CLS) with a 'shrinking strategy' proposed by Jia et al. [92] was adopted as follows,

$$x_i^{'t} = \left(1 - \lambda\right) x_i^t + \lambda \beta_c \tag{3-7}$$

where $x_i^{'t}$ is a new vector of individual x_i^t in *t* generation produced by the chaotic local search; β_c is generated by the equation $\beta_c = x_i^L + \beta_j^t \left(x_i^U - x_i^L \right)$; and λ is the shrinking scale given by:

$$\lambda = 1 - \left| \frac{FEs - 1}{FEs} \right|^{m} \tag{3-8}$$

where FEs are the current function evaluations; and *m* controls the shrinking speed. With higher m values, the shrinking speed is slower. In this study, the value of *m* was set at 1000, as suggested by Jia et al. [92].

β_j^t is a chaotic variable, which is obtained from the chaotic iteration. In this study, the logistic chaotic function was employed to construct a chaotic GA as follows:

$$\beta_j^{t+1} = \mu \beta_j^t \left(1 - \beta_j^t\right),\ t = 1,\ 2\ ,...;\ \beta_j \neq 0.25,\ 0.5 \text{ and } 0.75 \tag{3-9}$$

when μ=4, Eq.(3-9) reaches a complete chaotic state. Given β_j^1 an arbitrary initial value that is within the range of 0 to 1, but not equal to 0.25, 0.5 or 0.75, the chaos trajectory will finally search non-repeatedly any point within the range (0,1).

3.2.3 Performance of the new hybrid RCGA

To evaluate the performance of the proposed RCGA, six mathematical functions of different types were chosen as benchmark tests, which are usually used as benchmark tests to evaluate the performance of a new GA [141, 142]. Table 3.1 shows the selected benchmark tests with the optimum value corresponding to the best solution. In order to highlight the performance of the new RCGA, an extensive experimental study of various possible hybrid combinations of crossovers has been conducted. The other outstanding crossovers are Arithmetical Crossover (AC), Laplace Crossover (LX) and Bounded Exponential Crossover (BEX), which are described in Appendix I. Therefore, five different RCGAs have been defined and named as follows: AC+SPX+DRM, LX+SPX+DRM, BEX+SPX+DRM, SBX+SPX+DRM and SBX+SPX+DRM+Chaotic. For a fair comparison, the settings for each RCGA are the same except for the crossover, which has been changed according to a hybrid strategy. The settings for all the RCGAs are given in Table 3.2. In this study, six benchmark functions with 30 variables were adopted. The maximum number of generations was fixed at 100. For a uniform testing environment of all the RCGAs, the initial population size was taken to be ten times the number of decision variables. According to Poles et al. [143], using a well-distributed sampling can increase the robustness and avoid premature

convergence. Thus, the initial populations for all the RCGAs were generated by Sobol, which is a uniform random initialization method proposed by Sobol [28].

Table 3.1 Selected benchmark tests for evaluating the new GA

Test function	*x* domain	Optimum
1. Ackley's problem: $f_1 = -20\exp\left(-0.02\sqrt{\frac{1}{n}\sum_{i=1}^{n}x_i^2}\right) - \exp\left(\frac{1}{n}\sum_{i=1}^{n}\cos(2\pi x_i)\right) + 20 + e$	$-30 \le x_i \le 30$	$\min f(x^*) = 0$ with $x^* = (0,0,....,0)$
2. Exponential problem: $f_3 = -\left(\exp\left(-0.5\sum_{i=1}^{n}x_i^2\right)\right)$	$-1 \le x_i \le 1$	$\min f(x^*) = -1$ with $x^* = (0,0,....,0)$
3. Griewank problem $f_4 = 1 + \frac{1}{4000}\sum_{i=1}^{n}x_i^2 - \prod_{i=1}^{n}\cos\left(\frac{x_i}{\sqrt{i}}\right)$	$-600 \le x_i \le 600$	$\min f(x^*) = 0$ with $x^* = (0,0,....,0)$
4. Rosenbrock problem: $f_7 = \sum_{i=1}^{n-1}\left[100\left(x_{i+1} - x_i^2\right)^2 + (x_i - 1)^2\right]$	$-30 \le x_i \le 30$	$\min f(x^*) = 0$ with $x^* = (1,1,....,1)$
5. Schwefel problem: $f_8 = -\sum_{i=1}^{n}x_i \sin\left(\sqrt{\lvert x_i\rvert}\right) + 418.98288n$	$-500 \le x_i \le 500$	$\min f(x^*) = 0$ with $x^* = (420.98, 420.98, ..., 420.98)$
6. De-Jong's function with noise $f_{10} = \sum_{i=1}^{n}\left(x_i^4 + rand(0,1)\right)$	$-10 \le x_i \le 10$	$\min f(x^*) = 0$ with $x^* = (0,0,....,0)$

The performance of a GA is usually measured on the basis of two criteria, efficiency and accuracy. The efficiency of a GA is a measure of the rate of convergence, and the accuracy indicates the degree of precision in locating global minima. Figure 3.2 shows the evolution of the minimum objective value as the generation number increases. As shown in Figure 3.2, for RCGAs without local search, SBX+SPX+DRM performs well on problems 1, 3, 4 and 5, which indicates that SBX+SPX+DRM has an outstanding ability in tackling complex problems; BEX+SPX+DRM performs well on problem 2, and AC+SPX+DRM performs well on problem 6. For problems 2 and 6, although the performance of SBX+SPX+DRM is not the best, the difference in performance between SBX+SPX+DRM and the best RCGA is relatively small and can be regarded as the same. Therefore,

it can be seen that SBX+SPX+DRM has excellent search ability in detecting the optimal solution and a relatively faster convergence speed for various complex problems.

Table 3.2 Parameter settings for the five RCGAs

RCGA	Crossover (Probability)	Mutation (Probability)	CLS	Tournament size	Elitism
AC+SPX+DRM	AC (0.9)+SPX (0.5)	DRM (0.05)	NO	2	YES
LX+SPX+DRM	LX (0.9)+SPX (0.5)	DRM (0.05)	NO	2	YES
BEX+SPX+DRM	BEX(0.9)+SPX (0.5)	DRM (0.05)	NO	2	YES
SBX+SPX+DRM	SBX (0.9)+SPX (0.5)	DRM (0.05)	NO	2	YES
SBX+SPX+DRM+Chaotic	SBX (0.9)+SPX (0.5)	DRM (0.05)	YES	2	YES

However, the convergence speed of SBX+SPX+DRM does not satisfy all the benchmark tests. In order to improve the convergence speed, but without consuming much more computational time, a chaotic local search (CLS) was added to enhance the performance of SBX+SPX+DRM, and the resulting RCGA is referred to as SBX+SPX+DRM+Chaotic. The CLS was only applied at the 30th generation from the beginning. As shown in Figure 3.2, compared to SBX+SPX+DRM, the convergence speed was improved significantly by using the chaotic local search. For problems 4, 5 and 6, not only the convergence speed but also the accuracy of the optimal solution was further enhanced. All the comparisons demonstrate that the effectiveness of the CLS in accelerating convergence speed is excellent and should be adopted in the RCGAs.

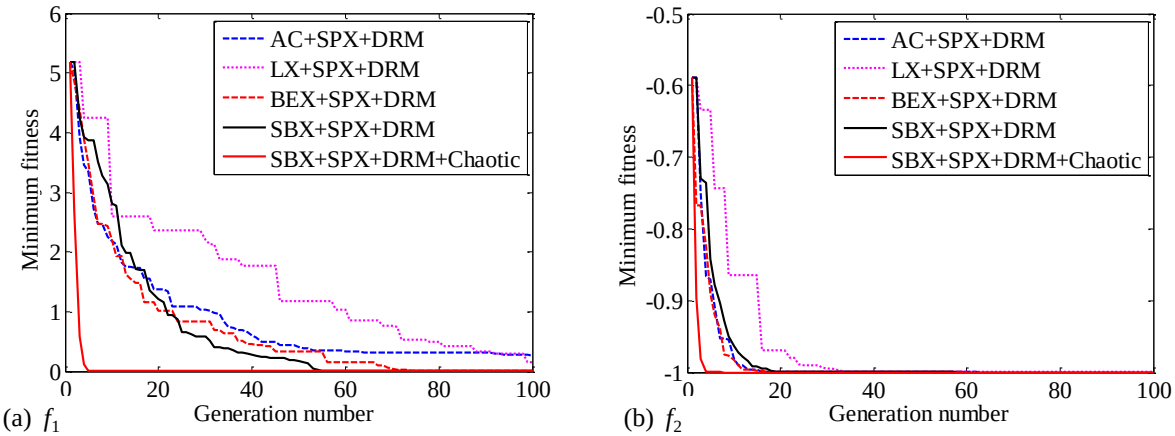

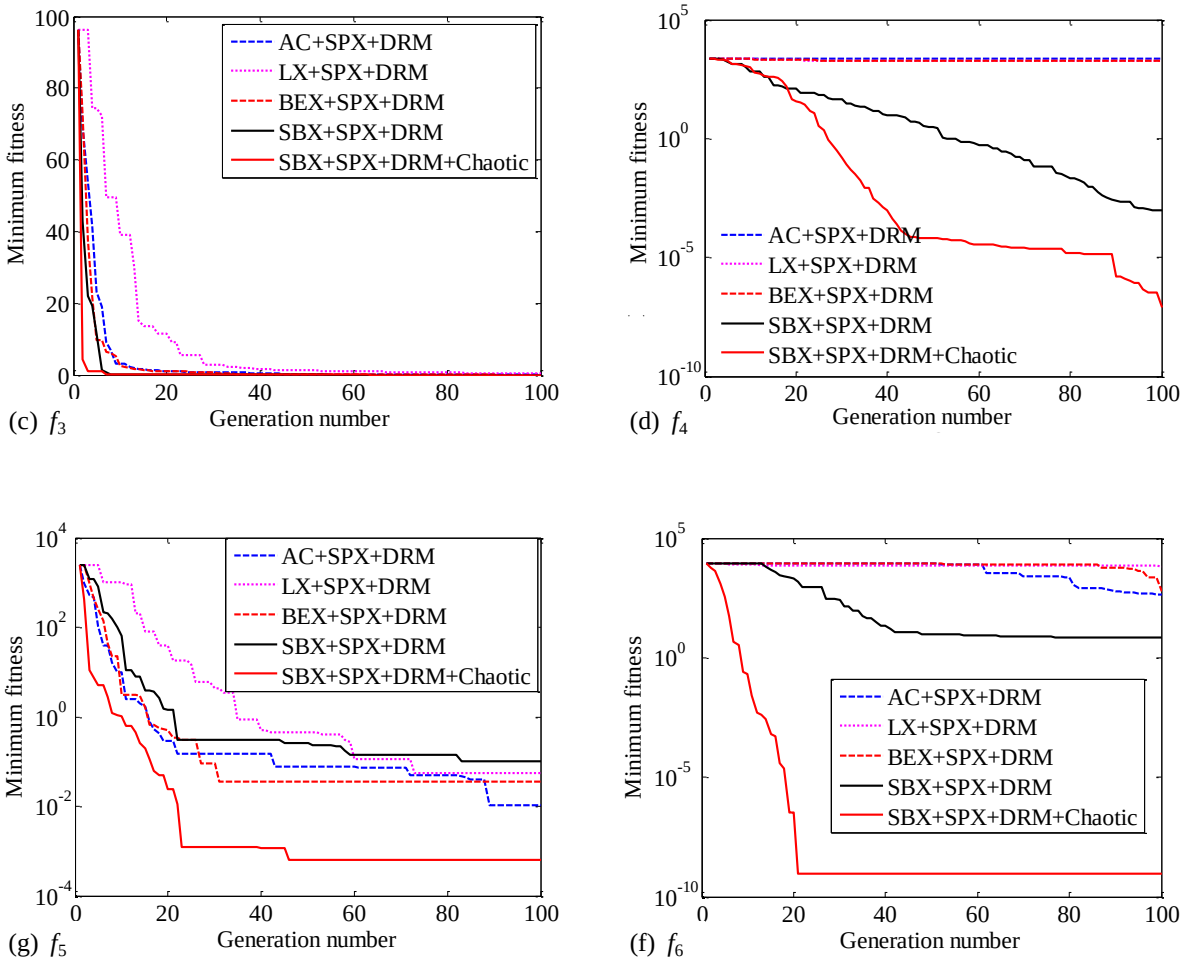

Figure 3.2 Comparisons of performance between six RCGAs for different benchmark tests

Overall, the results demonstrate that the proposed hybrid RCGA (SBX+SPX+DRM+Chaotic) has an outstanding search ability, and the efficiency and accuracy of the proposed RCGA are ideal for tackling different problems.

3.3 Applications in the identification of soil parameters

For further examining the ability of the proposed RCGA, the proposed hybrid RCGA has been applied to solve the problem of parameter identification.

3.3.1 Identification methodology

The aim of an optimization is to find values for the model parameters that provide the best attainable fit between model predictions and corresponding observations. For this purpose, the error

function is required, which is defined as follows, with 'Error' based on the least square method as introduced by Levasseur et al. [13]:

$$\mathrm{Error}(x)=\sqrt{\frac{\sum_{i=1}^{N}\left(\frac{U_{\exp}^{i}-U_{num}^{i}}{U_{\exp}^{i}}\times 100\right)^{2}}{N}}\% \tag{3-10}$$

where x is a vector of parameters; N is the number of values; $U_{\exp}^{i}$ is the value of measurement point i; U_{num}^{i} is the value at point i. The scale effects on the fit between the experimental and the simulated results can be eliminated by this normalized formulation. Additionally, the objective error calculated by this function is a dimensionless variable; thus, the difference in error can be avoided for different objectives.

Generally, deformation and strength are two extremely important indicators for showing the mechanical behavior of soil. In a laboratory triaxial test, the isotropic or anisotropic compression test is conducted first, followed by the shear stage. During the whole process, the model parameters accounting for compression and shear behaviors are measured and obtained. For field tests, such as the pressuremeter test, cone penetration test or vane shear test, the test results are usually displayed in the form of the displacement-pressure curve. The soil behavior (softening or hardening, contraction or dilation) are also implied in these curves, although some parameters related behavior cannot be directly measured. In other words, the results of selected tests can provide information to optimise the model parameters. Therefore, in this study, a mono-objective framework was considered, which includes two objectives regarding the strength and deformation of soil, respectively:

$$\min\left[\mathrm{Error}(x)\right]=\begin{bmatrix}\mathrm{Error}(q)\\ \mathrm{Error}(e)\text{ or }\mathrm{Error}(\Delta u)\end{bmatrix} \tag{3-11}$$

where Error(q) is the difference between the deviatoric stress from the simulations and that in the objectives; Error(e) is the difference between the void ratio from the simulations and that in the objectives for the drained tests; and Error(Δu) is the difference between the excess pore pressure from the simulations and that in the objectives for the undrained tests

Figure 1.8 shows the identification procedure based on the successive use of two different codes: the code for the integration of the constitutive model is written in the FORTRAN language and the

code for the optimization process is written in the MATLAB language. To demonstrate cases in more general, some relatively simple constitutive models were adopted.

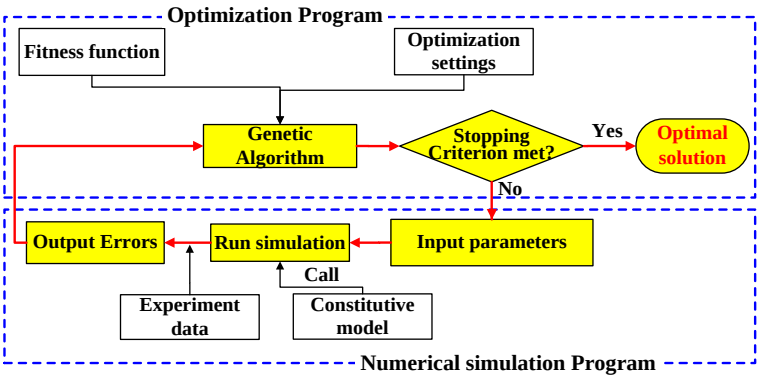

Figure 3.3 Identification procedure

3.3.2 Identifying parameters from laboratory testing

(1) For sand

The parameter identification for the sand using the RCGA was performed first. A Mohr-Coulomb-like model with nonlinear elasticity and plastic hardening (NLMC), similar to the Soil Hardening model proposed by Schanz et al. [144] in PLAXIS, was developed to simulate the objective tests. The constitutive equations are shown in Table 3.3. For the NLMC model, the Young's modulus is expressed as follows, according to Richart et al. [145]:

$$E = E_0 \cdot p_{at} \frac{(2.97-e)^2}{(1+e)} \left(\frac{p'}{p_{at}} \right)^{\zeta} \tag{3-12}$$

where E_0 is the reference value of the Young's modulus; e is the void ratio; p' is the mean effective stress; p_{at} is the atmospheric pressure used as reference pressure (p_{at} = 101.325 kPa); and ζ is a constant.

The NLMC model has six parameters (1) elastic parameters: E_0 and ζ, which can be obtained from isotropic compression tests; and (2) plastic parameters: plastic modulus, k_p, friction angle, ϕ, dilatancy angle, ψ and cohesion, c. Generally, a typical value of Poisson's ratio, υ=0.2 is assumed for the sand. All the parameters were then identified using the optimization method with the new hybrid RCGA from selected objective tests. The search domain and intervals of these parameters are

given in Table 3.4 and are much larger than those corresponding to typical values. The initial population for the RCGA was generated in SOBOL within the search domain.

Table 3.3 Constitutive relations of selected soil models

Models	NLMC	MCC
Elasticity	$\dot{\varepsilon}_{ij}^{e}=\frac{1+\upsilon}{E}\sigma_{ij}'-\frac{\upsilon}{E}\sigma_{kk}'\delta_{ij}$	
Yield function	$f=\frac{q}{p'}-H=0$	$f=\frac{q^2}{M^2}+p'\left(p'-p_c\right)=0$
Potential function	$\frac{\partial g}{\partial p'}=M_{pt}-\frac{q}{p'}$ with $\frac{\partial g}{\partial q}=1$ $M_{pt}=\frac{6\sin\phi_{pt}}{3-\sin\phi_{pt}}$ with $\phi_{pt}=\phi_{\mu}-\psi$	$g=f$
Hardening law	$H=\frac{M\varepsilon_d^p}{k_p+\varepsilon_d^p}$ with $M=\frac{6\sin\phi_{\mu}}{3-\sin\phi_{\mu}}$	$dp_c=p_c\left(\frac{1+e_0}{\lambda-\kappa}\right)d\varepsilon_v^p$
Number of parameters	6	5

Table 3.4 Search domain and intervals of parameters for NLMC and MCC

Model	NLMC					MCC			
Parameters	E_0	n	k_p	$\phi/^\circ$	$\psi/^\circ$	κ	λ	M	p'_{c0} /kPa
Lower bound	10	0.1	10^{-5}	10	0	10^{-4}	10^{-3}	0.5	10
Upper bound	500	1.0	0.1	50	20	0.1	0.5	2.0	200
Step	1.0	0.01	10^{-5}	0.1	0.1	10^{-4}	10^{-3}	0.01	0.5

A series of standard drained triaxial compression tests [146] with an isotropic compression test [147] performed on Fontainebleau sand were selected as the objective tests during the optimization process. All the tests were isotropically consolidated to the corresponding consolidation pressure before shearing. The experimental results for these drained triaxial tests are shown in Figure 3.4. Note that the cohesion, *c*, is taken equal to be zero, as dry Fontainebleau sand was used in the test. Thus two elastic parameters together with other plastic related parameters formed one set of model parameters, which were used to simulate objective tests during the optimization process.

Following the proposed identification procedure, optimization involving the NLMC model was performed using the proposed hybrid RCGA. The optimization was performed many times following the new GA with different set values in order to select the best result. The optimal set of parameters

obtained using the NLMC model corresponding to Fontainebleau sand is shown in Table 3.5. Figure 3.5 shows the simulation results for Fontainebleau sand from the NLMC model when the optimal parameters are used. However, comparisons between simulated and experimental results indicate that the new hybrid RCGA has the ability to detect the optimal parameters. Note that due to the limitations of the NLMC model, e.g., disregarding the interlocking effect [148-151], the strain softening behavior cannot be reproduced.

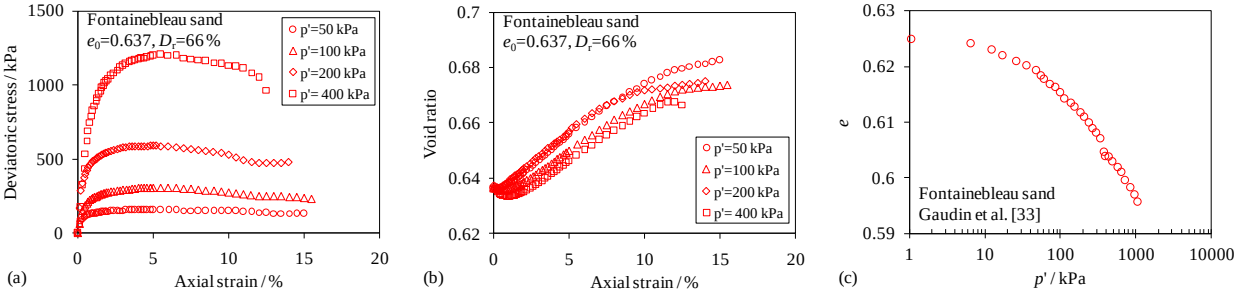

Figure 3.4 Results of drained triaxial tests on Fontainebleau sand: (a) deviatoric stress versus axial strain; (b) void ratio versus axial strain; (c) isotropic compression test

Table 3.5 Optimal sets of parameters for NLMC for Fontainebleau sand

Parameters	E_0	n	k_p	ϕ_μ / °	ψ / °
Values	180	0.55	0.00031	36.4	5.9

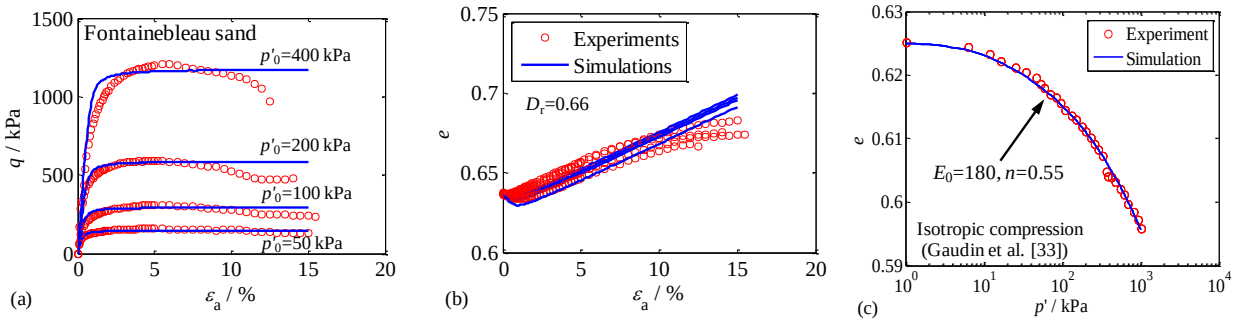

Figure 3.5 Simulation results based on optimal parameters for Fontainebleau sand: (a) deviatoric stress versus axial strain; (b) void ratio versus axial strain; (c) isotropic compression test

(2) For clay

As previously described, the new RCGA can succeed in identifying the model parameters for sand. In order to show the ability of the new RCGA in identifying soil parameters for clay, the widely

used Modified Cam Clay (MCC) model developed by Roscoe and Burland [152] and a series of tests on natural Shanghai clay conducted by Sheng [153] were selected.

Three drained compression triaxial tests and one oedometer test performed on Shanghai clay were selected as the objective to identify basic MCC parameters, as shown in Figure 3.6. Thus, in this case, a mono-objective framework with three different criteria is considered. A typical value of Poisson's ratio, υ=0.25 for Shanghai clay can be assumed. Thus, there are four parameters: swelling index, κ, compression index, λ, the slope of critical state line, M and the size of yield surface p'_{c0}, which need to be determined by an optimization method with the new hybrid RCGA. The search domain and intervals of these parameters are given in Table 3.4, and they are much larger than those corresponding to typical values.

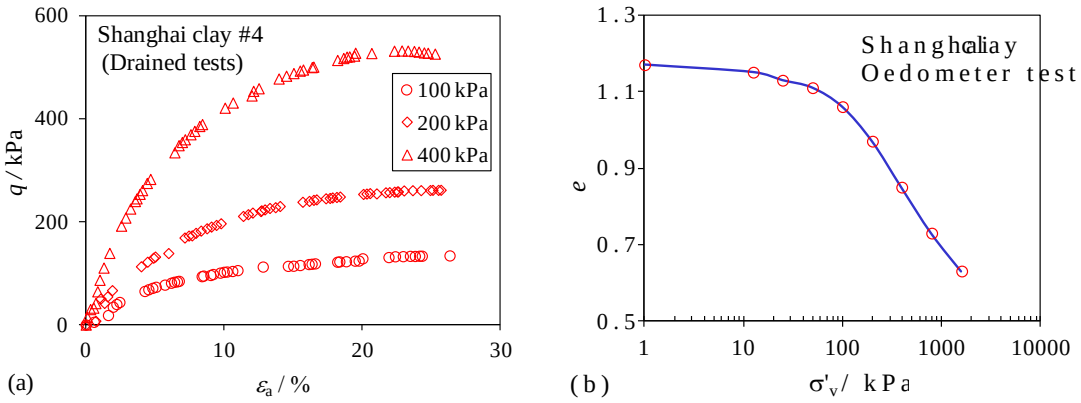

Figure 3.6 Results of Shanghai clay: (a) stress-strain of drained triaxial test; (b) oedometer test

The same optimization procedure as that used for the NLMC model was conducted again. The optimal parameters of the MCC model are presented in Table 3.6. All the optimal parameters are in a reasonable range and were obtained from the experimental measurements made by Sheng [153]. Using the optimal parameters, objective tests were simulated in the MCC model, as shown in Figure 3.7. The best fit between experiments and simulations by MCC model was detected. The big difference in volumetric strain is due to the limitation of the model in which the location of the critical state line in e-log p' plane is fixed and not suitable for a given clay [154], or for a lack of considering anisotropy, destructuration or time effect [155-160]. Therefore, all the comparisons between simulated and experimental results demonstrate that the optimal parameters from the MCC model corresponding to Shanghai clay detected by the hybrid RCGA are reasonable. Furthermore, this also demonstrates that the new hybrid RCGA performs well in identifying clay model parameters.

Table 3.6 Optimal sets of parameters of MCC for Shanghai soft clay

Parameters	κ	λ	M	p'_{c0} /kPa
Value	0.032	0.171	1.34	100

Overall, for the identification of parameters based on the laboratory tests, the proposed hybrid RCGA shows the strong and stable search ability for different constitutive models with various numbers of model parameters. Moreover, the parameters obtained from the optimization with the proposed hybrid RCGA are reliable and reasonable, which demonstrates that the optimization procedure is feasible and can be adopted as a tool in engineering practice.

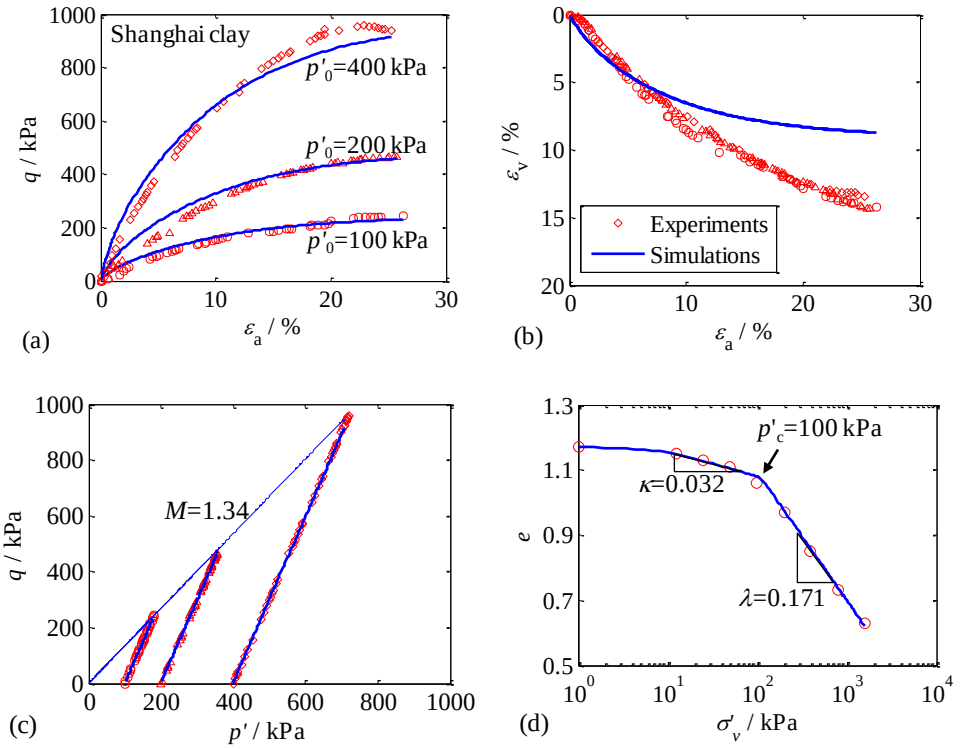

Figure 3.7 Simulation results based on optimal parameters for Shanghai clay: (a) deviatoric stress versus axial strain; (b) void ratio versus axial strain; (c) stress path; (d) oedometer test

3.3.3 Parameter identification based on field tests

The same identifications in the PMT and in the excavation used in chapter 2 were conducted again using the proposed algorithm. Table 3.7 shows the optimization results and Figure 3.8 shows the minimization process with increasing generation numbers, compared with other optimization

methods. It can be seen that the preset solution is finally found by the proposed algorithm with a faster convergence speed, which demonstrates the high performance of the proposed algorithm.

Table 3.7 Optimal parameters for different optimization methods with objective error and number of evaluations corresponding to convergence

Case	E /kPa	ϕ' / °	ψ / °(ν)	c / kPa	Objective error	Number of evaluations to convergence
PMT	30000	35.0	5.0	5.0	0.0	1111
Excavation	30000	35.0	0.3	5.0	0.0	661

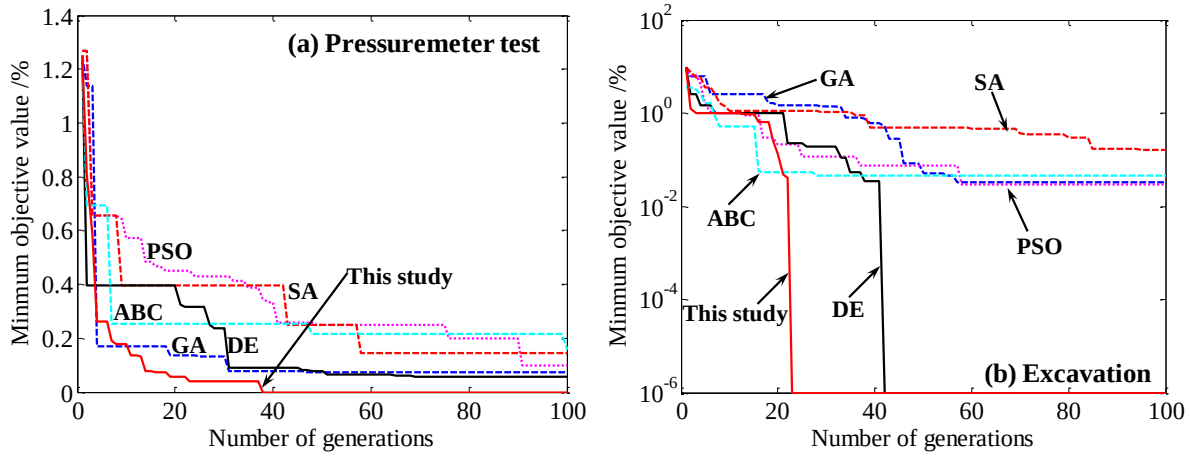

Figure 3.8 Minimization process in identifying parameters for all selected optimization methods (a) PMT; (b) excavation

3.4 Conclusions

A new combined hybrid real-coded genetic algorithm has been developed in this study. In this RCGA, a hybrid strategy was adopted by using two outstanding crossovers: the Simulated Binary crossover (SBX) and the Simplex crossover (SPX). A newly developed mutation operator, the Dynamic Random Mutation (DRM), was adopted to maintain the diversity of the population. Additionally, in order to accelerate the convergence speed, a newly developed chaotic local search (CLS) was applied conditionally.

The performance of the new RCGA was then first estimated in comparison with other hybrid RCGAs, which has the same hybrid strategy but with different crossovers. Six mathematical functions were selected as the benchmark to evaluate the performance of these RCGAs. The results

of all the benchmark tests demonstrate that the SBX+SPX+DRM algorithm has the best performance among these RCGAs without local search. In addition, when applying the chaotic local search in the SBX+SPX+DRM algorithm, all the optimization results were largely improved. All the results demonstrate that combining SBX+SPX+DRM+Chaotic can produce a better performance than the other RCGAs.

The performance of the proposed RCGA was then further evaluated by applying the RCGA to inverse analysis in identifying soil parameters based on laboratory tests. Three drained triaxial tests performed on the Fontainebleau sand were used to identify the parameters of a nonlinear Mohr-Coulomb model, and three drained triaxial tests with an oedometer test performed on natural Shanghai clay were selected as the objective tests to identify the parameters of the Modified Cam-Clay model. The optimization results demonstrate that the proposed RCGA has the ability to detect reliable and reasonable model parameters.

Finally, an inverse analysis of pressuremeter tests (PMT) was adopted to estimate the performance of the new hybrid RCGA. Two PMTs at different depths below the subsoil were simulated using the Mohr-Coulomb model. The optimal parameters were compared to those obtained from MOGA-II. The comparisons demonstrate that the parameters obtained using the new RCGA are more reasonable. In terms of the convergence speed, the new RCGA performed better than MOGA-II. Both aspects indicate that the performance of the proposed hybrid RCGA for this problem is better than MOGA-II.

Based on all the results, the proposed RCGA is recommended for conducting an inverse analysis to identify soil parameters. In the future, the proposed RCGA could be applied to various boundary value problems

Chapter 4 EPR-based prediction approach by optimization methods

4.1 Introduction

Over the last decades, soft computing techniques have been developed rapidly, and applied to different complicated engineering problems [161-164]. Among these techniques, the evolutionary polynomial regression (EPR) has been attracted more attention due to its more powerful ability in finding the target expression rather than the ability of artificial neural networks (ANNs) and genetic programming (GP) [165-167].

More recently, the EPR has been increasingly adopted in the field of geotechnical engineering and has been proved to be successful, for example in evaluating the liquefaction potential based on cone penetration test (CPT) results [167], assessing the earthquake-induced soil liquefaction and the lateral displacement [168], predicting the total sediment load of rivers [169], modeling the permeability and compaction characteristics of soils [170-172], evaluating the axial bearing capacity of piles [162, 173, 174], predicting the uplift capacity of suction caissons [161], modeling the soil behavior and applying in the finite elements analysis [175-177], predicting the stability of soil and rock slopes [178-180], etc. However, the application of EPR to evaluate the compressibility of soils has not been reported so far. Note that the compression index is extremely important in calculating the settlement of foundation, high accuracy of the correlation formulation is therefore needed. The EPR is recommended for improving current empirical equations for clay compressibility.

The best form of the EPR equation is usually acquired by means of a genetic algorithm (GA) over the values in the user defined vector of exponents. Thus, in order to improve the performance of EPR, it is necessary to find a GA with high ability for searching symbolic structures. The traditional GAs encoded as the binary strings were commonly used to conduct the search procedure in the EPR [181]. The performances of binary GAs are found to be satisfactory on small and moderately sized problems which do not require as much precision in the solution. But for high dimensional problems in which a high degree of precision is desired, binary GAs require huge computational time and memory [54, 141, 142]. To overcome these difficulties, real-coded GAs, in which the decision variables are encoded as real numbers, can be adopted. In other words, real-coded GAs are superior to binary coded GAs for continuous optimization problems [55]. However, this powerful tool has rarely been used to improve the performance of EPR. Thus, the EPR employing a high efficient

RCGA to search the best form of target expression is highly advised.

The aim of this chapter has been to propose an efficient RCGA to be applied to the EPR procedure for improving the performance of modeling the compression index of clays. First, a hybrid RCGA is proposed involving three different outstanding crossover operators under a new hybrid strategy. A self-adaptive mutation is also adopted in the proposed RCGA to improve the search efficiency. Then, the new RCGA is applied to propose an efficient EPR procedure in modeling the compression index with physical properties of remolded clays. Besides, three other excellent optimization algorithms are also respectively applied in EPR procedure for the same case to highlight the performance of the new RCGA in EPR.

4.2 Adopted hybrid RCGA

4.2.1 Basic scope of adopted RCGA

Due to the good performance of RCGA for solving the continuous problems, the enhanced RCGA proposed in the chapter 3 was employed to conduct the optimization in the EPR. The evolution of the proposed hybrid RCGA is similar to that of the GA proposed by Yamamoto and Inoue [182]. The main genetic operators used in the enhanced RCGA are selection, crossover, mutation, and replacement. First, the tournament selection was implemented for selecting the individuals to the mating pool, which has been successfully validated in RCGAs [134, 135]. In order to keep the diversity loss to the minimum, the tournament size was chosen as two in the proposed algorithm.

4.3 EPR procedure using RCGA

The evolutionary polynomial regression (EPR) is a data-driven method based on evolutionary computing, aimed to search for polynomial structures representing a system, first introduced by Giustolisi and Savic [181], with applications in hydroinformatics and environment related problems. A general EPR expression can be mathematically formulated as:

$$y = \sum_{j=1}^{m} F\left(\mathbf{X}, f\left(\mathbf{X}\right), a_j\right) + a_0 \tag{4-1}$$

where y is the estimated vector of output of the process; a_0 is an optional bias; a_j is an adjustable parameter for the jth term; F is a function constructed by the process; $\mathbf{X}$ is the matrix of input

variables; *f* is a function defined by the user; and *m* is the number of terms of the target expression.

According to Giustolisi and Savic [181], the first step in identifying the model structure is to transfer Eq.(4-1) to the following vector form:

$$\mathbf{Y}_{N\times 1}(\boldsymbol{\theta},\mathbf{Z}) = \left[\mathbf{I}_{N\times 1} \quad \mathbf{Z}^{j}_{N\times m}\right]\times\left[a_0 \quad a_1 \quad ... \quad a_m\right]^{\mathrm{T}} = \mathbf{Z}_{N\times d}\times\boldsymbol{\theta}^{\mathrm{T}}_{d\times 1} \tag{4-2}$$

where $\mathbf{Y}_{N\times 1}(\boldsymbol{\theta},\mathbf{Z})$ is the least-squares (LS) estimator vector of *N* target values; $\boldsymbol{\theta}_{d\times 1}$ is the vector of *d* (= *m*+1) parameters a_j and a_0 ($\boldsymbol{\theta}^{\mathrm{T}}$ is the transposed vector); and $\mathbf{Z}_{N\times d}$ is a matrix formed by **I** (unitary vector) for bias a_0, and *m* vectors of variables $\mathbf{Z}^{j}$. More details about the EPR can be found in Giustolisi and Savic [181].

Figure 4.1 shows the typical flow chart for the EPR procedure [181]. The general functional structure represented by $f(\mathbf{X}, a_j)$ in Eq.(4-1) is constructed from elementary functions by EPR using a GA strategy. In this study, the proposed RCGA is employed to select the useful input vectors from **X** to formulate the EPR. The building blocks (elements) of the structure are defined by the user based on understanding the physical process. The selection of feasible structures to be combined is an evolutionary process, whereas the parameters a_{j} in Eq.(4-2) are estimated by the least squares method.

For the RCGA process, a fitness function is necessary for directing the search to the best solution. In order to determine an optimal model corresponding to the smallest prediction error for training data, the sum of squared errors (SSE) was used to during the search towards the best-fit model:

$$\mathrm{SSE} = \frac{1}{N}\sum_{i=1}^{N}\left(\mathbf{Y}_{\mathrm{a}}\text{-}\mathbf{Y}_{\mathrm{p}}\right)^2 \tag{4-3}$$

where $\mathbf{Y}_{\mathrm{a}}$ are target values in the training data set and $\mathbf{Y}_{\mathrm{p}}$ are model predictions computed by using the polynomial expression obtained by EPR.

Note that the part “RCGA tool” in Figure 4.1 can also be replaced by other optimization methods to perform the EPR procedure.

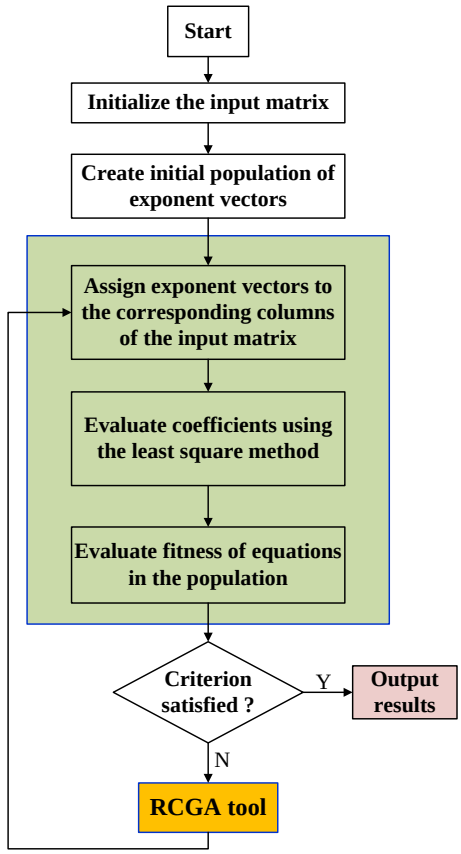

Figure 4.1 Typical flow chart for the EPR procedure using RCGA (after Giustolisi and Savic [181])

4.4 EPR-based modeling of compression index

In this section, the procedure for the formulation of correlation between the compression index and physical properties of remolded clays is presented using the EPR and the proposed RCGA. Furthermore, the performance of RCGA is also examined for the same case by compared to the use of three other excellent optimization algorithms.

4.4.1 Database

Compressibility is one of the important mechanical properties of clay. To obtain the compression index, an efficient and convenient way would be highly useful for geotechnical engineers. According to previous studies, the compression index of remolded clays was correlated with a number of physical properties of clays, such as the natural water content w_n, the initial void ratio e_0, the void ratio at liquid limit e_L, the specific gravity G_s, the activity A, the liquid limit w_L, the plastic limit w_P, the plastic index I_P and the shrinkage index I_S, etc., as summarized in Table 4.1. All

data from these references were assembled and used in the proposed EPR procedure. In order to obtain a correlation formulation which is suitable for all remolded clayey soils, the database must cover a sufficiently wide range of clays. In order to assess the adequacy of the database, certain indicators were determined, such as the statistics of variables summarized in Table 4.2, the plasticity chart of all selected data in Figure 4.2, and the histogram of some important variables in Figure 4.3.

Table 4.1 Some formulations of correlation for the compression index C_c of remolded soils

Formulations	References
$C_c = 0.007(w_L - 10)$	Skempton and Jones [183]
$C_c = 0.5 I_P G_s$	Wroth and Wood [184]
$C_c = 0.2237 e_L$	Nagaraj and Murthy [185]
$C_c = 0.329\left[0.027(w - w_P) + 0.0133 I_P\left(1.192 + A^{-1}\right)\right]$	Carrier III [186]
$C_c = 0.2343 e_L$	Nagaraj and Murthy [187]
$C_c = 0.256 e_L - 0.04$	Burland [188]
$C_c = 0.014(I_P + 3.6)$ $C_c = 0.007(I_s + 18)$	Sridharan and Nagaraj [189]
$C_c = 0.015 I_P - 0.0198$	Nath and DeDalal [190]

Remarks: C_c is compression index; w is water content; w_L is liquid limit; I_p is plastic limit; I_s is shrink limit; G_s is specific gravity; e_L is void ratio corresponding to liquid limit. A is activity of soil.

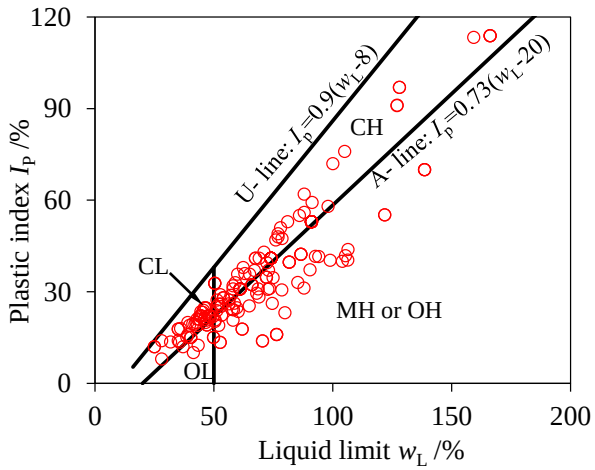

Figure 4.2 Classification of soils by liquid limit and plasticity index

Table 4.2 Statistics of variables used in the database

Soil type	Sample number	Variable	Maximum	Minimum	Mean	Standard deviation
OL	7	e_0	1.859	0.995	1.340	0.304
		w_L	49.8	37.0	45.1	4.8
		I_P	19.1	10.1	14.7	3.5
		C_c	0.309	0.182	0.240	0.041
CL	45	e_0	2.056	0.676	1.275	0.356
		w_L	49.6	25.0	41.5	6.4
		I_P	24.8	8.0	19.3	3.99
		C_c	0.421	0.120	0.277	0.064
CH	90	e_0	4.570	0.896	2.428	0.906
		w_L	166.2	50.4	78.1	26.0
		I_P	113.9	23.9	46.6	21.2
		C_c	1.340	0.230	0.542	0.218
MH or OH	58	e_0	4.643	1.377	2.523	0.786
		w_L	138.6	50.4	78.6	22.1
		I_P	70.0	13.4	32.4	13.4
		C_c	1.004	0.191	0.491	0.239

Remarks: w_L and I_P are in percent; OL is low plastic inorganic or organic silty clays; CL is low plastic inorganic clays, sandy and silty clays; CH is high plastic inorganic clays; and OH is high plastic organic clays.

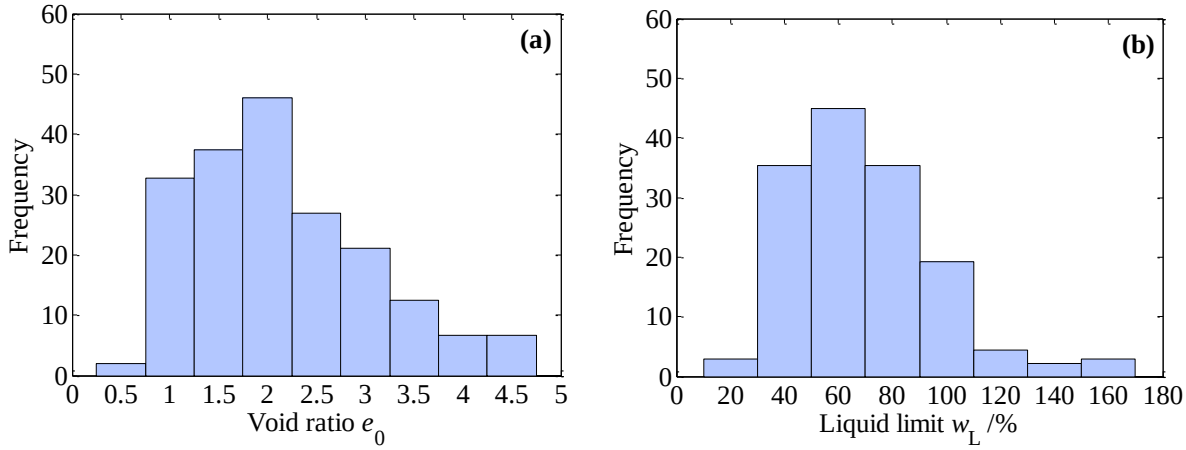

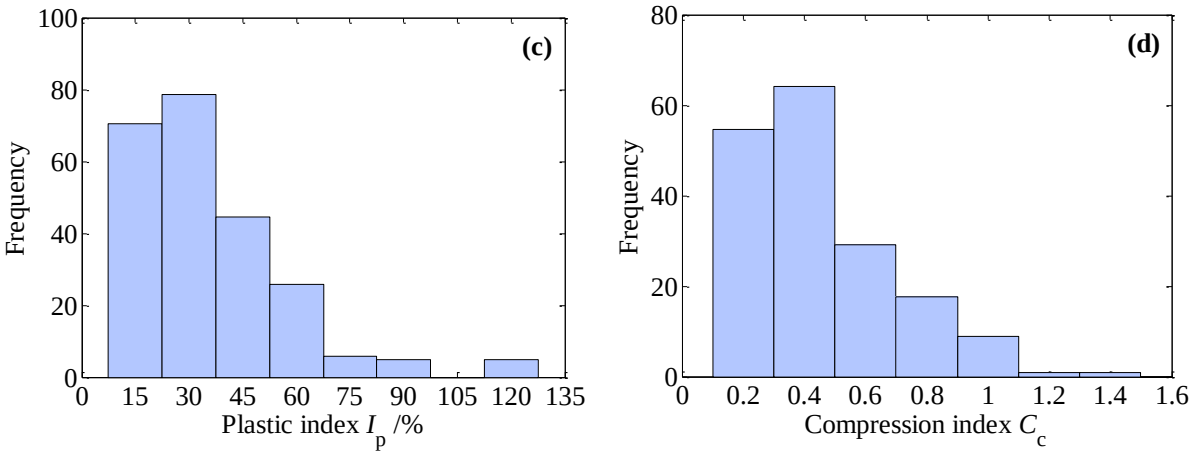

Figure 4.3 Histograms of variables in the database

Table 4.3 Correlations involving two and three variables by regression analysis

Combined variables	Correlations	R^2
e_0, w_L	$C_c = -0.0888 + 0.1388e_0 + 0.3573w_L$	0.80
e_0, I_p	$C_c = -0.0402 + 0.1515e_0 + 0.4834I_p$	0.82
w_L, I_p	$C_c = -0.0133 + 0.5436w_L + 0.2718I_p$	0.74
e_0, w_L, I_p	$C_c = -0.0362 + 0.1538e_0 - 0.0256w_L + 0.5079I_p$	0.83

Remark: the w_L and I_P are in real number, not in percent.

Similar to Table 4.1, the basic regression analyses were first investigated between C_c and e_0, w_L or I_p for single, two and three combined parameters. All the regression equations are summarized in Table 4.3 and all the comparisons are plotted in Figure 4.4 and Figure 4.5. For a single parameter, the C_c is relatively well correlated with e_0, and followed by w_L. However, all these basic regressions do not seem satisfying in terms of accuracy (R^2 <0.8). For two combined parameters, the correlation coefficient is increased to 0.82. Note that the combination w_L and I_p gives R^2<0.8, which reveals the importance of e_0 during the single parameter analysis. For three combined parameters, the correlation coefficient is only increased slightly to 0.83. Since a high correlation performance is always required in geotechnical design, the genetic optimization and EPR based correlation method should be a good choice and worth the attempt.

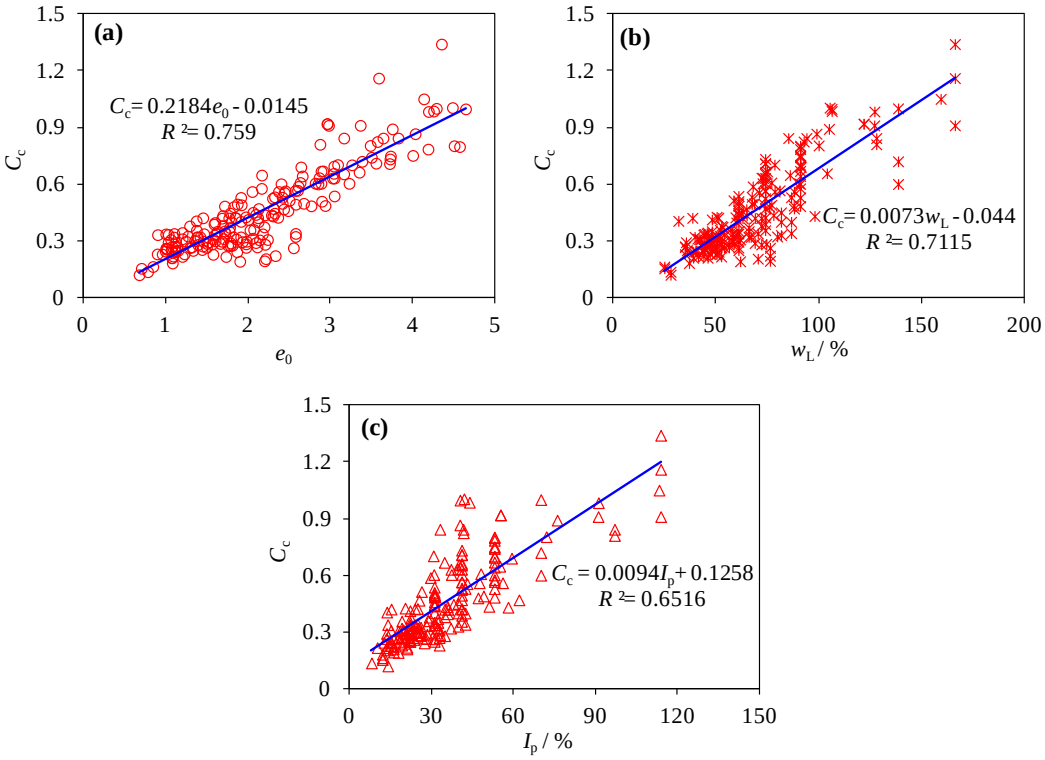

Figure 4.4 Correlations between C_c and (a) e_0, (b) w_L, (c) Ip and C_c

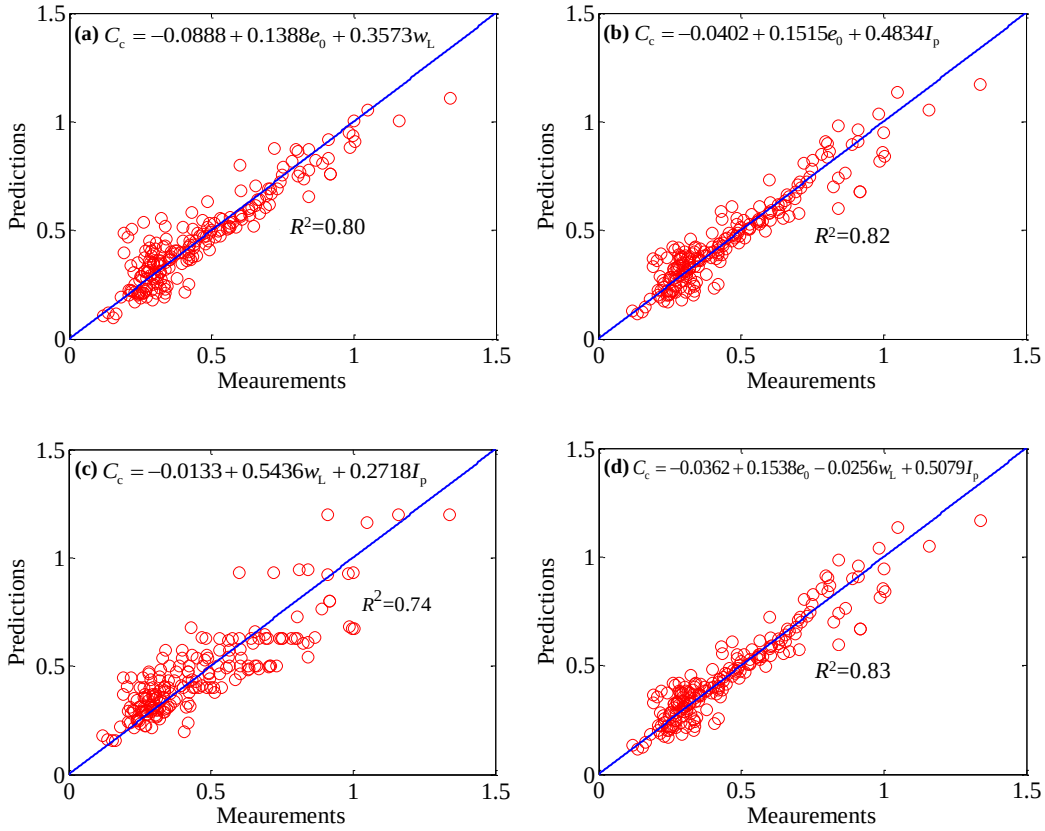

Figure 4.5 Correlations involving two and three variables by regression analysis

4.4.2 EPR-based modeling

Based on the equations shown in Table 4.1, the initial void ratio e_0, liquid limit w_L and plastic index I_P are the most common properties selected as the correlating variables. Then, these three properties were selected to provide a general structure of expression in this study:

$$C_c = f\left(e_0, w_L, I_P\right) + a_0 \tag{4-4}$$

where C_c is the compression index in e-log p' plane; e_0 is the initial void ratio; w_L is the liquid limit; I_P is the plastic index; a_0 is a constant.

More precisely, half the measurements from Table 4.1 were randomly selected as training results, with the rest for testing results. For the simplicity of the EPR expressions, all the exponents were constrained to [-2, 2] with a step size of 1. Also, the maximum number of terms of the target expression in Eq.(1) was set to 8, which was sufficiently for this case. Note that the data used cover a wide range of soil classification shown in Table 4.4, which can result in a more reliable and reasonable EPR-based correlation.

Table 4.4 Statistics of variables used in the database for both training and testing

Training (Testing)					
Sample number	Variable	Maximum	Minimum	Mean	Standard deviation
100 (100)	e_0	4.643 (4.570)	0.843 (0.676)	2.074 (2.202)	0.928 (0.916)
	w_L	166.2 (159.3)	25.00 (25.00)	73.33 (66.54)	33.34 (22.06)
	I_P	113.9 (113.3)	12.0 (8.0)	37.48 (34.02)	23.68 (17.26)
	C_c	1.340 (1.05)	0.164 (0.12)	0.452 (0.459)	0.255 (0.210)

Remark: w_L and I_P are in percent.

In order to examine the performance of the proposed RCGA in the EPR procedure, the same EPR procedure on compression index was conducted using different optimization algorithms (New RCGA (this study), MOGA-II [191], NSGA-II [139] and PSO [192] with details in Appendix II), respectively instead of RCGA. For all the optimization algorithms used in the EPR procedure, the number of the initial population and the maximum generations were set to 50. All the initial

population was generated by SOBOL (Sobol [28]). Many attempts at optimizing with different values of probability of crossover and the probability of mutation were made to find the best solution for each algorithm: for the new RCGA, the probabilities of crossover and simplex were set to 0.7 and 0.5, and the probability of mutation was set to 0.05; for the other three, the values of setting parameters by the developers [139, 191, 192] were employed. Therefore, all the results shown in the following are the best among many attempts of calculations.

Table 4.5 shows the results of a minimum number generation corresponding to the minimum SSE, with the minimum values of SSE for four selected optimization algorithms. Better performance was achieved by the proposed RCGA in terms of both the convergence speed and the search ability.

Table 4.5 Optimal results for the evaluation of compression index of remolded clays

Optimization algorithm	RCGA	MOGA-II	NSGA-II	PSO
Minimum generation number	20	21	42	45
Minimum SSE	6.46×10^{-4}	6.56×10^{-4}	6.91×10^{-4}	6.84×10^{-4}

All formulations for predicting the compression index optimized by the EPR procedure with different optimization methods are summarized in Table 4.6. Based on these formulations, the results of training and testing with the correlation coefficient (R^2) by using four optimization algorithms are plotted in Figure 4.6. In the case of the training results, the difference between four algorithms is slight, and the new RCGA has the best performance. With respect to the testing results, the difference becomes more significant. The prediction by the formulation of the new RCGA has a better agreement with the measurements than with that of other selected optimization algorithms. That is, the new RCGA is more reliable and accurate than other optimization algorithms in the EPR procedure.

In order to further evaluate the performance of accuracy for different optimized formulations, the root mean square error (RMSE) index was used,

$$\mathrm{RMSE} = \sqrt{\frac{1}{N}\sum_{i=1}^{N}\left(\mathbf{Y}_{\mathrm{a}} - \mathbf{Y}_{\mathrm{p}}\right)^2} \tag{4-5}$$

The lower the RMSE value, the better the model will perform. Meanwhile, both the mean value "u" and the standard deviation value "σ" of $\mathbf{Y}_a/\mathbf{Y}_p$ were also calculated. All the results are summarized in

Table 4.7, demonstrating that the EPR-based model optimized by the proposed RCGA is more accurate than those given by other selected optimization algorithms.

Table 4.6 Formulations of correlation optimized by EPR using different optimization algorithms

Optimization in EPR	Formulations of correlation
New RCGA	$C_c = \left(0.2413 + 0.3358 e_0 w_L - 0.063 \frac{(e_0)^2}{w_L I_P} + 0.1867 \frac{e_0}{(I_P w_L)^2} - 0.1585 \frac{(w_L)^2}{I_P} - 0.4416 (w_L I_P)^2 \right)$
MOGA-II	$C_c = \left(0.5925 + 0.1154 \left(\frac{w_L}{e_0 I_P} \right)^2 + 0.0117 \frac{(e_0)^2}{I_P} - 0.0189 \frac{w_L}{(I_P)^2} + 0.0476 e_0 (w_L)^2 I_P - 0.3365 \frac{w_L}{e_0 I_P} \right)$
NSGA-II	$C_c = \left(0.1551 - 0.0027 \left(\frac{e_0}{I_P} \right)^2 + 0.0978 \cdot e_0 + 0.0129 \frac{(e_0)^2}{I_P} + 0.0272 e_0 (w_L)^2 I_P - 0.0215 e_0 w_L (I_P)^2 \right)$
PSO	$C_c = \left(-0.3225 + 0.3186 \cdot e_0 - 0.0075 \frac{w_L}{(I_P)^2} - 0.0043 \frac{e_0}{w_L I_P} + 0.0393 \frac{1}{e_0} \right)$

Note : the w_L and I_P are in real number, not in percent.

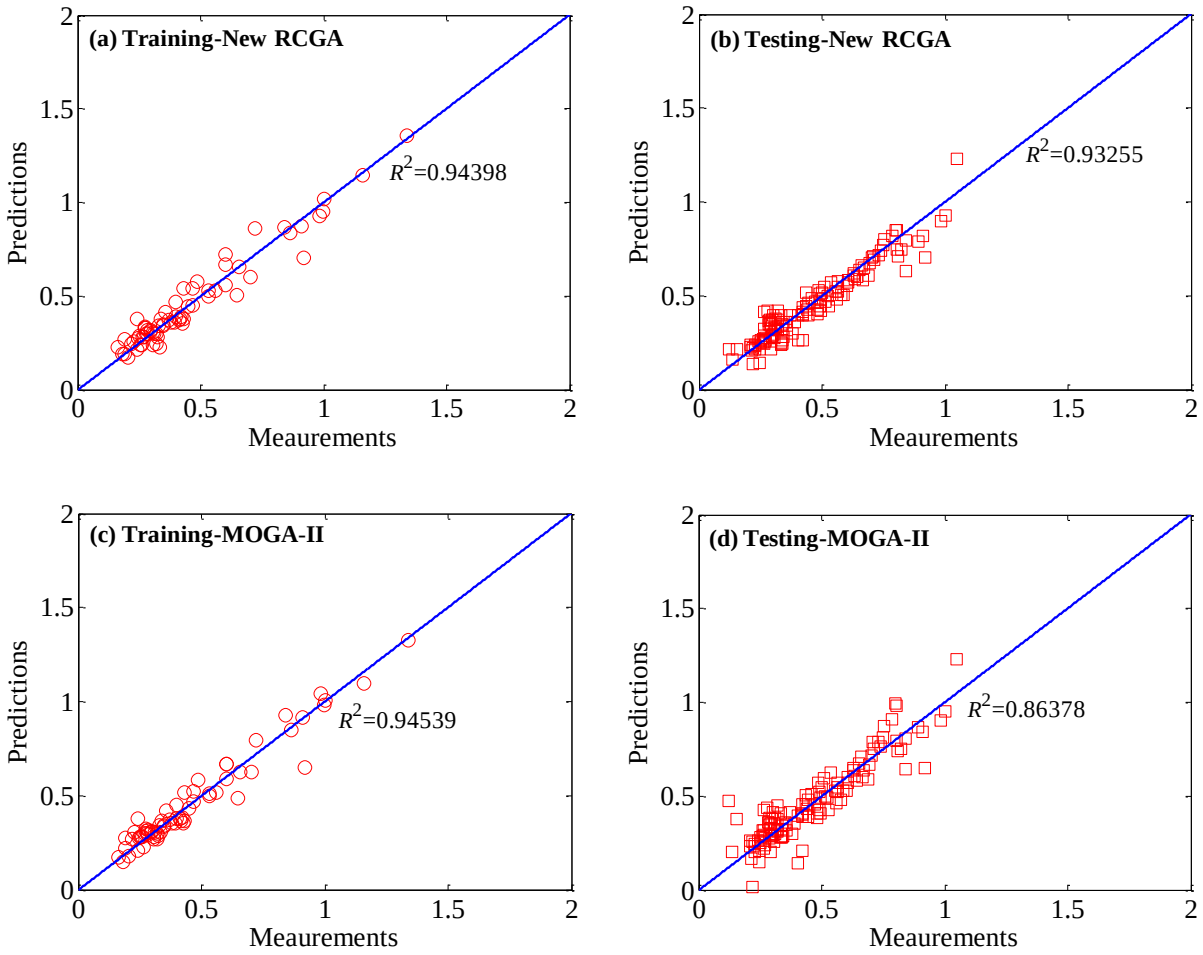

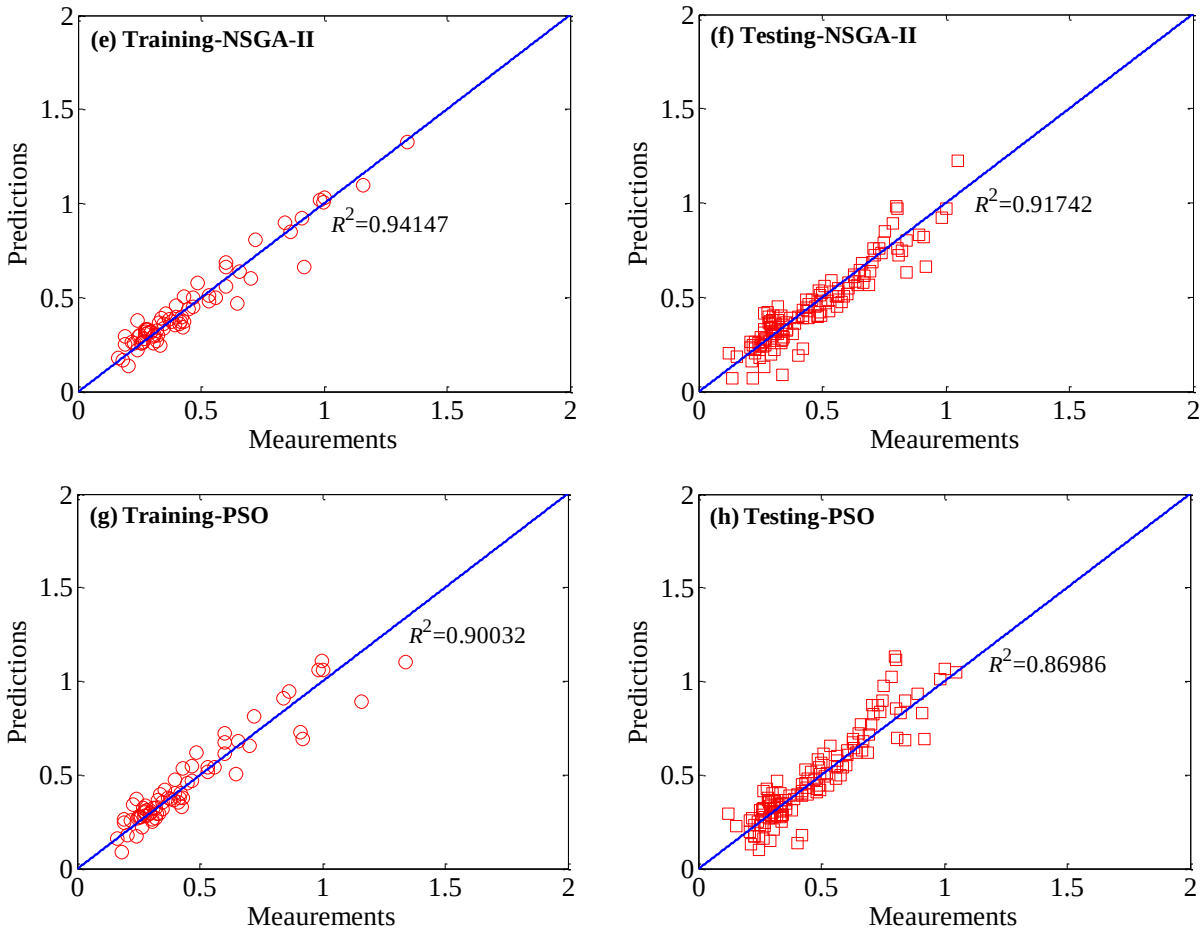

Figure 4.6 Training and testing results of evaluating the compression index by using four optimization algorithms

Table 4.7 RMSE index, the mean value and standard deviation value of $\mathbf{Y}_a/\mathbf{Y}_p$ of optimized formulations

Optimization algorithm	RMSE	u	σ
New RCGA	3.43×10^{-4}	1.0044	0.1872
MOGA-II	0.0031	1.0452	0.3658
NSGA-II	0.0095	0.9932	0.1914
PSO	0.0055	1.0106	0.2559

4.4.3 Application to other remolded clays

To evaluate the performance of the proposed EPR-based correlation on predicting the compression index of remolded clays, the proposed ERP-based correlation was applied to evaluate the compression index of some other natural clays not used in the training and testing data. The clays

from [193-197] were adopted and predicted by the proposed EPR-based correlation. Meanwhile, the same data was also predicted by empirical correlations based on regression analysis presented in Figure 4.5 for comparisons, shown in Figure 4.7. It can be seen that the EPR-based correlation for predicting C_c has a better performance than empirical correlations. Since these data were randomly selected, the proposed ERP-based correlation can be considered reliable for evaluating the compressibility of remolded clays.

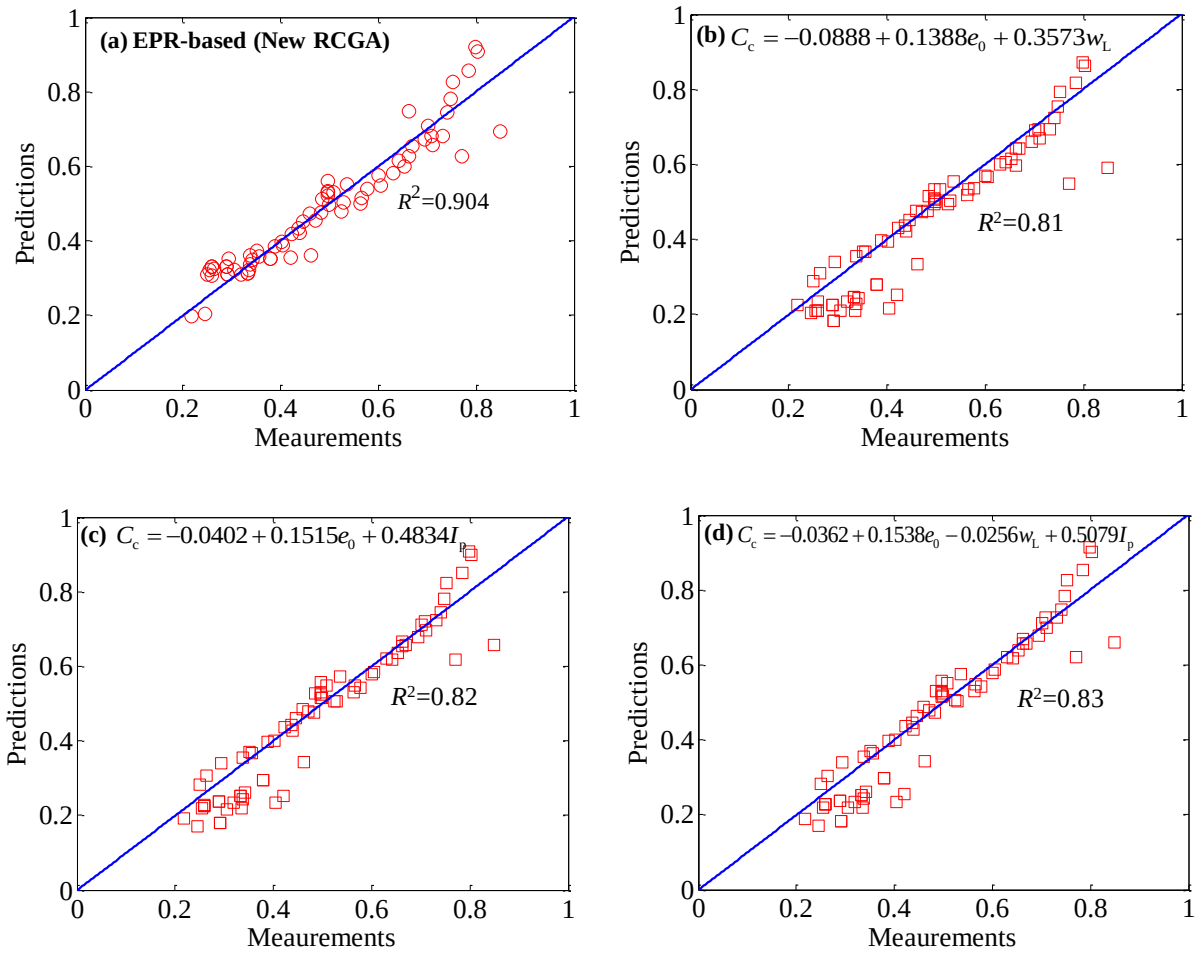

Figure 4.7 Comparison between measurements and predictions of evaluating the compression index by using EPR-based and empirical correlations

4.4.4 Discussion of EPR-based correlations

According to the above results, a better performance of EPR-based correlations was obtained compared to empirical correlations for predicting the compression index of remolded clays. Note that the reliability of EPR-based correlations depends extremely on the range and quantity of the database (e.g., C_c of remolded clays in our case) used in the training data. In this study, the proposed

EPR-based correlations have a good performance on 200 sets of data which covers worldwide typical natural clays. It must be admitted that more database involved in training data would result in even more reliable and reasonable EPR-based correlations, which will also be practically useful.

However, it should be pointed out that the general trend between C_c and each input (e.g., e_0, w_L and I_p) individually cannot be obtained by EPR-based correlations. In this sense, some simple regressions with clear trends are more understandable, even though their performances are not as good as EPR-based correlations.

In fact, apart from three selected physical properties e_0, w_L and I_p, the C_c is also affected by other factors, e.g., w_0, e_L, G_s, I_s, and A shown in Table 1. The non-monotonous trend of C_c with e_0 or w_L or I_p by EPR based on large amount of database can be somehow understood as a supplement due not fully considering of all the factors during the EPR procedure. This discrepancy not be developed in this stud, should be further studied.

4.5 Conclusions

A new EPR-based modeling approach for evaluating the compressibility of remolded clays, for which a hybrid real-coded genetic algorithm has been adopted to improve the performance of EPR has been proposed. Prior to the EPR procedure, the correlations between C_c and a number of major physical properties were investigated. Wherever a single variable was involved, the C_c is highly correlated to e_0. When the two variables were involved, the correlation by e_0 and I_p gives a relatively good performance compared to measurements. When the number of variables increases from two to three, the performance is only slightly improved; this leads to attempting a modeling based on the EPR.

Then, the EPR with the propoesd RCGA was applied to evaluate the compression index of remolded clays with physical properties. Meanwhile, three existing optimization algorithms (MOGA-II, NSGA-II and PSO) were selected to perform the same procedure for a comparison. The compression index was correlated with three most frequently used properties (initial void ratio, liquid limit and plastic index) for remolded clays. The training results demonstrated that each optimization algorithm can provide a reasonable EPR formulation with a high value of correlation coefficient. However, the testing results demonstrated a better performance with the proposed RCGA than with others in the EPR. Finally, a EPR-based formulation for predicting the compression index with three physical properties for remolded clays was finally proposed using the proposed RCGA.

Chapter 5 Identifying parameters of natural soft clay

5.1 Introduction

Natural soft clays usually exhibit anisotropy, destructuration and creep behaviors, based on which different constitutive models have been proposed in recent decades (e.g., Kimoto and Oka [198]; Karstunen and Yin [4]; Yin et al. [199]). These models may contain parameters which cannot be determined directly by conventional laboratory or field tests. Laboratory tests on both intact and reconstituted soil samples are then usually necessary for determining parameters in a more straightforward way, which implies relatively high testing costs (e.g., test numbers, working days) in engineering practice. If there is a way to obtain such parameter values by simulating conventional laboratory or field tests and minimizing the difference between experimental and theoretical results, (so-called optimization), this will become useful to the practice of engineering.

Different optimization techniques for identifying soil parameters have been successfully used in the geotechnical field in the last few decades. The existing optimization techniques can be divided into two categories: (1) Deterministic optimization techniques, such as gradient based algorithms and simplex (Lecampion et al. [42]; Calvello and Finno [19]; Yin and Hicher [31]; Papon et al. [12]) work with a single solution and are focused on reaching local minima, because they begin the search procedure with a first guess solution (often chosen randomly in the search space). If this guess solution is not close enough to the global minimum solution, it is likely to be trapped in a local minimum solution. (2) Stochastic optimization techniques, such as evolutionary algorithms (Pal et al. [11]; Javadi et al. [131]; Levasseur et al. [13]; Rokonuzzaman and Sakai [18]; Papon et al. [12]; Vardakos et al. [24]; Moreira et al. [200]) and simulated annealing (Yepes et al. [201]), rely significantly on computational power.

All these optimization techniques are usually applied to laboratory tests, in-situ testing or field measurements. Among these, evolutionary algorithms are found to be very promising global optimizers. Genetic algorithms (GA) are perhaps the most commonly used evolutionary algorithms (Deb [202]). However, the application of GAs for soil parameters accounting for combined anisotropy, creep and destructuration has not been reported to date. Therefore, enhancing a more efficient GA, based on recent developments and applying it to tackle the problem of parameter identification for soft structured clays, may be a helpful approach.

The aim of this chapter is to propose an efficient optimization procedure for identifying parameters using a GA with conventional soil characterization tests on intact samples of soft structured clay. For this purpose, three conventional triaxial tests on Wenzhou marine clay have been selected for the model and a newly developed elastic viscoplastic model considering anisotropy, destructuration and creep features has been enhanced and adopted. A classic and popularly adopted genetic algorithm, the Non-dominated Sorting Genetic Algorithm, NSGA-II, has been chosen for comparison with the new proposed RCGA to highlight the effectiveness and efficiency of the new RCGA. For both GAs, the uniform sampling method by Sobol[28] has been adopted to generate the initial individuals. Then the parameters identified by the two genetic algorithms are compared with measurements, and the more reasonable one is used to predict other tests on the same clay for further validation.

5.2 Adopted real-coded genetic algorithm

The genetic algorithm (GA) originally developed by Holland [52] is a simulation mechanism of Darwinian natural selection and a genetic computational model of the biological process of evolution. It is also a process to search for the optimal solution by simulating natural evolution. In GAs, first an encoding scheme has been used to represent a point (individual) in the search of decision variables, and then each individual of the population is assigned its fitness based on some criteria. There are two types of GAs, namely, fixed-length binary coded GAs and real coded GAs (RCGA). The performance of binary GAs is found to be satisfactory on small and moderately sized problems not requiring as much precision in the solution. For high dimensional problems in which a higher degree of precision is desired, the binary GAs require huge computational time and memory (Goldberg [54]). To overcome these difficulties, RCGAs are now becoming popular. It is commonly accepted that RCGAs are more suitable for continuous optimization problems than the binary coded GAs (Herrera et al. [203]).

Furthermore, some outstanding operators have recently been developed and applied individually to some genetic algorithms. However, these outstanding operators were not well combined and applied to the geotechnical field for solving complex optimization problems. Thus, it is necessary to develop a new genetic algorithm with high efficiency to improve the performance of the optimization process.

Therefore, the proposed RCGA in chapter 3 is employed to conduct the optimization. Only difference is the newly developed Dynamic Random Mutation operator. The DRM applies the mutation rule as follows:

$$x_i^* = x_i + s_m \Phi_0 \left(x_i^U - x_i^L \right) \tag{1}$$

where x_i^* is the offspring after the mutation; s_m is mutation step size; Φ_0 is a random perturbation vector in the n-dimensional cube $[-\phi_0,+\phi_0]^n$, in which ϕ_0 is a user-specified number chosen between 0 and 1.

The step size was dynamically adjusted using the following update rules,

$$s_m = \frac{1}{3} \cdot \arctan\left(a\left(1 - 2 \cdot \frac{k}{k_{\max}} \right)^b \right) + \frac{1}{2} \tag{2}$$

where the parameters, a and b are used to control the decay rate of s_m, with k and $k_{\max}$ denoting the current generation number and the maximum number of generations, respectively.

It is clear that the mutation range decreases as the number of generations increases, with its decay rate being controlled by the parameters a and b. The influences of a and b are shown in Figure 5.1, in which a controls the rate of decrease, and parameter b controls the position of decrease. The highlights of this dynamic step size are that a large step size can be kept in the initial generations, which leads to a high mutation range as the number of generation increases. The step size is degraded to a small value to guarantee that the evolution process converges to an optimum solution. Additionally, the DRM mutation is a self-adaptive operator, which can improve the search efficiency of the proposed genetic algorithm.

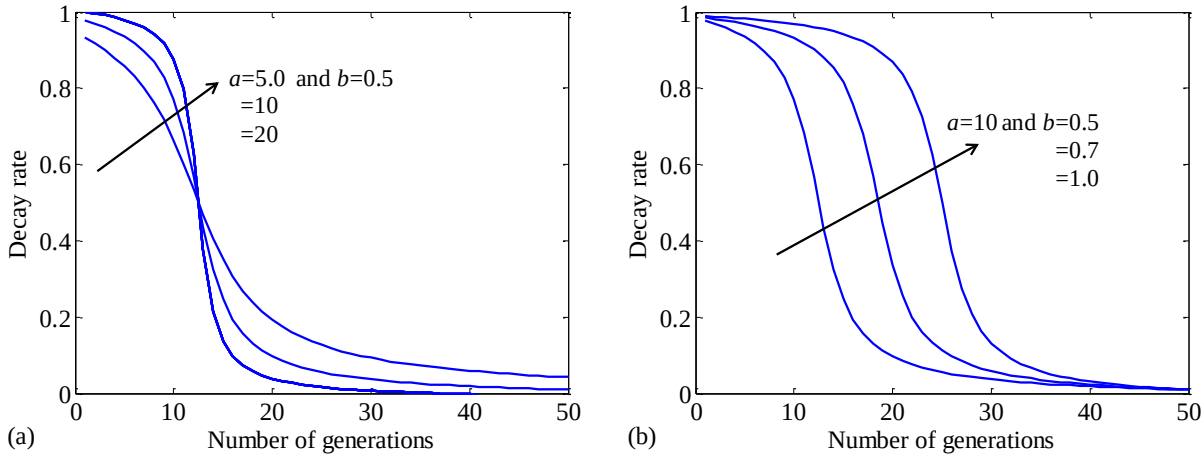

Figure 5.1 Effects of a and b on the decay rate for the DRM

5.2.1 Method of sample initialization

Using a well-distributed sampling to generate the initial population can increase the robustness of the algorithm and allow premature convergence to be avoided. This initial population is governed by the number of individuals, their domain (range), and the method controlling the distribution of the individuals within their domain. In accordance with the approach taken by Poles et al. [143], the sampling method SOBOL, proposed by Sobol [28], was adopted in the new GA. SOBOL is a deterministic algorithm that imitates the behavior of the random sequence, through which a uniform sampling in the design space can be obtained.

5.3 Identification procedure based on RCGA

5.3.1 Error function

In order to carry out an inverse analysis, the user must define a function that can evaluate the error between the experimental and the numerical results, and then minimize this function. In order to make the error independent of the type of test and the number of measurement points, an advanced error function proposed by Levasseur et al. [13] has been adopted. The difference between the measured and the simulated results is expressed in the form of the least square method,

$$\mathrm{Error}(x)=\sqrt{\frac{\sum_{i=1}^{N}\left(\frac{U_{\exp}^{i}-U_{num}^{i}}{U_{\exp}^{i}}\times 100\right)^{2}}{N}}\% \tag{3}$$

where x is a vector of the parameters; N is the number of values; $U_{\exp}^{i}$ is the value of measurement point i; U_{num}^{i} is the value of calculation at point i.

The scale effects on the fitness between the experimental and the simulated results can be eliminated by this normalized formula. Additionally, the objective error calculated by this function is a dimensionless variable; thus, any difference in error can be avoided for different objectives with different variables.

5.3.2 Identification methodology

Generally, deformation and strength are two extremely important indicators to illustrate the mechanical behavior of soil. For a laboratory triaxial test, the isotropic or anisotropic compression

test has been conducted first, followed by the shearing stage. During the whole process, the model parameters accounting for the compression behavior and the shear behavior are measured and obtained. At the same time, some other parameters concerning features such as sensitivity or destructuration and creep are also implied in the stress-strain-time relationship (softening or hardening, contraction or dilation), although these variables cannot be directly measured. Therefore, the results of selected laboratory tests can provide information to optimize the model parameters. In this study, a mono-objective framework with three different criteria is considered:

$$\min\left[\text{Error}(x)\right]=\begin{bmatrix}\text{Error}(K_0)\\ \text{Error}(q)\\ \text{Error}(\Delta u \text{ or } \Delta e)\end{bmatrix} \tag{4}$$

Note that the errors can be calculated between measurements and simulations based on strains along the stress level or stresses along the strain level. It will be more convenient in strain-controlled tests to compute the errors based on p' for K_0-compression test (marked as Error (K_0)), and based on q and Δu or Δe (marked as Error (q) and Error (Δu or Δe)) for undrained or drained triaxial tests.

The total error function is expressed as:

$$\text{Error}\left(x\right)=\sum_{\text{i=1}}^{m}\left(l_i\cdot\text{Error}\left(x\right)_i\right) \tag{5}$$

where m is the number of objectives involved in the optimization; $\text{Error}\left(x\right)_i$ is the value of error corresponding to the objective, i. l_i is the weight factor with $\sum(l_\text{i}) = 1$; The weight factor, l_i is taken as 1/3 in this case, as each test plays the same important role in evaluating soil behavior. Then the average error is taken as being equal to (Error (q) + Error (Δu or Δe) + Error (K_0))/3, with Error (q), Error (Δu), Error (Δe) and Error (K_0) representing the difference between the experimental results and the numerical simulation values for deviatoric stress, excess pore pressure for undrained tests, the change in void ratio for drained tests and vertical stress for the K_0-consolidation stage, respectively.

5.3.3 Numerical validation by identifying soil parameters

To evaluate the performance of the adopted RCGA, a set of synthetic objective tests (one oedometer test and one undrained triaxial test on isotropically consolidated clay) was first generated by the Modified Cam-Clay model [152] using a set of typical parameters (υ=0.25, e_0=1.0, κ=0.02, λ=0.20, M_c=1.2, p'_{c0}=100), as shown in Figure 5.2. Then, except for υ and e_0, the rest of the

parameters were optimized by the new RCGA and NSGA-II, respectively. The initial population size and the maximum number of generations were taken to 50 and 100. The interval of each parameter is shown in Table 5.1. Figure 5.3 shows the evolution of the minimum objective value as the generation number increases in identifying MCC parameters for both RCGA and NSGA-II. The Procedure with RCGA converges faster than that with NSGA-II, which demonstrates an improved search ability by RCGA.

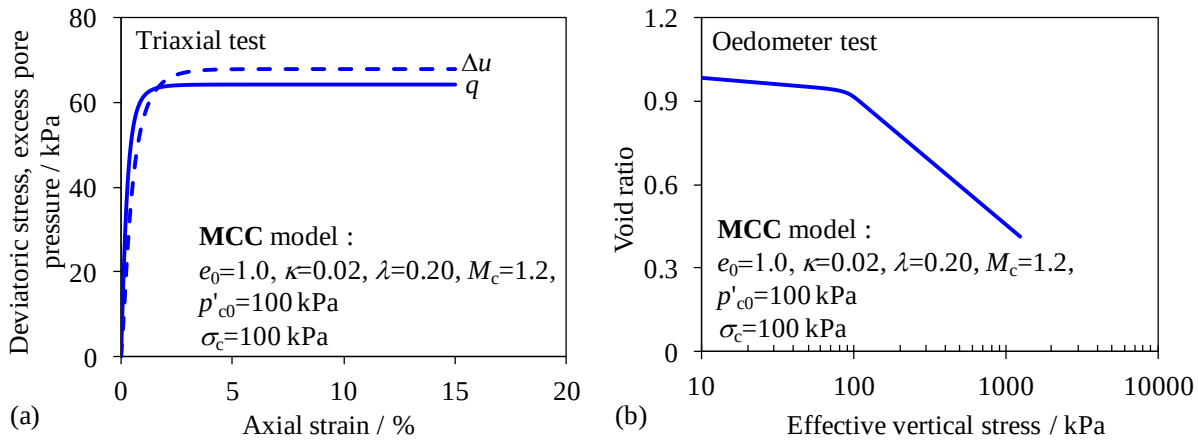

Figure 5.2 Results of synthetic objective tests generated by MCC model

Table 5.1 Search domain and intervals of parameters for MCC model

Parameters	κ	λ	M_c	p'_{c0}
Lower bound	0.001	0.1	0.5	50
Upper bound	0.1	0.5	1.5	150
Step	0.001	0.01	0.01	1.0

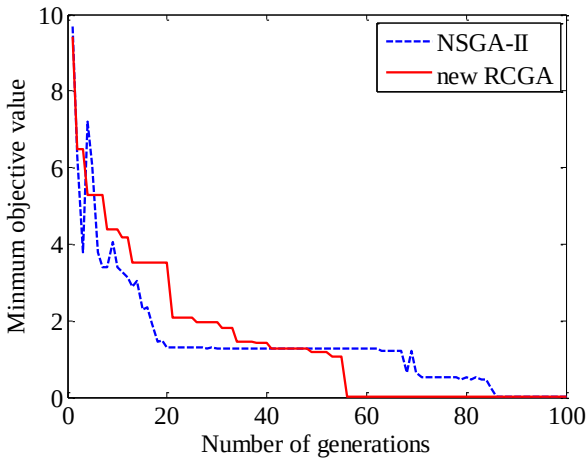

Figure 5.3 Comparison of optimized results in identifying MCC parameters for RCGA and NSGA-II

Therefore, the excellent performance of the proposed RCGA was validated by conducting four benchmark mathematic tests and one constitutive model test, based on which the proposed RCGA is recommended for tackling more complex problems.

5.4 Application to identify model parameters of soft structured clay

5.4.1 Experimental observations on coupling of creep and destructuration

Experimental observations show a strong coupling of creep and destructuration (Leroueil et al. [204]; Rocchi et al. [205]; Yin and Karstunen [206]; Yin and Wang [207]; Yin et al. [159]). For instance, Fig. 7 shows a schematic plot of a typical 1D compression curve and the evolution of a secondary compression coefficient with the vertical stress for both intact and reconstituted soft clays. By extending the compression curve of the reconstituted sample, an intersection point with the compression curve of the intact sample can be obtained. The difference between the intact and the reconstituted samples is due to the state of the soil structure which can be influenced by cementation or chemical bonding during the natural deposition of the clay. The initial value of the post-yield secondary compression coefficient of the intact sample is large, and it then decreases with increasing vertical stress due to the debonding process induced by the plastic strain, and it finally approaches the value of the secondary compression coefficient of the reconstituted sample. Thus, creep and destructuration are strongly coupled. This coupling can also be found in the triaxial condition and can significantly influence the stability of geotechnical structures.

5.4.2 Discrepancy in standard parameter determination

Since the secondary compression coefficient changes with the state of bonding for soft structured clays, the coupling effect links two soil properties: the secondary compression coefficient of soil without bonding (corresponding to the reconstituted clay) $C_{\alpha ei}$, and the soil sensitivity S_t. As shown by Zhu et al. [208], the global secondary compression coefficient $C_{\alpha e}$ of intact samples depends on two soil properties: the intrinsic secondary compression coefficient $C_{\alpha ei}$ of its reconstituted samples and the state of bonding represented by the soil sensitivity S_t or the bonding ratio χ_0 (Note that $C_{\alpha ei}$ and S_t or χ_0 are independent). In numerical or analytical methods for geotechnical applications, the $C_{\alpha ei}$ and the bonding ratio χ_0 reflecting S_t (see Fig. 7) are

simultaneously estimated with the soil constants controlling the debonding rate (e.g., ξ and ξ_d in constitutive models of structured clays by Yin et al. [199] and Gens and Nova [209]).

For determining $C_{\alpha ei}$, a conventional consolidation test on a reconstituted sample is usually required for most soft structured clays in which the interparticle bonding is generally not fully destroyed during mechanical loading. Thus, reconstituted samples need to be tested, which requires additional time (about one month) and considerable cost. For determining the initial bonding ratio, χ_0, 1D compression tests on both intact and reconstituted samples are also needed (see Figure 5.4). The determination of the destructuration constants, ξ and ξ_d requires both 1D and isotropic compression tests on intact and reconstituted samples, as they control different debonding mechanisms (Yin et al. [199]).

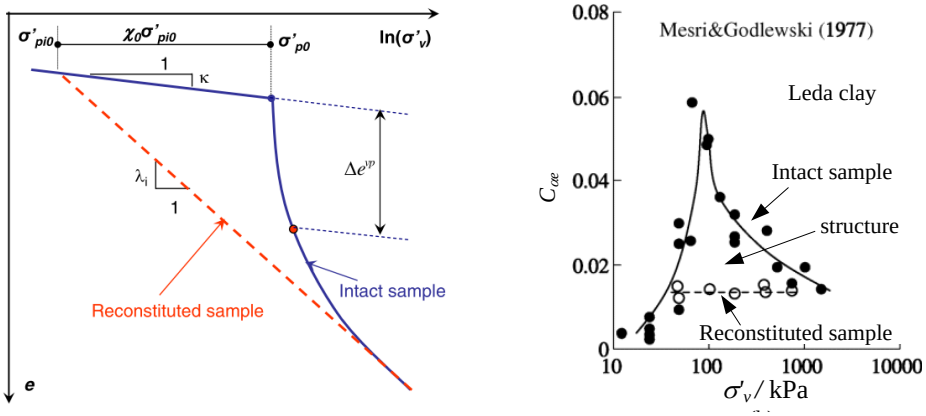

(a) (b)

Figure 5.4 Typical results of oedometer test for intact and reconstituted soft clays

Thus, 1D and 3D tests on both intact and reconstituted samples of soft structured clay are currently required. This leads to high demands on time and testing costs, and can lead to difficulties in engineering practice. Finding a more efficient way to determine these parameters with conventional tests on intact clay alone is essential.

5.4.3 Brief introduction of laboratory tests and identification philosophy

The Wenzhou clay deposit is a marine clay characterized as slightly organic and highly plastic. A relatively homogenous layer of Wenzhou clay from 10.5 to 11.5 m was selected for this study. Some common physical properties are presented in Table 5.2.

Intensive laboratory tests were carried out along various stress paths, focusing on the rate-dependent mechanical properties of Wenzhou clay (Yin et al. [159]). The tests selected for this study were three conventional undrained triaxial tests on K_0-consolidated Wenzhou clay under different confining stresses. The K_0-consolidation was performed over 2 days up to a vertical stress of 75 kPa, for another 2 days up to 150 kPa, and finally for another 2 days up to 300 kPa. The average stress-rate was 2.08 kPa/h. For the undrained triaxial shearing stage, a strain rate of 2 %/h was applied during tests in accordance with the ASTM standard, and this was also adopted in the simulations. The results of these undrained triaxial tests with their K_0-consolidation curves are shown in Figure 5.5.

Table 5.2 Typical physical properties of Wenzhou clay

Depth (m)	γ (kN/m^3)	e_0	w (%)	w_L (%)	w_P (%)	σ'_{p0} (kPa)	σ'_{v0} (kPa)
10.5-11.5	15.5	1.895	67.5	63.4	27.6	81.3	75.4

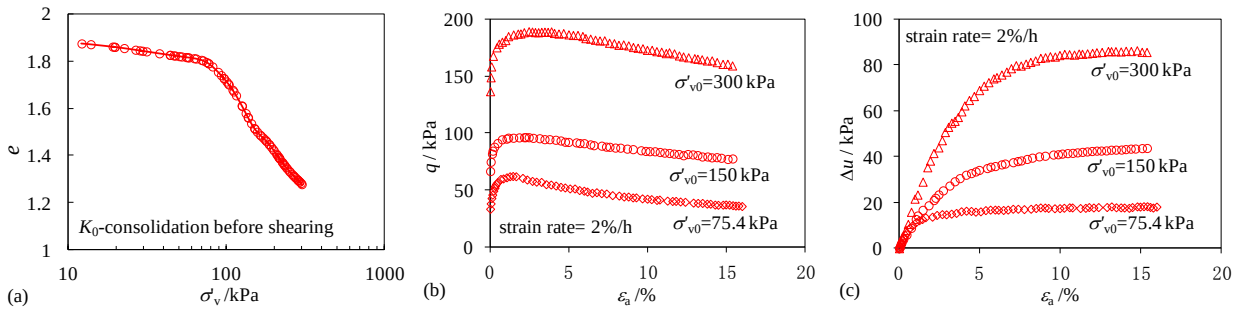

Figure 5.5 Results of triaxial tests on Wenzhou clay: (a) K_0-consolidation stage; (b) deviatoric stress versus axial strain; and (c) excess pore pressure versus axial strain.

Since the stress-strain-time relationship is uniquely controlled by the secondary compression coefficient and the applied strain-rate of test (see Yin et al. [156]), and the destructuration behavior is also uniquely controlled by a test with a stress-path of varying stress ratio, an undrained triaxial shearing test with its consolidation stage is theoretical enough for identifying related parameters. Then for higher accuracy, three triaxial tests under different confining stresses with their consolidation stages as recommended in engineering design, usually for simple elastoplastic models, were adopted in this study. If successful, the application of the design-based test requirement can be directly extended to more advanced constitutive models.

5.4.4 Adopted constitutive model

For soft structured clays, creep and destructuration related parameters are important not only for constitutive modeling but also for engineering practice (e.g. directly relating to secondary compression coefficient and sensitivity). A newly developed elastic viscoplastic model (Yin et al. [199]) accounting for the main features of a natural soft clay (e.g., soil viscosity, anisotropy and destructuration) can reproduce the decrease of the secondary compression coefficient with the inter-particle debonding, and is thus adopted to simulate all selected tests in this study. A brief introduction to this model with its associated parameters can be found in the Appendix. Due to its natural deposition, the soil exhibits naturally inherent cross-anisotropy of elasticity (see Yin and Chang [210]; Chang and Yin [211]; Yin *et al.* [149, 206, 212]). This anisotropic elastic behavior was considered to enhance the model of Yin et al. [199] by adopting the following matrix of elastic stiffness:

$$\begin{bmatrix} \dot{\varepsilon}_x \\ \dot{\varepsilon}_y \\ \dot{\varepsilon}_z \\ \dot{\varepsilon}_{xy} \\ \dot{\varepsilon}_{yz} \\ \dot{\varepsilon}_{zx} \end{bmatrix} = \begin{bmatrix} 1/E_v & -\upsilon'_{vv}/E_v & -\upsilon'_{vv}/E_v & 0 & 0 & 0 \\ -\upsilon'_{vv}/E_v & 1/E_h & -\upsilon'_{vh}/E_h & 0 & 0 & 0 \\ -\upsilon'_{vv}/E_v & -\upsilon'_{vh}/E_h & 1/E_h & 0 & 0 & 0 \\ 0 & 0 & 0 & 1/2G_{vh} & 0 & 0 \\ 0 & 0 & 0 & 0 & \left(1+\upsilon'_{vh}\right)/E_h & 0 \\ 0 & 0 & 0 & 0 & 0 & 1/2G_{vh} \end{bmatrix} \begin{bmatrix} \dot{\sigma}'_x \\ \dot{\sigma}'_y \\ \dot{\sigma}'_z \\ \dot{\sigma}'_{xy} \\ \dot{\sigma}'_{yz} \\ \dot{\sigma}'_{zx} \end{bmatrix} \quad (6)$$

with $E_h = nE_v$, $\upsilon'_{vh} = \sqrt{n}\upsilon'_{vv}$, where E_v and E_h are the vertical and horizontal Young's modulus, respectively, υ'_{vv} and υ'_{vh} are the vertical and horizontal Poisson's ratio, respectively and G_{vh} is the shear modulus (see Graham and Houlsby [213]). For stress-controlled isotropic compression with incremental stress of $\dot{\sigma}'_x = \dot{\sigma}'_y = \dot{\sigma}'_z = \dot{p}'$, then

$$\dot{\varepsilon}_v = \dot{\varepsilon}_x + \dot{\varepsilon}_y + \dot{\varepsilon}_z = \left(1 - 4\upsilon'_{vv} + 2/n - 2\upsilon'_{vv}/\sqrt{n}\right)\frac{\dot{p}'}{E_v} \quad (7)$$

Based on the definition of bulk modulus, $K=\delta p'/\delta\varepsilon_v$, the vertical Young's modulus can be obtained as follows, with the shear modulus, G_{vh}:

$$E_v = \left(1 - 4\upsilon'_{vv} + 2/n - 2\upsilon'_{vv}/\sqrt{n}\right)\left(\frac{1+e_0}{\kappa}\right)p' \quad (8)$$

$$G_{vh} = \frac{\sqrt{n}E_v}{2\left(1+\sqrt{n}\upsilon'_{vv}\right)} \quad (9)$$

Then for input parameters (κ, υ'_{vv}, n), one additional parameter, n, varying between 0 and 1, needs to be identified for anisotropic elasticity unlike the isotropic elasticity.

Overall, the recently developed 'ANICREEP' model considering soil viscosity, anisotropy and destructuration was adopted and enhanced with cross-anisotropy of elasticity. Apart from the Poisson's ratio (varying from 0.1 to 0.35 for clays, and the stress-strain response in 1D and triaxial conditions is not sensitivity to these values (see Biarez and Hicher [214]; Yin and Hicher [31]), taken as 0.25, a typical value for clays) and the initial void ratio e_0, all other input parameters of the model are set for optimization in this study. The intervals of these parameters given in Table 5.3 are much larger than those corresponding to their typical values (see Biarez and Hicher [214]; Yin et al. [156, 199]; Zhu et al. [208]; Yao et al. [215-217]). Note that this is necessary to insure that the real solutions are within the range, and that no measurement or pre-judgment is necessary based on stress-strain or stress path curves. If successful, the high performance of the proposed identification procedure using the proposed RCGA can be highlighted.

Table 5.3 Search domain for creep and destructuration parameters of ANICREEP model

Parameters	κ	λ_i	M	$C_{\alpha ei}$	χ_0	ξ	ξ_d	n
Lower bound	0.001	0.001	0.5	0.0001	0	0	0	0.1
Upper bound	0.2	0.5	2.0	0.1	50	20	0.5	2.0
Step size	0.001	0.001	0.01	0.0001	0.5	0.1	0.05	0.05

5.5 Optimization results and validation

5.5.1 Optimization results and discussion

Table 5.4 Parameters of selected algorithms

Algorithm	PopSize	NumGens	Selection	Probability of Crossover	Probability of Mutation	Elitism strategy
New RCGA	100	50	Tournament	0.7	0.05	Yes
NSGA-II	100	50	Tournament	0.7	0.05	Yes

The optimization procedure was initially conducted using the new RCGA. In order to estimate the performance of the new RCGA, the classic and widely adopted Non-dominated Sorting Genetic Algorithm (NSGA-II) proposed by Deb et al. [139] was selected to carry out the same optimization analysis. The controlling parameters of NSGA-II have the same values as the new RCGA, as shown in Table 5.4. Note that these parameter settings are typical and common, as recommended by many researchers (Deb et al. [139], Deep and Thakur [142], Jin et al. [25, 26]), the sensitivity of these parameters will not be presented here.

According to Deep and Thakur [142], computational effectiveness and efficiency are two important aspects for assessing an optimization algorithm. The computational effectiveness signifies the degree of precision in locating global minima, and the efficiency of a GA is the measure of the rate of convergence. Following the same optimization procedure, the optimal solution with minimum average error was respectively obtained by RCGA and NSGA-II. Generally, GA provides a population of individuals, which has to be selected according to a satisfaction criterion. All individuals, whose error value is lower than a reference value, are called 'satisfactory' (Papon et al. [12]). In this paper, the optimal solution is selected based on the minimum average error (average error=(Error(q)+Error(Δu)+Error(K_0))/3) from a thousand set of parameters generated during optimization, as shown in Table 5.5. This optimal solution is unique for different optimization runs when the number of generations and initial individuals are big enough in GA (see Papon et al. [12]). The significant difference between the optimal parameters obtained using both algorithms was found, which indicates that the two GAs used in this study have different search abilities in finding the best solution. Based only on the value of the objective error, the set of parameters obtained using the new RCGA is much more satisfying than that of NSGA-II. In other words, the new RCGA has a perfect search effectiveness and is more suitable than NSGA-II for identifying soil parameters.

Table 5.5 Simulation errors with three typical sets of parameters optimized by Genetic Algorithm for Wenzhou clay

Algorithm	Convergence generation	Optimal parameters								Objective error /%
		κ	λ_i	M	$C_{\alpha ei}$	χ_0	ξ	ξ_d	n	
RCGA	50	0.052	0.225	1.18	0.0081	5	11.5	0.425	0.80	7.94
NSGA-II	49	0.059	0.250	1.13	0.0041	3.5	8.5	0.50	0.70	9.69

Remark: Objective error representing minimum average error of (Error(q)+Error(Δu)+Error(K_0))/3 during optimization.

For evaluating the search efficiency, the number of generations to convergence is a key criterion. Figure 5.6 shows the evolution of the minimum objective error in each generation with the number of generations. It can be seen that the new RCGA in general has a smaller error than the NSGA-II, which demonstrates that a higher search efficiency is obtained with the new RCGA.

It is apparent that the advanced search mechanism and the maintenance of population diversity can lead to a good performance for the GAs. Unlike in the NSGA-II, the mutation operators adopted in the RCGA are self-adaptive. The DRM provides a greater chance of population variation by producing a relatively large allowable step size for the mutation at every initial evolution period, which can result in a higher probability of escaping from the local traps. When the population is gradually converging to the optimum solution, a small mutation region produced by the DRM can enhance the precision of the obtained solution.

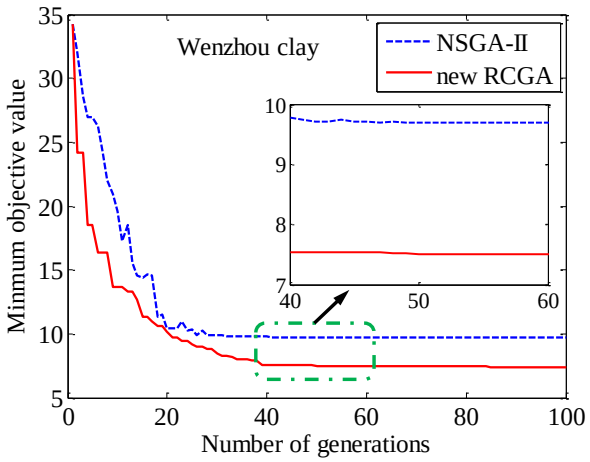

Figure 5.6 Evolution of minimum objective value in each generation with the increase of the number of generations

All the comparisons demonstrate that the new RCGA is robust and suitable for identifying parameters of soft structured clay, in terms of computational effectiveness and efficiency. With regard to the reasonableness and reliability of optimal parameters, this will be further validated in the following sections.

5.5.2 Validation based on experimental measurements

Additional test data on the same Wenzhou marine clay (Zeng [218]; Wang and Yin [219]; Yin et al. [159]) have been used to determine which set of parameters obtained by different GAs is the most appropriate.

For the parameter concerning the compression behavior, the intrinsic compression index λ_i (corresponding to the reconstituted clay) cannot be directly measured for intact samples except under very high stress levels. According to Biarez and Hicher [214], the compression index λ_i=0.197 can be estimated using the empirical form C_c=0.009(w_L-13). Based on a study by Zeng [218] on reconstituted clay from the same location, a compression index of λ_i =0.202 was obtained. In the comparison, the value given by RCGA is closer to the actual measurement than that given by NSGA-II. Likewise, for the slope of the critical state line M, as shown in Figure 5.7, the value of M given by RCGA ($M_{\_RCGA}$=1.18) appears more reasonable than that given by NSGA-II($M_{\_NSGA}$=1.13).

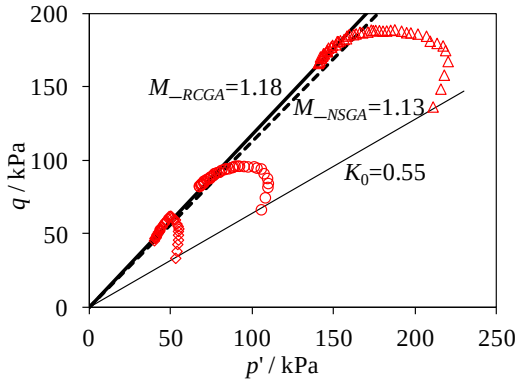

Figure 5.7 Comparisons of M_c obtained by RCGA and NSGA-II between simulated and experimental results

The measured value of sensitivity, S_t, for Wenzhou marine clay is approximately 5.45, as shown in Figure 5.8. From the optimization analysis, a S_t value of 6 was obtained using the new RCGA, and a value of 4.5 using NSGA-II. Compared to the measured value, the one obtained using the RCGA appears more reasonable than the one obtained using NSGA-II. For this reason, the performance of the new RCGA is suitable for identifying soil parameters.

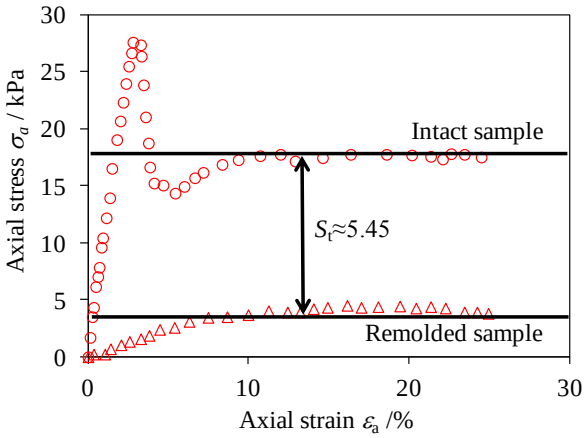

Figure 5.8 Unconfined compression tests on intact and remolded Wenzhou marine clay.

For $C_{\alpha ei}$, a higher value of $C_{\alpha ei}$= 0.0081 is obtained using the new RCGA and a smaller value of $C_{\alpha ei}$= 0.0041 is obtained using NSGA-II. Compared with the measurements given by Dan [220] and Zeng [218] based on reconstituted clay from the same location, the value determined using RCGA is closer to the average measured value ($C_{\alpha ei}$ = 0.007) than that given using NSGA-II, as shown in Figure 5.9. It can be seen that the value obtained using the new RCGA appears more reasonable.

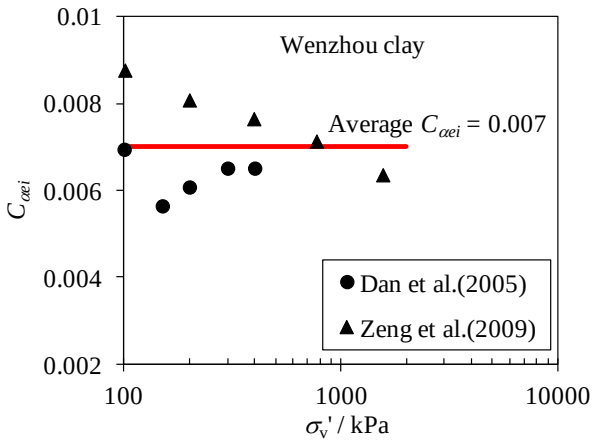

Figure 5.9 Evolution of $C_{\alpha ei}$ with vertical stress for Wenzhou marine clay.

Considering the uniqueness of the solution and the comparisons between measurements and optimization results in term of the intrinsic compression index λ_i, the critical state line M, the initial bonding χ_0 and the intrinsic secondary compression coefficient $C_{\alpha ei}$, the new RCGA appears more robust and suitable than the NSGA-II for identifying parameters. Finally, the optimal set of parameters using the new RCGA was selected, shown in Table 5.5, for further validation by simulating other tests on the same clay.

5.5.3 Validation based on test simulations

One-dimensional multi-staged CRS (Constant Rate of Strain) tests, undrained triaxial tests in compression and extension, and undrained creep tests on the same Wenzhou clay (Yin et al. [159]) were simulated using an enhanced ANICREEP model with the optimized parameters shown in Table 5.5.

5.5.3.1 Oedometer tests at constant rate of strain

Two one-dimensional multi-staged CRS tests with strain rates varying between 0.2 %/h and 20 %/h were simulated and compared with experimental results, as shown in Figure 5.10. A good

agreement between experiments and simulations was achieved for the two tests. This demonstrates that the enhanced ANICREEP model can predict the 1D rate-dependent behavior of Wenzhou marine clay, and that the soil parameters optimized by the new RCGA are suitable.

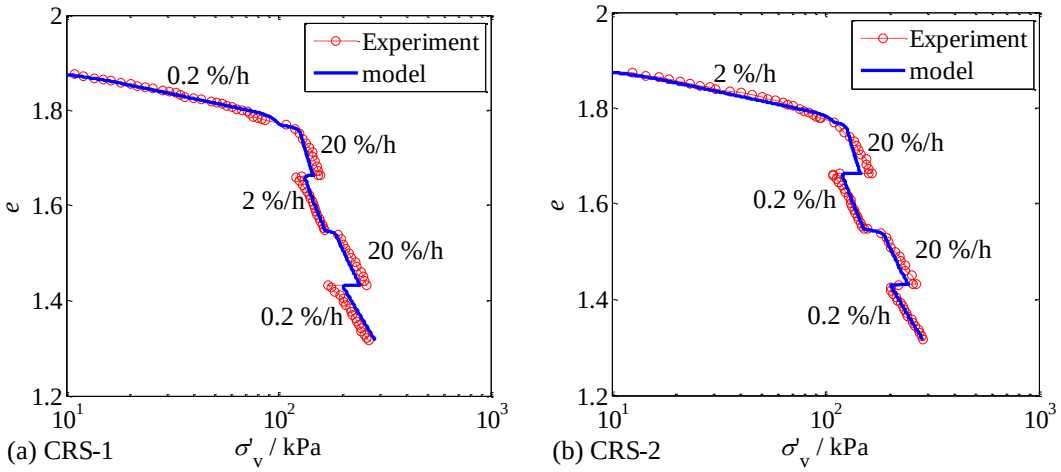

Figure 5.10 Comparisons between simulated and experimental results of multi-staged one-dimensional tests with axial strain-rate varying between 0.2%/h and 20%/h.

5.5.3.2 Undrained triaxial tests at constant rate of strain

Three sets of undrained triaxial tests in compression and extension on K_0-consolidated samples under three vertical effective stresses (σ'_{v0}=75.4, 150 and 300 kPa) at strain-rates of 0.2%/h, 2%/h and 20%/h were simulated. Figure 5.11 to Figure 5.13 show the comparisons between the predicted and the measured results for deviatoric stress vs. axial strain and effective stress path. Good agreement between experimental results and simulations was generally achieved by the enhanced ANICREEP model with the set parameters optimized using the new RCGA method. This demonstrates that (1) the enhanced model has a good ability to reproduce the 3D rate-dependent and destructuration behavior of soft structured clay; and (2) the parameters obtained from the new RCGA are representative of the 3D behavior of Wenzhou clay.

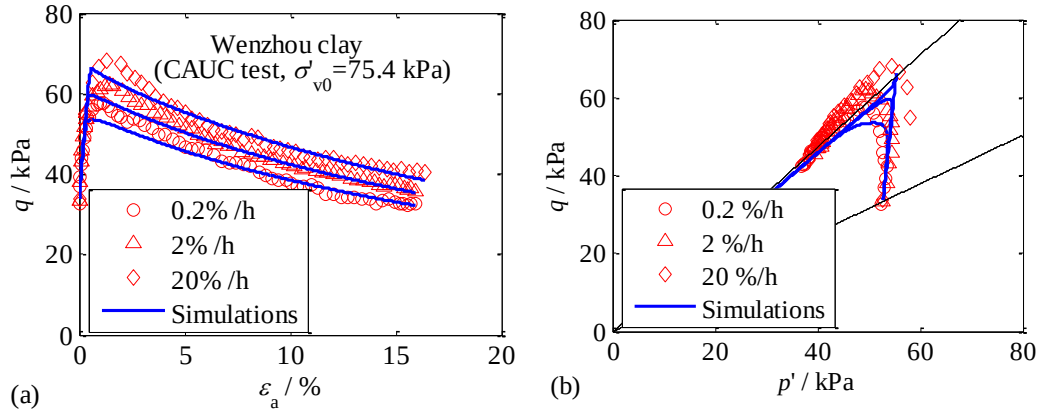

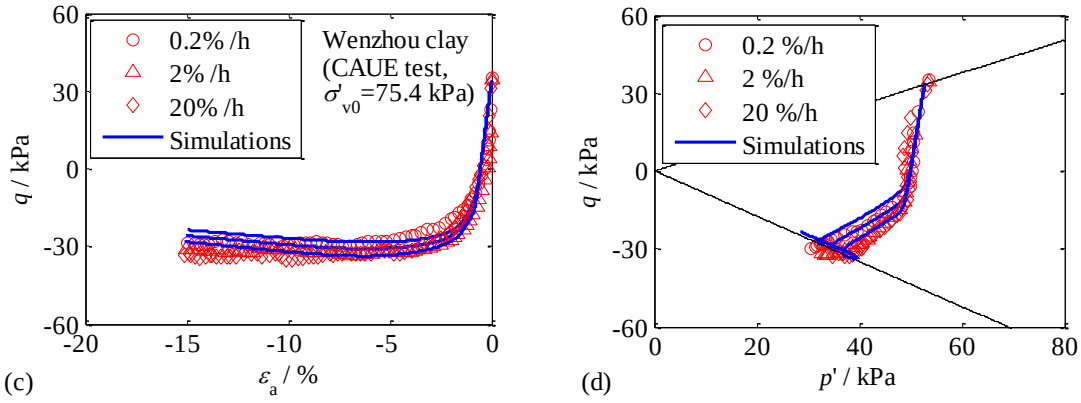

Figure 5.11 Comparisons between simulated and experimental results of undrained triaxial CRS tests on samples K_0-consolidated at a vertical stress of 75.4 kPa: (a, b) in compression and (c, d) in extension.

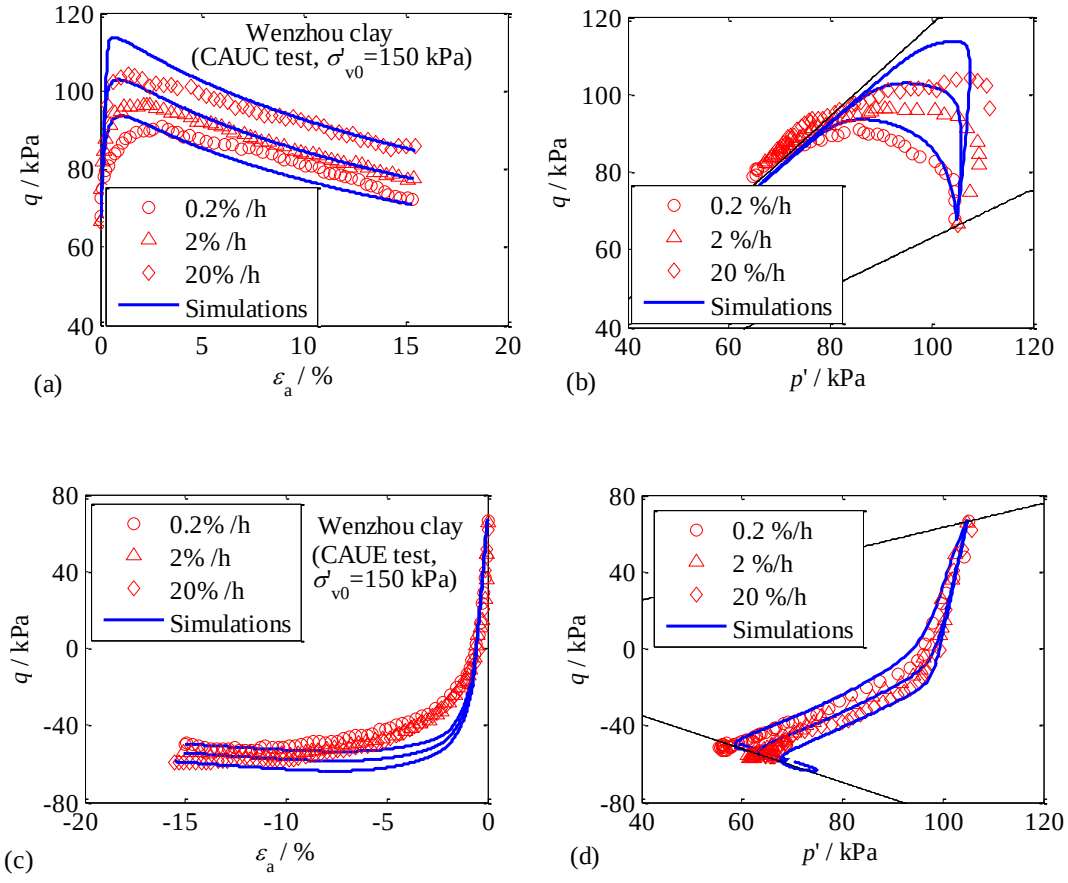

Figure 5.12 Comparisons between simulated and experimental results of undrained triaxial CRS tests on samples K_0-consolidated at a vertical stress of 150 kPa: (a, b) in compression and (c, d) in extension.

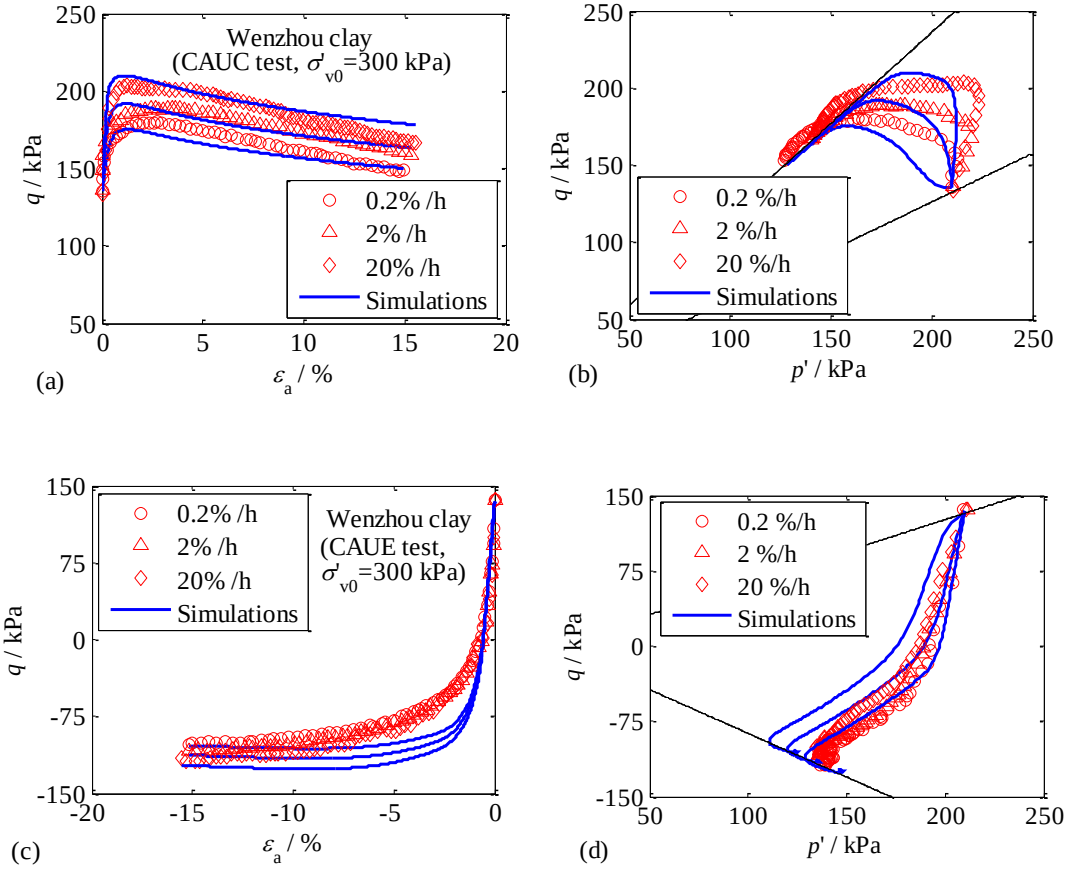

Figure 5.13 Comparisons between simulated and experimental results of undrained triaxial CRS tests on samples K_0-consolidated at a vertical stress of 300 kPa: (a, b) in compression and (c, d) in extension.

5.5.3.3 Undrained triaxial creep tests

Four undrained triaxial creep tests on K_0-consolidated samples (σ'_{v0}=150 kPa) under different applied stress levels ($\Delta\sigma'_{v0}$=12.6, 16.8, 20.5 and 25.6 kPa) were simulated using the enhanced ANICREEP model with parameters obtained using the new RCGA. The comparison between experimental and simulation results is shown in Figure 5.14, demonstrating again the good predictive ability of the model and the good quality of the optimization procedure of the new RCGA. Note that the simulation performance of mean effective stress-time relations is less good than that of axial strain, which can be improved by revising the stress-dilatancy relation in the model according to Wang and Yin [219].

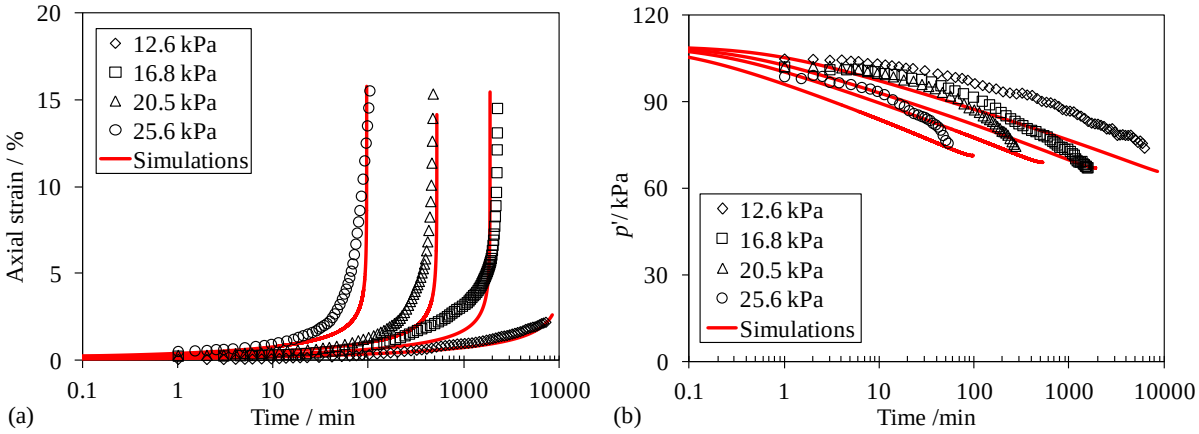

Figure 5.14 Comparisons between simulated and experimental results of undrained triaxial creep tests: (a) axial strain versus time; (b) mean effective stress versus time.

5.6 Discussion

As shown in the previous validation, the error between experiments and simulations for tests with different stress paths and loading rates is different. Then, if different tests are combined as objectives, the optimized parameters will be different. In this part, a comparative study is presented for the choice of the loading rates and load paths during the optimization based parameters identification.

Table 5.6 Three sets of optimal parameters with objective errors for Wenzhou clay based on different objective combinations

Combinations	Optimal parameters								Objective error /%
	κ	λ_i	M	$C_{\alpha ei}$	χ_0	ξ	ξ_d	n	
Comb-2	0.062	0.294	1.16	0.0078	10	5.5	0.35	0.75	6.96
Comb-3	0.070	0.221	0.99	0.0071	5.0	11.0	0.50	0.90	10.41
Comb-4	0.050	0.201	1.17	0.0066	9.0	13.5	0.275	0.9	9.46

The influence of the loading rate on parameter identification was first evaluated by adopting the undrained triaxial compression tests with strain-rates of 0.2%/h, 2%/h and 20%/h under a same vertical effective stresses (σ'_{v0}= 150 kPa) in the optimization (marked as "Comb-1"). Then, for investigating the influence of loading path, three undrained triaxial extension tests (σ'_{v0}=75.4, 150 and 300 kPa) at a same strain-rate of 2%/h were selected as objectives (marked as "Comb-2"), and

two undrained triaxial compression tests (σ'_{v0}=75.4 and 300 kPa) with one undrained triaxial extension test (σ'_{v0}=150 kPa) at a same strain-rate of 2%/h were selected as objectives (marked as "Comb-3"). The same K_0-compression test was used together for all three combinations. The same identification procedure was used for the above three combinations unlike the one based on undrained triaxial compression tests.

All the optimized parameters were summarized in Table 5.6. Together with the previous case in Table 6 (marked as "Std"), the combination with different loading rates gives a smallest objective error, followed by the "Std", "Comb-3" and "Comb-2". To evaluate the performance of each choice or combination, optimized values of λ_i, M, $C_{\alpha ei}$ and χ_0 were compared to measurements respectively, shown in Figure 5.15. It can be observed that, the combination with different loading rates gives a smallest objective error, followed by the "Std", "Comb-3" and "Comb-2".

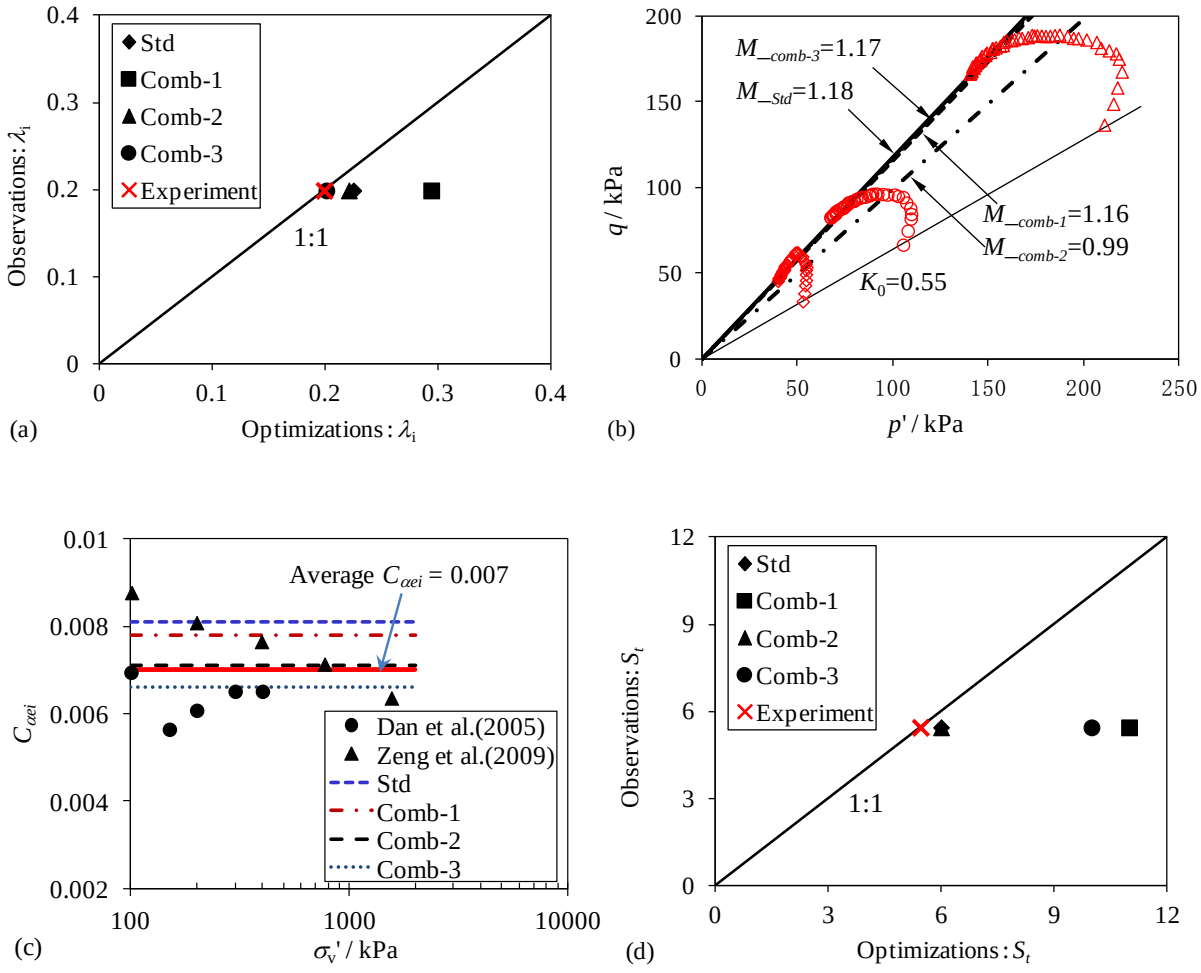

Figure 5.15 Comparisons of different optimal parameters obtained from different combinations of objective tests

For each combination, all optimized parameters were used to simulate other oedometer and triaxial test. The total average errors between experimental data and simulations were calculated and plotted in Figure 5.16 for comparison. The combination with different loading rates gives the smallest objective error, followed by the "Std", "Comb-3" and "Comb-2". , the extension test combining with compression tests involved in the objective can result in more accurate parameters.

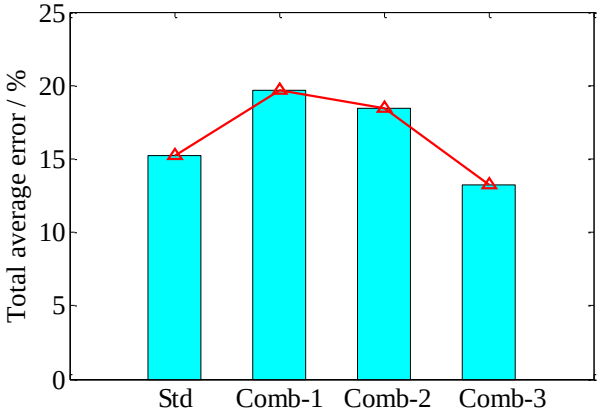

	Vertical stress (kPa)	Strain rate (% /h)	Compression (C) or Extension (E)
Std:	75.4, 150 and 300	2.0	3C
Comb-1:	150	0.2, 2.0 and 20	3C
Comb-2:	75.4, 150 and 300	2.0	3E
Comb-3:	75.4, 150(E) and 300	2.0	2C+1E

Figure 5.16 Comparisons of total average errors simulated by optimal parameters for different combinations of objective tests

Overall, the "Std" and "Comb-3" have relatively better performance compared to others. Note that the undrained triaxial extension test is not a conventional test in laboratory and more difficult to be conducted, because by adding the extension test into objective can increase the difficulty in identifying model parameters, which is not our original intention. Thus, the proposed optimization method using three undrained triaxial compression tests as the objective is more suitable in terms of the accuracy of parameters and practical convenience.

5.7 Conclusions

An efficient optimization method for identifying parameters of soft structured clay using standard experimental tests has been proposed, in which an appreciation of genetic algorithms and constitutive models are required. A newly developed elastic viscoplastic model accounting for soil

viscosity, anisotropy and destructuration was adopted and enhanced with cross-anisotropy of elasticity for simulating laboratory tests on soft structured clays.

The new RCGA with uniform samplings was first examined and discussed in terms of the optimization performance. The results demonstrate that an optimal solution can be guaranteed by the new RCGA. The computational effectiveness and efficiency of the new RCGA, was considered to be better compared to the commonly used NSGA-II. The optimization performance of the new RCGA was further examined by comparing the optimized values for the intrinsic compression coefficient, the slope of the critical state line, the initial bonding ratio and the intrinsic secondary compression coefficient with specific experimental measurements. The results demonstrate that the new RCGA solution is more suitable than the NSGA-II. The new RCGA solution was then further validated by simulating other tests on the same clay with different stress paths: 1D CRS tests with various strain-rates, 3D CRS tests in compression and extension with various strain-rates and 3D undrained creep tests, which demonstrate that the new RCGA solution is reliable. Therefore, it can be concluded that the new RCGA optimization is a suitable and efficient way to identify parameters of soft structured clays. All the results demonstrate that the determination of the whole set of parameters of an advanced elastic viscoplastic model for natural structured clays can be determined by simply using a limited number of conventional soil tests, if an appropriate identification procedure is undertaken.

The application of the advanced optimization methods in combination with advanced constitutive models could in the future be applied to field tests or measurements.

Chapter 6 Selection of sand models and identification of parameters

6.1 Introduction

Over the last few decades, the constitutive modeling of the mechanical soil behavior has achieved development. Numerous sand models have been proposed and applied within the framework of classical elasto-plasticity theory. They range from elementary and simple models (e.g., the Mohr-Coulomb model), to nonlinear models (the hardening soil model [221]), and to critical state based advanced models (e.g., the NorSand model [222], the Severn-Trent model [223] and the SANISAND model [224]). The micromechanical based models have attracted more attention and perform well in simulations (Yin et al. [148-150, 225]). Each of them has its advantages but also disadvantages in applications. Some models incorporating simple formula with few parameters are easy to use, if they are not accurate in their predictions. However, others incorporating complex formula with more parameters can give a relatively better prediction performance, but are difficult to apply in terms of the determination of parameters. Nowadays, engineers and researchers still lack knowledge about how to select model with the necessary features, and parameters which can be easily identified.

In recent years, the optimization methods have become increasingly been used and attracted more attention in geotechnical field as their application are capable of reducing the high cost of laboratory testing or in-situ monitoring. In terms of parameter identification, many optimization algorithms have been successfully applied: (1) Gradient based algorithms and Simplex (Calvello and Finno [19]; Papon et al. [12]); (2) Genetic Algorithms (GA) (Levasseur et al. [13]; Papon et al. [12]); (3) Neural Networks Algorithms (Ghaboussi and Sidarta [226]; Obrzud et al. [21]); and (4) Particle Swarm Optimizer (PSO) Algorithms (Knabe et al. [30]). Among these advanced algorithms, genetic algorithms are based on stochastic principles, which are considered more robust than the gradient methods [12, 13]. For a single-objective problem, uniqueness of the optimal solution can be guaranteed by GA, which is independent of the initial populations compared to gradient-based methods [12]. Moreover, the GA is more powerful in solving the multi-objective problems than the gradient-based methods. Furthermore, a set of uniformly distributed Pareto solutions can be detected by GA compared to gradient-based methods [12, 13]. It has been reported that the use of a genetic algorithm to identify soil parameters is particularly suitable when the topology of the error function

is complex (Papon et al. [12]). Therefore, the optimization method using a genetic algorithm is considered appropriate for model selection and parameter identification.

The Genetic Algorithm (GA) originally developed by Holland [52] is a simulation mechanism based on Darwinian natural selection, and a genetics computational model of the biological evolutionary process. It is also a process used to search for an optimal solution by simulating natural evolution. In recent years, different advanced genetic algorithms based on the theory of the original GA have been proposed, and have been used to solve many geotechnical problems (Wöhling et al. [227]; Rokonuzzaman et al. [18]; Papon et al. [12]). There are two types of GA: namely fixed-length binary coded GA and real coded GA (RCGA). The performances of binary GAs are found to be satisfactory on small and moderate sized problems which don't require much precision in the solution. But for high dimensional problems in which a higher degree of precision is desired, binary GAs require huge computational time and memory (Goldberg [54]). In the other hand, the RCGAs are designed especially for continuous optimization problems (Herrera et al. [203]; Mokhade and Kakde [135]), which is the case for the identification problems in geotechnical fields. Thus, it is more suitable to adopt the RCGA to tackle these problems. Then, an efficient RCGA is necessary for parameter identification.

This chapter aims to discuss the selection of sand models and the identification of their parameters with a genetic algorithm. A real-coded genetic algorithm has been enhanced for the optimization with high efficiency. Conventional triaxial tests on Hostun sand have been chosen as the objectives. Four relative simple constitutive models with gradually increasing numbers of features, referred to as MC (Mohr-Coulomb model), NLMC (Nonlinear Mohr-Coulomb model), CS-NLMC (Critical state based nonlinear Mohr-Coulomb model) and CS-TS (Critical state based two-surface model) have been selected for optimization. For each model, the optimized parameters were used to simulate other tests on the same sand to evaluate the model's predictive ability. Once the appropriate model with its associated features was determined, then the selection of the type of tests (e.g., drained and/or undrained tests) as the objectives to identify the model parameters was evaluated. The number of tests in the objective is then examined to obtain the relative accuracy and reliability of the parameters. Finally, the strain levels of objective tests for identifying parameters are estimated.

6.2 Genetic algorithm based optimization

In this section, the genetic algorithm-based optimization is introduced. Before conducting the optimization, three key points need to be clearly introduced: (1) the error function, to measure the

difference between model predictions and corresponding observations; (2) the initialization method, to generate the initial population for the optimization; and (3) the optimization algorithm, to control the optimization process.

6.2.1 Error function

The discrepancy between the measured and the modeled behavior has been expressed by a scalar error function, 'Error', in the sense of the least square method introduced by Levasseur et al. [13],

$$\mathrm{Error}(x)=\sqrt{\frac{\sum_{i=1}^{N}\left(\frac{U_{\exp}^{i}-U_{num}^{i}}{U_{\exp}^{i}}\times 100\right)^{2}}{N}}\%\qquad(6\text{-}1)$$

where x is a vector of parameters; N is the number of values; $U_{\exp}^{i}$ is the value of measurement point i; U_{num}^{i} is the value of calculation at point i.

Note that different cost function made of error functions or the error function with different weights for different variables can result in different results, as discussed in Levasseur et al. [13]. In our case, the scale effects on the fitness between the experimental and the simulated results can be eliminated by this normalized formula of Eq.(1), and the same weight for different variables is adopted for ensuring the whole performance. Additionally, the objective error calculated by this function is a dimensionless variable; thus, any difference in error can be avoided for different objectives with different variables.

6.2.2 Adopted hybrid real-coded genetic algorithm and initialization method

The newly developed RCGA in chapter 3 was employed to conduct this optimization process. The initial population for a genetic algorithm is usually generated by a uniform sampling method. For uniform sampling, a method introduced by Sobol [28] has been adopted in this study. It is a deterministic algorithm that imitates the behavior of the Random Sequence. The aim is to obtain a uniform sampling of the design space. It has been reported as being suitable for problems with up to twenty variables.

6.2.3 Optimization procedure

The aim of the inverse modeling procedure (see Figure 6.1) is to find values for the model parameters that provide the best attainable fit between model predictions and corresponding observations. In this study, a mono-objective framework with two criteria was considered:

$$\min\left[\text{Error}(x)\right] = \min\left[\frac{\text{Error}(q) + \text{Error}(e)}{2}\right] \tag{6-2}$$

where Error(q) is the average difference in deviatoric stress between simulations and objectives; and Error(e) is the average difference in void ratio between simulations and objectives.

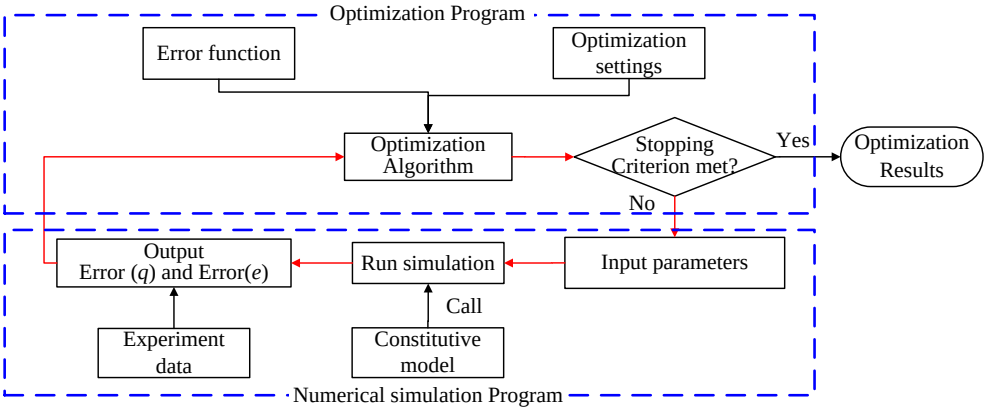

Figure 6.1. Identification procedure

In order to focus on the key parameters which are not easily determined or where their determination could involve more experimental costs, parameters such as Young's modulus and Poisson's ratio which can be directly measured from experiment are not considered in the optimization. Thus, the number of parameters and their physical attributes for each model are not always the same, and they depend on which model is selected. Therefore the intervals of parameters for every selected model are given in the following sections according to the sand models selected in this study.

For the optimization algorithm, each population was generated using the initialization algorithm Sobol. The initial population was set to 100 individuals and the size of the population kept constant during the optimization process. The number of generations was set to 50 and was tested sufficiently to obtain the optimal results for this study.

6.3 Selection of features of sand necessary for constitutive modeling

This section is based on laboratory tests on sand and the use of the genetic optimization method to identify which features of sand have to be taken into account in constitutive modeling. The purpose is to find a constitutive model which can adequately describe the sand behavior with only a limited number of parameters to be identified. Note that the study is based on industry-demand conventional triaxial tests, and thus high-level features (such as anisotropy, non-coaxial behavior, cyclic behavior, etc.) are not considered in this study.

6.3.1 Brief introduction of selected tests

The tests selected for this study are drained triaxial tests performed on Hostun sand by Liu et al. [228] and Li et al. [229]. Hostun sand has a high siliceous content.

Table 6.1 Index properties of Hostun sand

Particle Shape	SiO_2	G_s	d_{50}/mm	e_{max}	e_{min}	C_u
angular to sub-angular	>99.24 %	2.6	0.35	0.881	0.577	1.4

Table 6.1 shows the main physical properties of Hostun sand. In the optimization, three drained triaxial tests (p'_0=100 kPa, e_0=0.66; p'_0=200 kPa, e_0=0.83; and p'_0=400 kPa, e_0=0.82) were selected as the objective to obtain the critical state related parameters. All the tests were isotropically consolidated to the corresponding consolidation pressure before shearing. The experimental results for the three drained triaxial tests are shown in Figure 6.2.

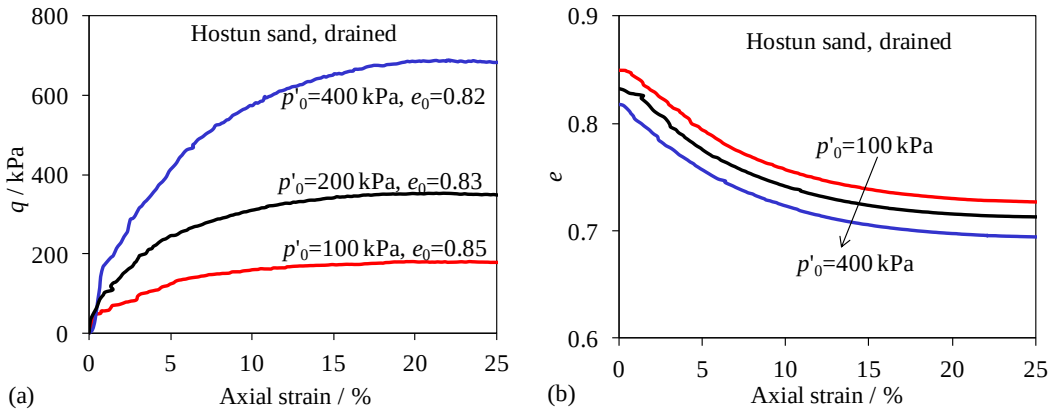

Figure 6.2. Results of drained triaxial tests on Hostun sand: (a) deviatoric stress versus axial strain; (b) void ratio versus axial strain

In order to identify the sand features which should be considered in constitutive modeling, four sand models with a gradually increasing number of features and different numbers of parameters were chosen to simulate the objective tests, which are (1) an elastic-perfectly plastic Mohr-Coulomb model (MC), (2) a nonlinear Mohr-Coulomb model (NLMC), (3) a critical state based nonlinear Mohr-Coulomb model (CS-NLMC) and (4) a critical state based two-surface model (CS-TS). The comparisons of constitutive laws for the four sand models are shown in Table 5.3. For MC, the Young's modulus is constant. For NLMC, CS-NLMC and CS-TS, the Young's modulus is expressed as follows, according to Richard et al. [145],

$$E = E_0 \cdot p_{at} \frac{(2.97-e)^2}{(1+e)} \left(\frac{p'}{p_{at}} \right)^{\zeta} \tag{6-3}$$

where E_0 is the reference value of Young's modulus; e is the void ratio; p' is the mean effective stress; p_{at} is the atmospheric pressure used as reference pressure (p_{at} = 101.3 kPa); and ζ is a constant.

The parameters of each selected model can be divided into: (1) elastic parameters; (2) plastic shear hardening related parameters; (3) stress-dilatancy related parameters, and (4) critical state related parameters for critical state based models. The two elastic parameters, E_0 and ζ, were easily obtained from isotropic compression tests as shown in Figure 6.3. A typical value of Poisson's ratio υ=0.2 was assumed for the sand. All the other parameters were identified by the optimization method. Note that for MC, the elastic parameter was selected for optimization because the overall deformation before the maximum shear strength is entirely controlled by the elastic stiffness. For the optimization, the intervals of the parameters are given in Table 6.3, which cover their typical values for sand.

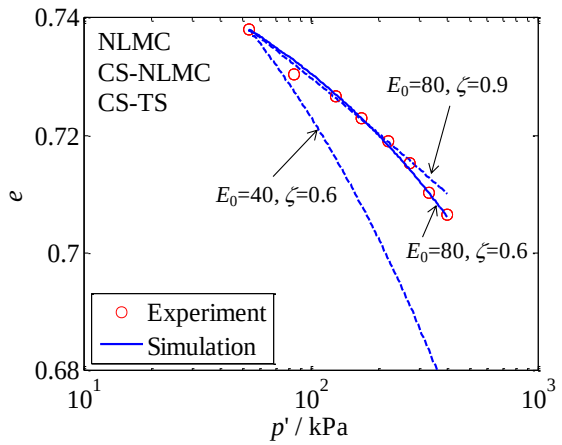

Figure 6.3. Calibration of elasticity parameters by using isotropic compression test on Hostun sand

Table 6.2 Typical constitutive relations of four selected sand models

Constitutive models	MC	NLMC	CS-NLMC	CS-TS
Elastic behavior	$\dot{\varepsilon}_{ij}^{e}=\frac{1+\upsilon}{E}\sigma'_{ij}-\frac{\upsilon}{E}\sigma'_{kk}\delta_{ij}$			
Yield function	$f=\frac{\sigma_1-\sigma_3}{2}-\frac{\sigma_1+\sigma_3}{2}\sin\phi$	$f=\frac{q}{p'}-H=0$	$f=\frac{q}{p'}-H=0$	$f=\left(q-p\alpha\right)^2-m^2p^2=0$
Potential function	$g=\frac{\sigma_1-\sigma_3}{2}-\frac{\sigma_1+\sigma_3}{2}\sin\psi$	$\frac{\partial g}{\partial p'}=M_{pt}-\frac{q}{p'}$ with $\frac{\partial g}{\partial q}=1$ $M_{pt}=\frac{6\sin\phi_{pt}}{3-\sin\phi_{pt}}$ with $\phi_{pt}=\phi_{\mu}-\psi$	$\frac{\partial g}{\partial p'}=A_d\left(M_{pt}-\frac{q}{p'}\right)$ with $\frac{\partial g}{\partial q}=1$ $M_{pt}=\frac{6\sin\phi_{pt}}{3-\sin\phi_{pt}}$	$D=A_d\left(M_{pt}-\alpha\right)$ $M_{pt}=\frac{6\sin\phi_{pt}}{3-\sin\phi_{pt}}$
Hardening law	-	$H=\frac{M_p\varepsilon_d^p}{k_p+\varepsilon_d^p}$ with $M_p=\frac{6\sin\phi_p}{3-\sin\phi_p}$	$H=\frac{M_p\varepsilon_d^p}{k_p+\varepsilon_d^p}$ with $M_p=\frac{6\sin\phi_p}{3-\sin\phi_p}$	$h=k_p\frac{\left\|\mathbf{b}:\mathbf{n}\right\|}{b_{ref}-\left\|\mathbf{b}:\mathbf{n}\right\|}$
Critical state	-	-	$e_c=e_{ref}-\lambda\ln\left(\frac{p'}{p_{at}}\right)$	$e_c=e_{ref}-\lambda\ln\left(\frac{p'}{p_{at}}\right)$
Inter-locking	-	-	$\tan\phi_p=\left(\frac{e_c}{e}\right)^{n_p}\tan\phi_{\mu}$; $\tan\phi_{pt}=\left(\frac{e_c}{e}\right)^{-n_d}\tan\phi_{\mu}$	$\tan\phi_p=\left(\frac{e_c}{e}\right)^{n_p}\tan\phi_{\mu}$; $\tan\phi_{pt}=\left(\frac{e_c}{e}\right)^{-n_d}\tan\phi_{\mu}$
Number of parameters	4	5	10	10

Table 6.3 Search domain for different parameters of constitutive models

Model	MC			NLMC			CS-NLMC and CS-TS							
Parameters	E_0	ϕ_u	ψ	ϕ_μ	ψ	k_p	e_{ref}	λ	ϕ_μ	k_p	k_p (CS-TS)	A_d	n_p	n_d
Lower bound	0	10	0	10	0	0	0.5	0	10	0	0	0	0	0
Upper bound	50000	50	20	50	20	0.1	1	0.1	50	0.1	100	5	10	10
Step	1000	0.5	0.5	0.5	0.5	10^{-4}	0.001	0.0001	0.5	10^{-4}	1	0.1	0.1	0.1

6.3.2 Performance of the enhanced RCGA

The optimization is performed by using the CS-NLMC model and one test result (p'_0=200 kPa, e_0=0.83) as example, the computational effectiveness and efficiency of the enhanced RCGA was assessed. In order to highlight the advantages of the new RCGA, the Multi-Objective Genetic Algorithm (MOGA-II, a binary-coded genetic algorithm) presented by Poles et al. [191] with high search ability (see Papon et al. [12]) was chosen as a comparative objective to conduct the same optimization. The parameters of two GAs are shown in Table 6.4. The optimal parameters are presented in Table 6.5. It can be seen that two sets of parameters are almost the same. It demonstrates that the new RCGA has also an outstanding search ability for tackling the problem of parameter identification.

Table 6.4 Parameters of selected algorithms

Algorithm	PopSize	NumGens	Selection	p_C	p_D	p_M	Elitism
New RCGA	100	50	Tournament	0.9	0.5	0.05	Yes
MOGA-II	100	50	Tournament	0.9	0.5	0.05	Yes

Moreover, the efficiency is important for assessing an algorithm. Figure 6.4 shows the evolution of the minimum objective in each generation with the increase of the number of generations. It can be seen that the convergence speed is lower during small number of generations and higher in a high number of generations for the new RCGA, compared to MOGA. This is due to the DRM used in the new RCGA. The DRM is a self-adaptive mutation, which provides a greater chance of population variation by producing a relatively large allowable step size for the mutation at every beginning evolution period. This can result in a higher probability for escaping from the local traps. When the population gradually converges to the optimum solution, a small mutation region produced by DRM

is likely to enhance the precision of the obtained solution. The number of generations corresponding to convergence is 26 for the new RCGA and 33 for the MOGA-II, which indicates that the new RCGA shows a faster convergence speed than MOGA-II. This is a key point for GA optimization in identifying parameters from tests.

Overall, the proposed enhanced RCGA performs well in searching the optimal solution and has a faster convergence speed than MOGA-II. Furthermore, judging from the continuity of the geotechnical problem, the new RCGA is more suitable than other classical binary GAs due to its advantages in encoding. Therefore, only the new RCGA is used to conduct the optimization procedure in the following sections.

Table 6.5 Optimal parameters with the optimal errors of testing for two selected GAs

Initialization method	Optimal parameters							Average error /%
	e_{ref}	λ	ϕ_μ	k_p	A_d	n_p	n_d	
RCGA	0.745	0.030	28.9	0.0039	1.1	2.8	1.9	3.88
MOGA-II	0.743	0.029	28.9	0.0037	1.0	2.8	2.4	3.82

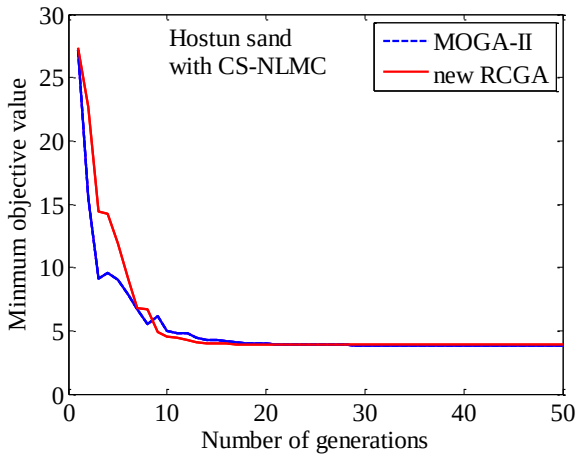

Figure 6.4. Evolution of minimum objective error in each generation with increasing the number of generations

6.3.3 Optimization results and discussion

The optimization using the MC model was conducted first, followed by NLMC, CS-NLMC and CS-TS in sequence. Since this problem is mono-objective, the set of parameters with the lowest error

was selected and was considered as the optimal set of results. The optimization results with objective error are shown in Table 6.6.

Table 6.6 Optimal parameters and error for four sand models

Model	MC			NLMC			CS-NLMC (CS-TS)						
Parameters	E_0	ϕ_u	ψ	ϕ_μ	ψ	k_p	e_{ref}	λ	ϕ_μ	k_p	A_d	n_p	n_d
Values	15500	27.0	0.0	31.5	0.0	0.022	0.739 (0.739)	0.0253 (0.0253)	29.0 (29.0)	0.0061 (29)	0.8 (0.7)	1.9 (1.7)	4.3 (5.4)
Error / %	36.43			5.31			2.91 (2.81)						

The comparisons between the optimal simulations and the objective tests are shown in Figure 6.5. The errors between the optimal simulations and the objective tests of the four selected models are shown in Figure 6.6. It can be seen that the worst performance of the simulations is found in MC, followed by NLMC. Both CS-NLMC and CS-TS perform well and are much better in stress-strain behavior than the MC and NLMC models. The reason for this is that the four selected models have different features in describing the sand behavior. First, since the MC model is an elastic-perfectly plastic model, the stress-strain nonlinearity cannot be described. In contrast to MC, a nonlinear plastic stress-strain behavior is incorporated into NLMC, which results in a better performance than that given by MC. In other words, the incorporation of nonlinear elastic and plastic stress-strain features is essential for all sand models. In terms of CS-NLMC and CS-TS, a better agreement between the simulations and the experiments is obtained than when using NLMC. This indicates that it is necessary to incorporate the critical state concept in sand models for simulation. Note that the comparison of predictions is not surprising based on studies on critical states of sand during the last few decades, and this section also serves to show the performance of GA optimization as a basis for the following sections.

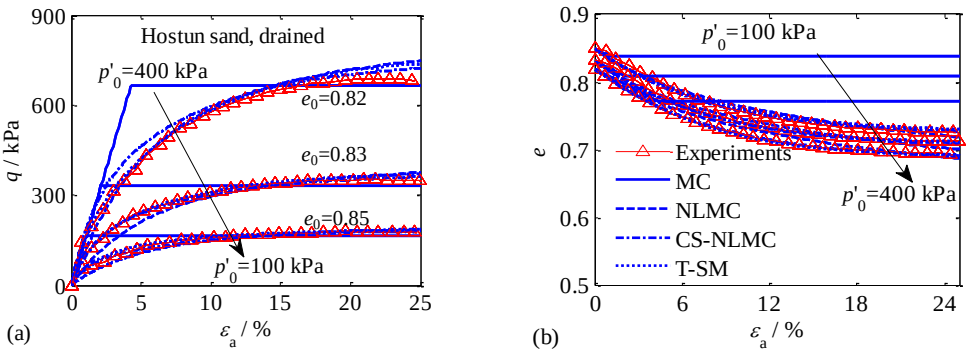

Figure 6.5. Comparisons between the simulations and the objective tests for four selected models

Additionally, the slight difference between CS-NLMC and CS-TS is related to the plastic hardening law. In contrast to CS-NLMC, which incorporates a hyperbolic plastic hardening law, the CS-TS model incorporates the bounding surface concept based hardening law with an small elastic domain proposed by Manzari and Dafalias [230], which is slightly more accurate in the simulation.

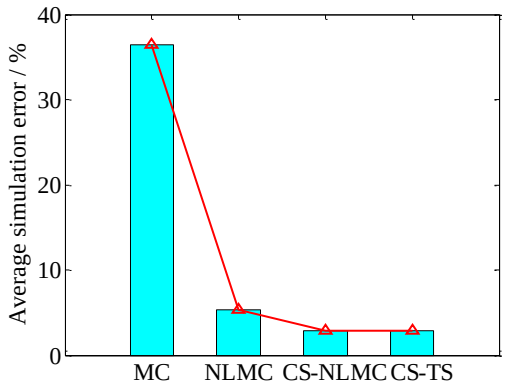

Figure 6.6 Average errors between optimal simulations and objective tests of four selected models

Overall, the features of sand necessary in constitutive modeling are nonlinear plastic hardening behavior, and the critical state concept with an interlocking effect. On the basis of these feathers, both the CS-NLMC and the CS-TS models are recommended to simulate sand behavior.

In order to further validate the ability of the selected models to describe the sand behavior, other triaxial tests performed on the same Hostun sand were simulated by selected models using the optimized parameters. The error between simulations and experiments was calculated simultaneously. Figure 6.7 shows the average simulation error of the four models for all the tests. Again, the CS-TS model results in the best performance in the simulation, followed by CS-NLMC, NLMC and MC.

Figure 6.8 shows the comparisons between the simulations and the experiments for CS-NLMC and CS-TS, and based on these, the CS-NLMC and CS-TS models are still recommended. When two numerical models perform equally well in predicting test phenomena, additional criteria need to be selected to judge the merit of the models. One useful guideline is to evaluate the complexity of the formulae adopted in the model and the type and number of parameters. According to this criterion, the CS-NLMC model is more suitable due to its relatively simple formulae compared to those in CS-TS. Numerical convergence is easier to obtain when the simple formulae are used to deal with complex geotechnical problems. Since the bounding surface concept is not necessary for describing

monotonic behavior, the CS-NLMC model was chosen as an appropriate sand model for the following sections.

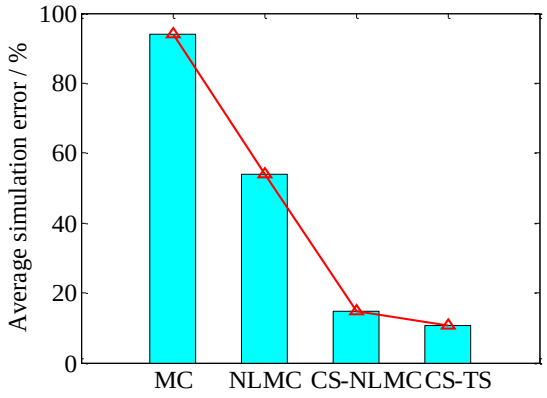

Figure 6.7 Average simulation errors of MC, NLMC, C-SNLMC and CS-TS

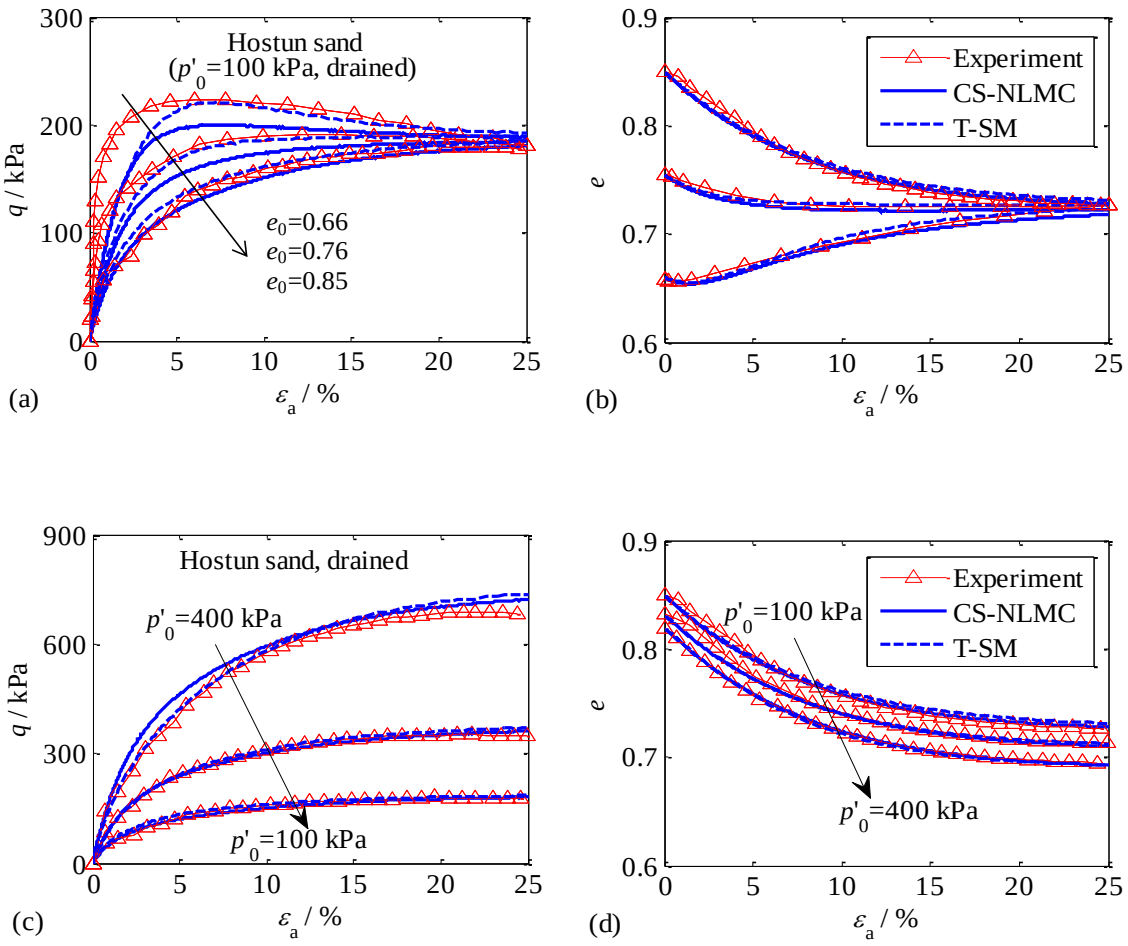

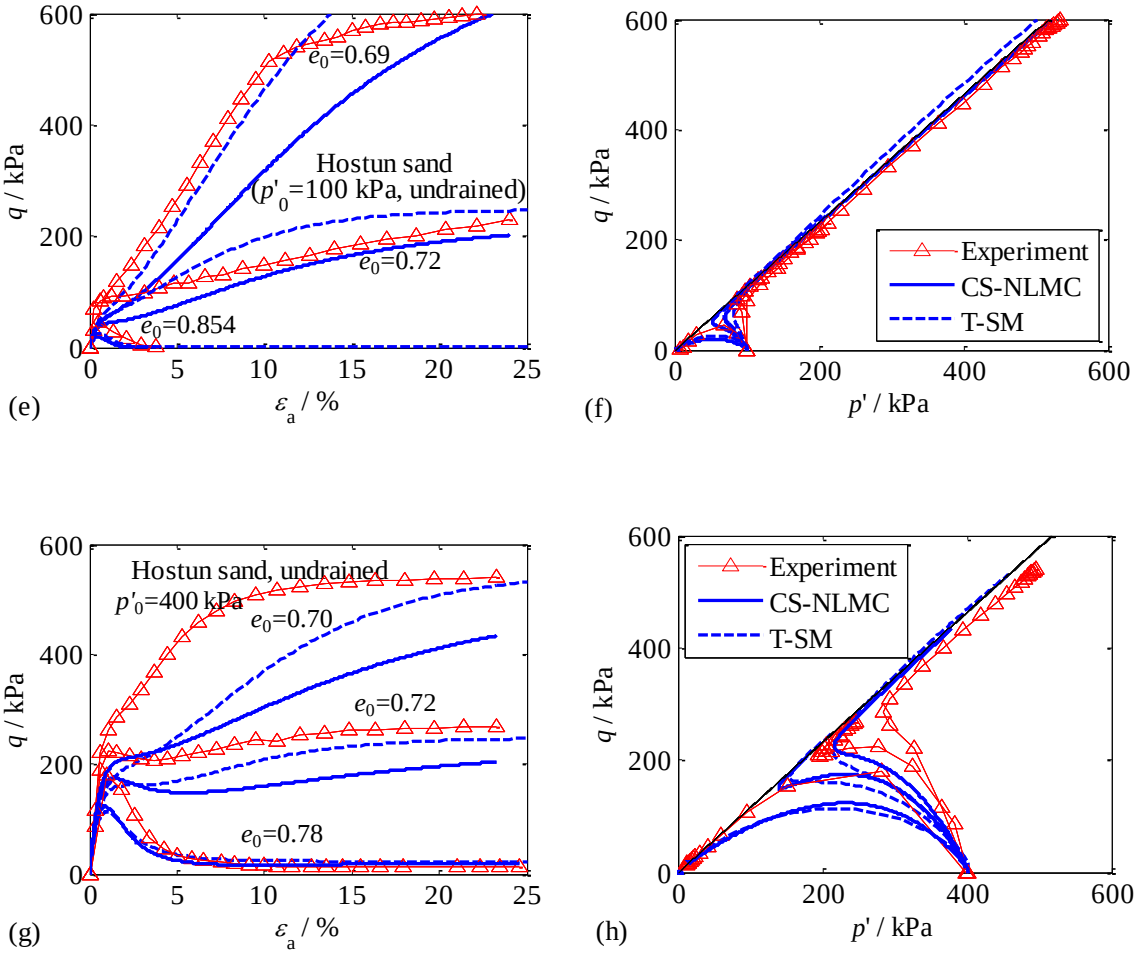

Figure 6.8. Comparisons between simulation and experiments for CS-NLMC and CS-TS

6.4 Selection of test type for identification of parameters

Besides drained triaxial tests, undrained triaxial tests can also be conducted for estimating soil properties. To better identify the parameters, the performance of different combinations of drained and undrained triaxial tests as objective tests needs to be examined. For this purpose, three drained and three undrained triaxial tests performed on Hostun sand were selected for possible combinations of the GA objective. The results of the selected tests are shown in Figure 6.9 and are marked by the sequence number. The sequence number and the information for the corresponding test are presented in Table 6.7. Three tests were selected randomly as a combination from the total of six tests. Thus, twenty different combinations in total are examined in this section, and are summarized in Table 6.8.

In order to analyze the effect of the test type on the identification of parameters, all the combinations in Figure 6.7 were divided into four groups according to the number of undrained tests

in the objective, and were marked as 3CDs, 2CDs+UD, CD+2UDs and 3UDs (CD and UD representing drained and undrained tests, respectively). Four groups with simulation errors are plotted in Figure 6.10. It can be found that the average error first decreases and then increases with the increasing number of undrained tests in the objective. However, there are scatter points with large simulation errors among all the combinations.

Table 6.7 Number of optimum objectives

Number of tests	Initial void ratio e_0	Confining pressure σ_3 / kPa	Drainage conditions
①	0.85	100	CD
②	0.83	200	CD
③	0.82	400	CD
④	0.72	100	UD
⑤	0.73	200	UD
⑥	0.72	400	UD

A possible reason that leads to poor simulations is the determination of CSL parameters, as found in Figure 6.11, which comprises critical state line between predictions and experiments for different combinations. Note that the experimental critical states in the figure are apparent points corresponding to a strain level of 25%. It can be seen that the combinations with close final states of e, p' in the e-log p' space could lead to an incorrect CSL, as found in combinations 8, 10 and 20. These incorrect CSLs may lead to poor simulated results. In contrast, the combinations with dissimilar final states of e, p' may give a generally accurate critical state line and result in a good simulation performance, such as combinations 5 and 15. Figure 6.12 shows the comparison of results between experiment and simulation for three typical CSLs.

The same optimization procedure was carried out for all combinations. The optimal parameters and the corresponding objective errors for the different combinations are listed in Table 6.8. In order to evaluate the performance of each combination, the optimal set of parameters was applied to simulate five drained tests and six undrained tests with different confining pressures and void ratios on the same Hostun sand, as performed by Liu et al. [228] and Li et al. [229]. Simulation errors were also calculated, as shown in Table 6.8.

Table 6.8 Optimal parameters and errors of different combinations

Number	Combinations	Optimal parameters							Objective error/%	Average error / %
		e_{ref}	λ	ϕ_μ	k_p	A_d	n_p	n_d		
1	①②③	0.739	0.0253	28.5	0.0038	1.1	2.4	2.6	3.46	13.43
2	①②④	0.735	0.0188	29.0	0.0025	0.7	3.1	5.0	5.16	11.11
3	①②⑤	0.739	0.0212	29.0	0.0013	1.7	4.1	0.2	8.98	14.28
4	①②⑥	0.735	0.0181	29.0	0.0023	0.9	3.3	3.6	5.04	12.00
5	①③④	0.739	0.0260	28.5	0.0037	0.8	2.7	4.6	5.11	10.46
6	①③⑤	0.743	0.0281	29.0	0.0017	1.7	4.2	0.0	7.71	11.47
7	①③⑥	0.740	0.0262	29.0	0.0023	0.9	3.9	3.4	4.83	11.29
8	①④⑤	0.733	0.0117	28.0	0.0017	0.7	1.7	5.0	15.21	15.09
9	①④⑥	0.732	0.0142	28.0	0.0018	1.0	2.5	3.9	6.91	14.09
10	①⑤⑥	0.734	0.0127	28.5	0.0017	1.6	3.5	1.4	12.76	18.16
11	②③④	0.744	0.0286	29.0	0.0058	0.7	2.4	5.0	5.42	10.77
12	②③⑤	0.753	0.0340	29.0	0.0026	1.7	3.7	0.0	5.04	11.18
13	②③⑥	0.749	0.0314	29.0	0.0031	1.0	3.5	2.6	3.03	10.57
14	②④⑤	0.750	0.0334	29.5	0.0057	0.8	2.1	3.7	11.89	10.89
15	②④⑥	0.738	0.0219	29.0	0.0035	0.7	2.6	5.0	6.93	10.09
16	②⑤⑥	0.755	0.0374	28.5	0.0018	1.9	3.10	0.0	5.97	11.26
17	③④⑤	0.749	0.0317	29.0	0.0056	0.9	2.8	3.0	11.87	11.01
18	③④⑥	0.745	0.0294	29.5	0.0054	0.6	2.9	5.0	7.79	10.15
19	③⑤⑥	0.752	0.0333	28.0	0.0023	1.6	3.7	0.5	5.64	11.93
20	④⑤⑥	0.760	0.0467	28.5	0.0028	0.8	0.5	2.3	11.64	19.61

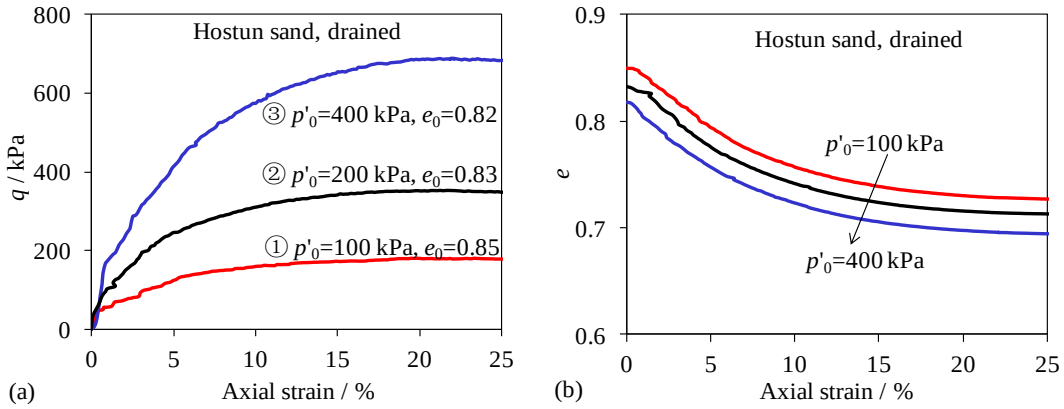

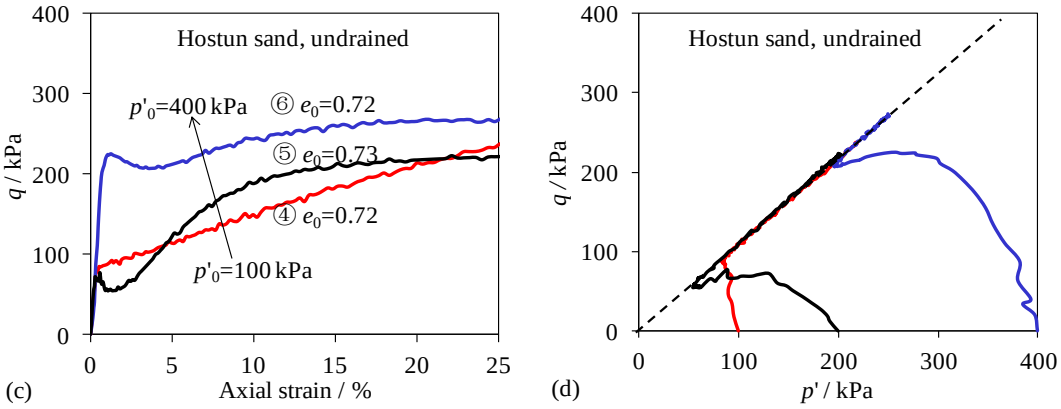

Figure 6.9. Results of drained and undrained triaxial tests of Hostun sand

In order to analyze the effect of the test type on the identification of parameters, all the combinations in Table 6.8 were divided into four groups according to the number of undrained tests in the objective, and were marked as 3CDs, 2CDs+UD, CD+2UDs and 3UDs (CD and UD representing drained and undrained tests, respectively). Four groups with simulation errors are plotted in Figure 6.10. It can be found that the average error first decreases and then increases with the increasing number of undrained tests in the objective. However, there are scatter points with large simulation errors among all the combinations. A possible reason for the poor simulations is the determination of CSL parameters, as shown in Figure 6.11, which shows a comparison of the critical state line between predictions and experiments for different combinations. Note that the experimental critical states in the figure are apparent points corresponding to a strain level of 25%. It can be seen that the combinations with close final states of e, p' in the e-log p' space could lead to an incorrect CSL, as found in combinations 8, 10 and 20. These incorrect CSLs may lead to poor simulated results. In contrast, the combinations with dissimilar final states of e, p' may give a generally accurate critical state line and result in a good simulation performance, such as combinations 5 and 15. Figure 6.12 shows the comparison of results between experiment and simulation for three typical CSLs.

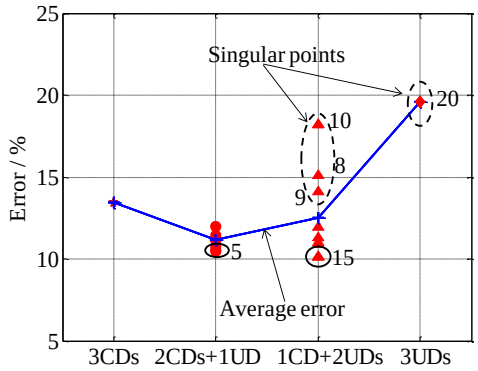

Figure 6.10. Simulation errors based on optimal parameters of different combinations

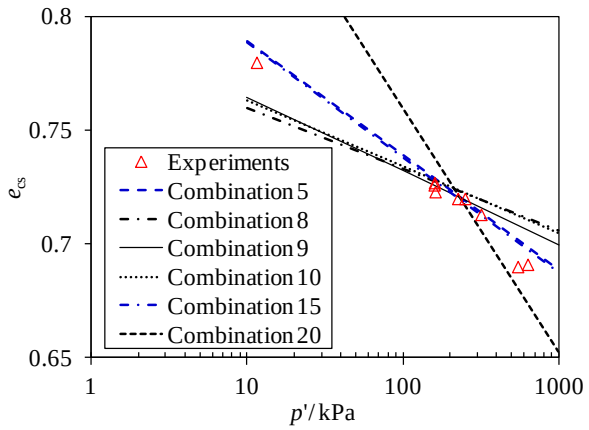

Figure 6.11. Critical state lines of different combinations

Overall, the performance of parameter identification can be further improved by using the combinations which contain both undrained and drained tests as objectives, apart from those combinations with close final states of e, p' which cause incorrect CSLs.

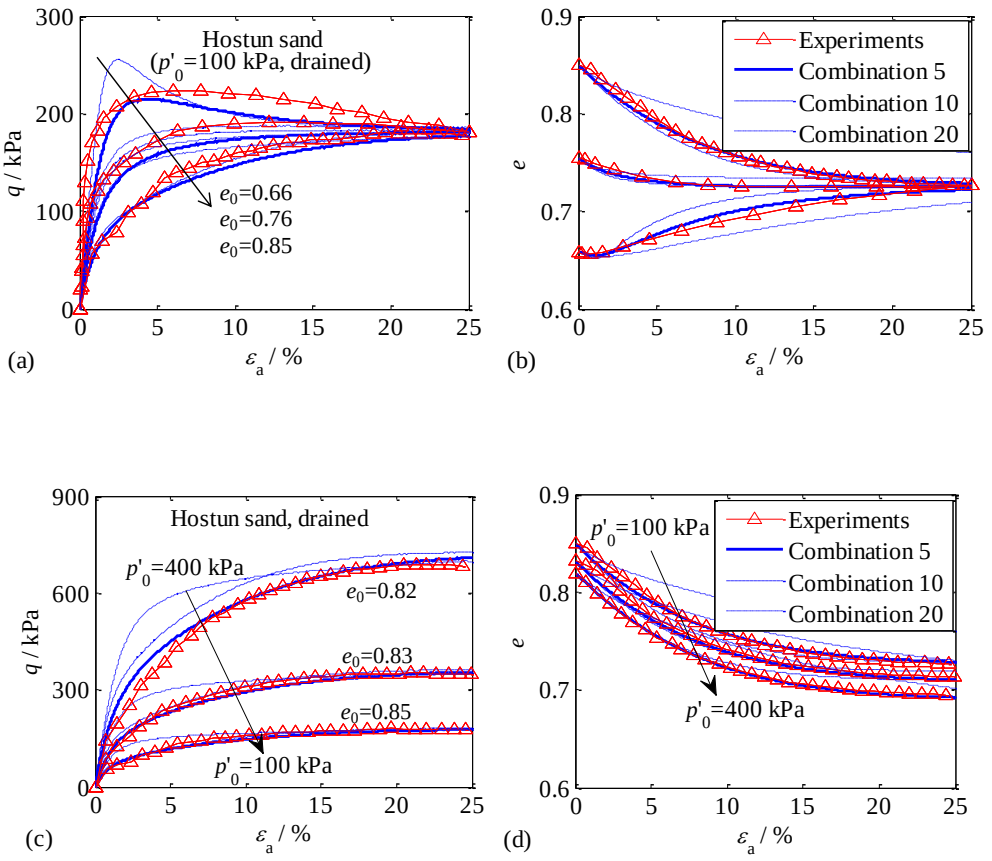

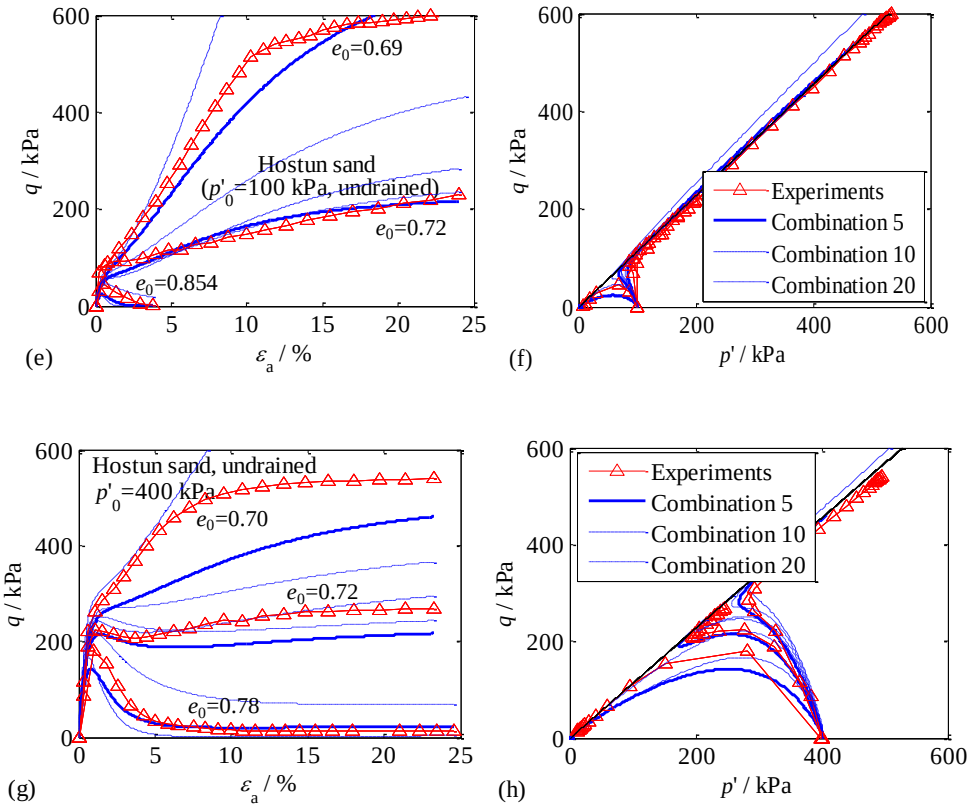

Figure 6.12. Results of simulation based on different combinations

6.5 Estimation of minimum number of tests for identification of parameters

As previously mentioned, the objective with one undrained test could result in a generally better performance. At the same time, the inaccurate CSL determined using selected tests could result in unsatisfactory parameters and simulations, which was highlighted previously. One possible way to avoid this problem is to add more tests to the objective in the optimization. Traditionally, three triaxial tests have been proposed for estimating strength parameters (e.g., cohesion, c, and friction angle, ϕ). However, for critical state based modeling, more tests should be used. Thus, this section aims to estimate the minimum number of tests required for modeling based on critical state.

In this case, in order to focus on the effect of the number of tests for the identification of parameters, there are two possibilities for adding more tests to the standard set of three drained tests. These are: (1) adding drained tests and (2) adding undrained tests. For adding drained tests, one or two more tests (marked as 3+1 or 3+2) were examined. For adding undrained tests, one to four more tests (marked as 3+1, 3+2, 3+3 and 3+4) were examined, based on the available tests carried out by Liu et al. [228] and Li et al. [229]. The test which is easy to carry out in the laboratory at low cost

should be selected first. Following this rule, the test on dense sand with relatively low confining pressure was first selected, and then the test with high confining pressure was subsequently added. The program for choosing tests is presented in Figure 6.13.

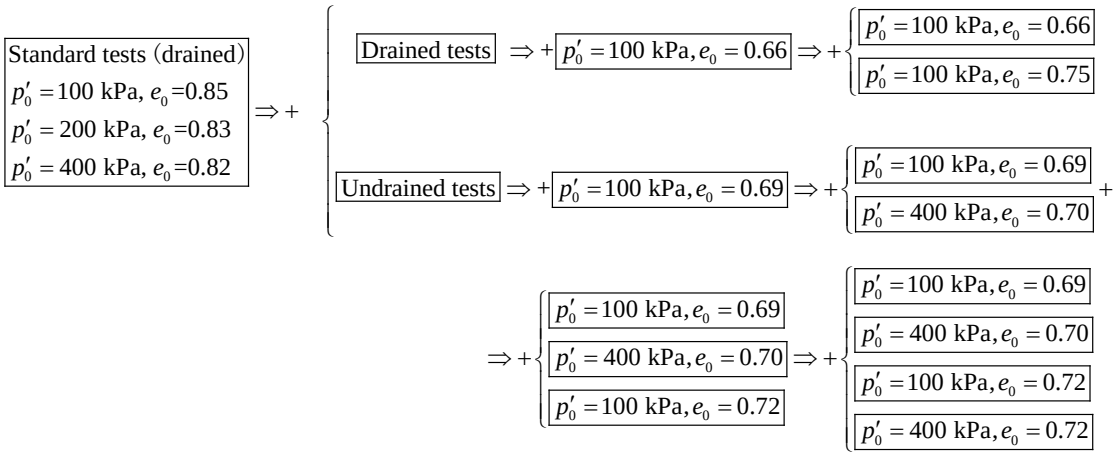

Figure 6.13. Program for selecting the effective number of tests

Table 6.9 Optimization parameters and error based on critical state sand model

Total Quantity	Additional tests		Optimal parameters							Average error /%
	drained	undrained	e_{ref}	λ	ϕ_μ	k_p	A_d	n_p	n_d	
3	0	0	0.739	0.0253	28.5	0.0038	1.1	2.4	2.6	13.43
3+1	+1		0.736	0.0273	28.5	0.0035	0.7	2.8	4.6	12.75
		+1	0.740	0.0275	29.0	0.0023	0.8	3.4	4.3	10.04
3+2	+2		0.737	0.0241	29.5	0.0033	0.8	2.9	3.8	10.60
		+2	0.740	0.0268	29.0	0.0019	0.8	3.4	4.3	10.66
3+3		+3	0.741	0.0272	29.0	0.0031	0.8	3.1	4.3	9.60
3+4		+4	0.742	0.0279	29.0	0.0022	1.0	3.4	2.7	10.04

The same optimization procedure was conducted for objectives with different numbers of tests. The optimal parameters are summarized in Table 6.9. In order to estimate the number of tests, other tests in addition to the objectives were simulated by CS-NLMC using each set of optimal parameters. Meanwhile, the differences between simulations and experiments were also computed, and the values of simulation errors are summarized in Table 6.9. The variation of errors with the increasing number of drained or undrained tests is plotted in Figure 6.14. It can be found that adding two tests

to the basic standard combination is sufficient to obtain accurate parameters. By using the optimal parameters obtained by adding two tests to the basic standard combination, the comparisons between experimental and simulated results are shown in Figure 6.15. Moreover, the results suggest also that model parameters identified by using three tests in practice are not reliable for critical state based constitutive models. Therefore, the minimum recommended number of tests for critical state based modeling is five.

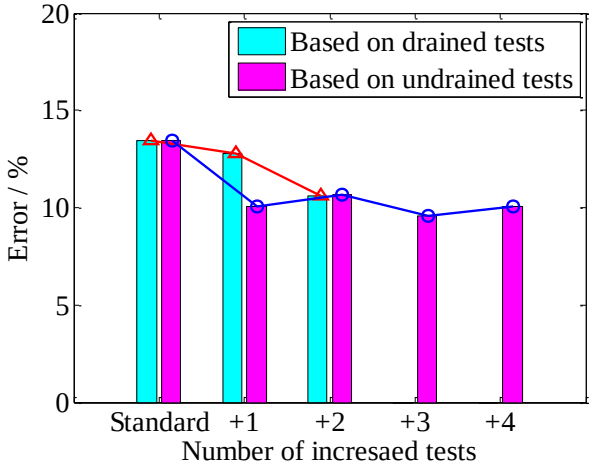

Figure 6.14. Variation tendency of errors with the increase of the number of drained or undrained tests

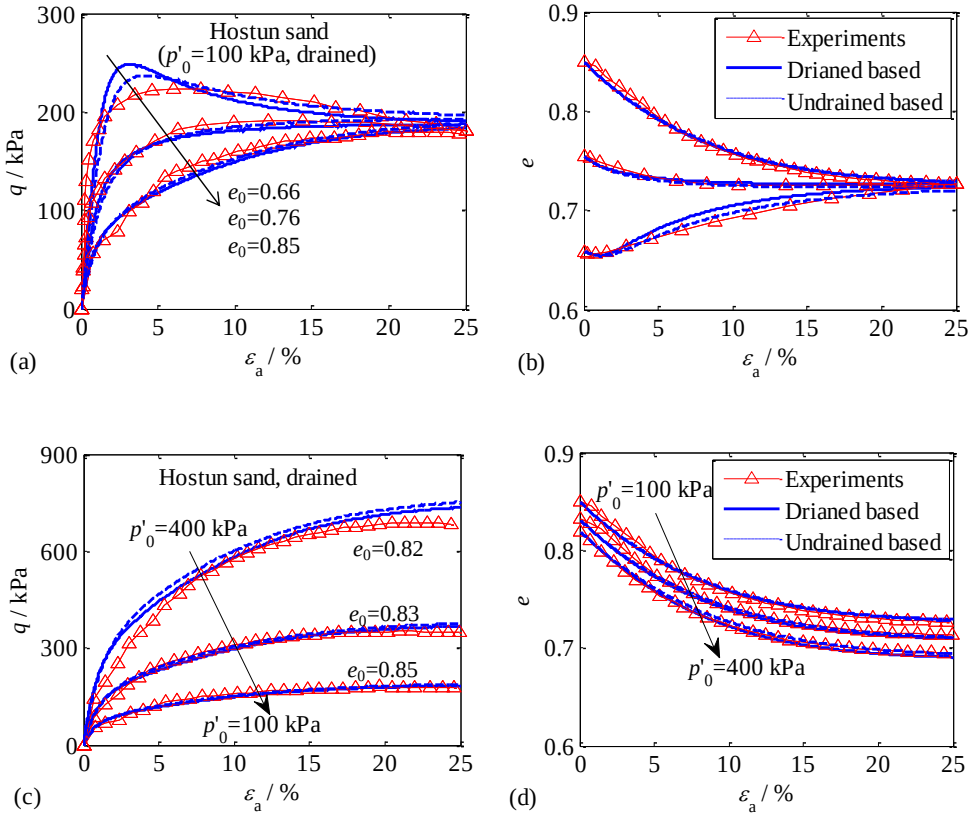

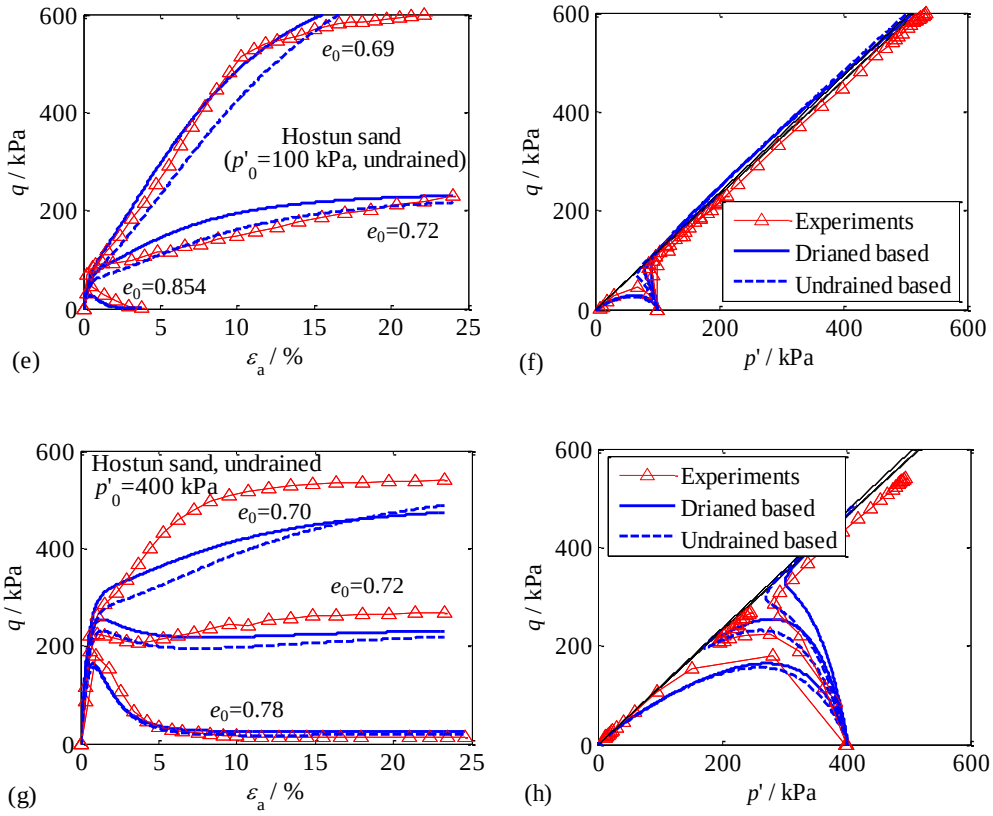

Figure 6.15. Simulation results of Hostun sand based on the optimal parameters

6.6 Estimation of strain level of tests for identification of parameters

It is well known that the critical state cannot be accurately reached during conventional triaxial tests on sand. The reason is that the sample becomes inhomogeneous with the increase of the strain level due to localizations or instabilities. In reality, therefore, the critical state parameters cannot be directly measured from triaxial tests. In this case, the optimization method should be applied to the tests at limited strain levels with samples being still more or less homogenous. Therefore, it is necessary to confirm the smaller suitable strain level of tests for the identification of parameters by the optimization method.

According to the conclusions from previous section, two groups with five tests (3CDs+2CDs, 3CDs+2UDs) were selected as the objective to examine the smaller suitable strain level of tests for the identification of parameters. The optimization procedure was conducted based on the objective tests with strain levels of 5%, 10%, 15%, 20% and 25% successively. The optimization results are shown in Table 6.10. In order to evaluate the performance of the optimal parameters by GA optimization, other drained and undrained tests on the same Hostun sand were simulated again by using the optimal parameters. The errors were then taken average based on all test simulations. The

variation of errors with the increasing strain level for all tests is plotted in Figure 6.16. It can be found that the parameter identification based on all drained tests becomes acceptable when the strain level of tests becomes bigger than 20%, and based on drained combined with undrained tests that is not stable due to high nonlinear undrained stress-strain curves, as found in Figure 6.14. Therefore, the minimum strain level is recommended as 20% when all five drained tests are adopted and as 25% when three drained tests with two undrained tests are adopted.

Table 6.10 Optimal parameters of Hostun sand for different strain levels

Strain levels /%	3CDs+2CDs (3CDs+2UDs)						
	e_{ref}	λ	ϕ_μ	k_p	A_d	n_p	n_d
5	0.750 (0.765)	0.0565 (0.038)	28.3 (28.4)	0.0021 (0.0048)	0.6 (0.7)	3.0 (3.2)	5.3(5.0)
10	0.735 (0.780)	0.0345 (0.0445)	29.0 (29.0)	0.0020 (0.0076)	0.8 (0.8)	2.8 (2.5)	3.5(4.8)
15	0.740 (0.760)	0.0335 (0.036)	29.5 (29.0)	0.0029 (0.0046)	0.8 (0.8)	2.9 (2.9)	3.4(4.7)
20	0.736 (0.78)	0.0273 (0.0505)	29.5 (29.0)	0.0035 (0.0048)	0.8 (1.1)	2.8 (3.2)	4.3(2.3)
25	0.737 (0.74)	0.0241 (0.0268)	29.5 (29.0)	0.0033 (0.0019)	0.8 (0.8)	2.9 (3.4)	3.8(4.3)

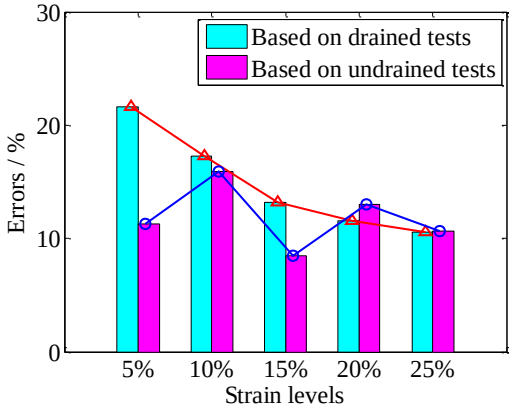

Figure 6.16. Evolution of average simulation errors with the strain levels for Hostun sand

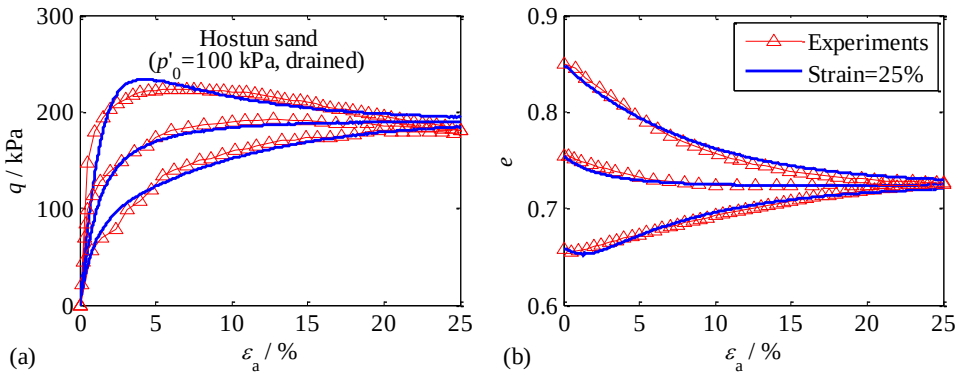

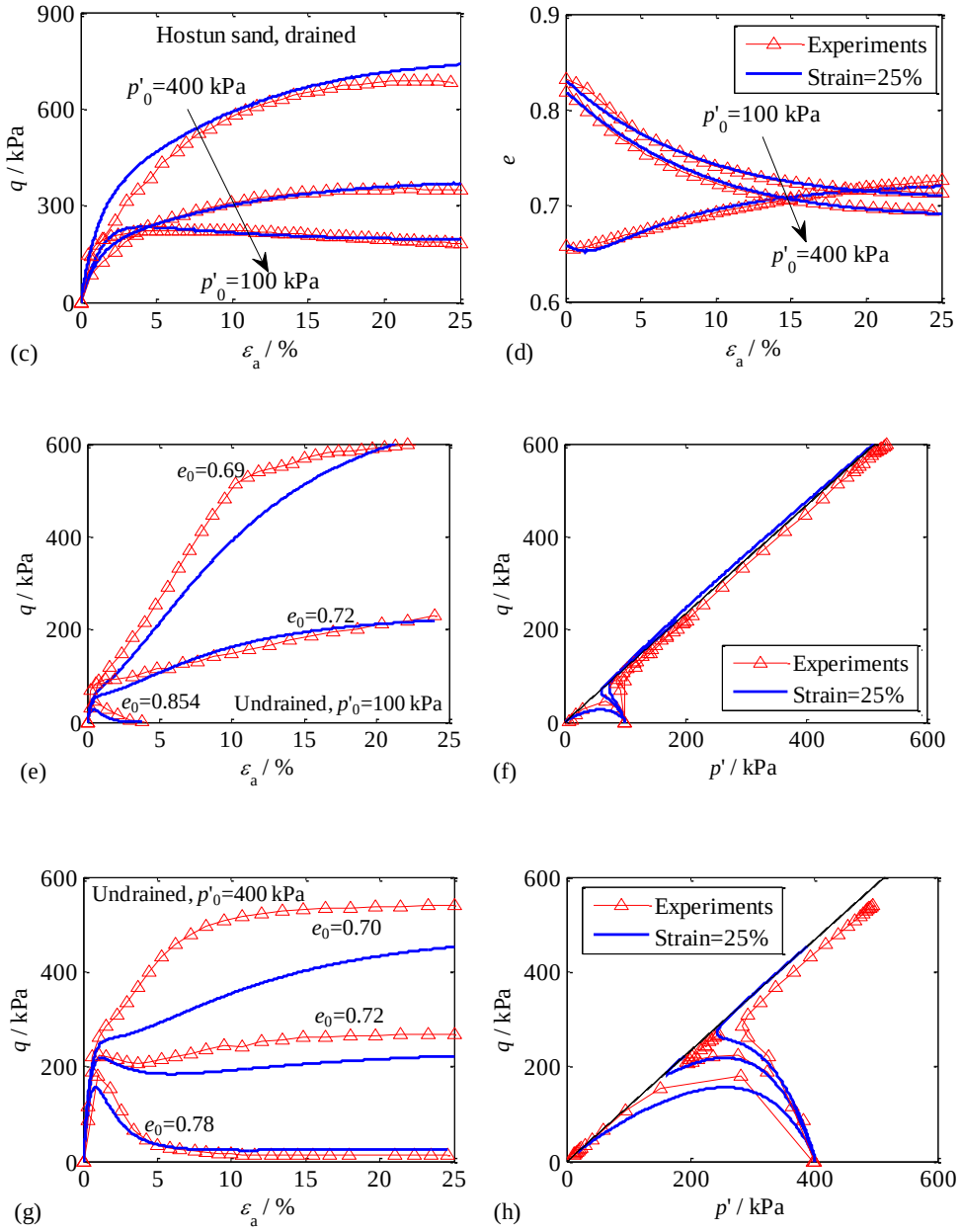

Figure 6.17. Comparisons between experimental and simulated results for Hostun sand using identified parameters from five drained tests at a strain level of 25%

Comparisons between experimental and simulated results using parameters identified from five drained tests at a strain level of 25%, as shown in Figure 6.17, demonstrate a good agreement. Overall, the objective tests up to an axial strain of 25% can give the relatively reliable and reasonable parameters by optimization.

6.7 Conclusions

The selection of sand model and the parameter identification by genetic algorithm have been discussed in this chapter. The computational effectiveness and efficiency of the new RCGA were highlighted by a comparison with the MOGA-II algorithm. The proposed RCGA with a uniform sampling initialization method was adopted to conduct the optimization procedure. Conventional triaxial tests on Hostun sand were selected as the objective in the optimization.

Firstly, the determination of which features are required to be included in constitutive modeling of sand was discussed. Four models with gradually differing features were chosen from numerous sand models as examples for optimization. The results demonstrate that the appropriate sand model should incorporate nonlinear plastic stress-strain hardening, and the critical state concept with an interlocking effect. As a result, the critical state based models (CS-NLMC and CS-TS) were recommended. For the simplicity of modeling monotonic behavior, the CS-NLMC was selected for further study.

Then, the type of tests (drained and/or undrained) to be selected for parameter identification was discussed. It was found that the objective consisting of the drained test and the undrained test could result in relatively accurate optimal parameters in the optimization. Based on the criterion of least cost, two drained tests and one undrained tests were found to satisfy the requirement of obtaining the optimal parameters. In addition, the accuracy of optimal parameters would increase with the increasing number of tests in the objective. However, attention needs to be paid to the test combinations to avoid close final states of e, p' which may cause an incorrect determination of the CSL.

Thirdly, the minimum number of objective tests for identifying parameters was estimated. Optimizations based on two possibilities of adding tests were conducted. Comparisons between simulation and experiment demonstrate that five tests in the objective could give a good performance of parameter identification by genetic algorithm.

Finally, the smaller suitable strain level for identifying parameters was evaluated. Optimizations based on objectives with different strain levels were conducted. Comparisons between simulation and experiment suggest that five drained tests should be selected as the objective, and tests with a strain level of 20% can give relatively reliable and reasonable parameters by optimization.

In the future, investigations could involve applying the advanced optimization methods, combined with the CS-NLMC model, to boundary value problems.

Chapter 7 General conclusions and perspectives

7.1 General conclusions

In the thesis, the identification of soil parameters by using optimization methods has been investigated. The main conclusions were presented as follows:

(1) A review of optimization techniques for identifying parameters in geotechnical engineering has first been presented. The identification methodology is introduced and current optimization methods are reviewed with an introduction to their basic principles and applications in geotechnical engineering.

(2) A comparative study was performed for identifying Mohr-Coulomb parameters from a synthetic PMT and excavation. The GA, PSO, SA, DE and ABC were selected to conduct the optimizations. All the comparisons demonstrate that the DE has the strongest search ability with the smallest objective error but on the other hand, it also has the slower convergence speed.

(3) A new efficient hybrid real-coded genetic algorithm (RCGA) has been developed by adopting two crossovers with outstanding ability. The performance of the proposed RCGA has been validated by optimising six mathematical functions and then further evaluated by identifying soil parameters based on both laboratory tests and field tests, for different soil models. All the comparisons demonstrate that the proposed RCGA has an excellent performance of inverse analysis for identifying soil parameters.

(4) The evolutionary polynomial regression (EPR) based modeling of clay compressibility using an enhanced hybrid real-coded genetic algorithm has been conducted. The results demonstrate that the EPR-based modeling of clay compressibility using the enhanced RCGA gives a more accurate and reliable correlation between the compression index and the physical properties of remolded clays.

(5) An efficient optimization method for identifying the parameters of advanced constitutive model for soft structured clays from only limited conventional triaxial tests is proposed. All comparisons demonstrate that a reliable solution can be obtained by the new RCGA optimization combined with an elasto-viscoplastic soil model, which is useful in practice with a reduction in testing costs.

(6) The selection of sand models and parameter identification by using the optimization method have been discussed. Four key points are discussed in turn: (1) which features are necessary to be accounted for in constitutive modeling of sand; (2) which type of tests (drained and/or undrained) should be selected for an optimal identification of parameters; (3) what is the minimum number of tests that should be selected for parameter identification; and (4) what is the suitable and the lower strain level of objective tests for obtaining reliable and reasonable parameters. The results demonstrate that the appropriate sand model should incorporate nonlinear plastic stress-strain hardening, and the critical state concept with an interlocking effect. Then, based on the criterion of the lower cost, two drained tests and one undrained tests can satisfy the requirement for obtaining the optimal parameters. Finally, comparisons between simulation and experiment suggest that five drained tests should be selected as the objective, and tests with a strain level of 20% can give relatively reliable and reasonable parameters by optimization.

7.2 Perspectives

Although the parameter identification of geomaterials using advanced optimization methods has been presented, and the outstanding performance of adopted optimization methods in identifying parameters was highlighted, there are some shortcomings which need to be further investigated and to be overcome:

(1) In terms of the optimization method, the performance of other newly developed methods with new search mechanism needs to be evaluated to further improve the performance in identifying soil parameters.

(2) In terms of the constitutive model, the proposed approach of parameter identification needs to be applied to more advanced models, such as hyperplastic-based models, and micromechanical based models.

(3) In terms of application, future investigations need to involve the application of advanced optimization methods, combined with advanced models, to a great number of real engineering problems, such as excavation, tunneling and foundation.

Appendixes

(I) Main genetic operators

1. Bounded exponential crossover (BEX)

The Bounded exponential crossover (BEX) has newly been proposed by Thakur et al. [231]. It is a parent centric crossover operator and introduced as follows:

$$\begin{aligned} \xi_i &= x_i^1 + \beta_i^1 \left(x_i^2 - x_i^1 \right) \\ \eta_i &= x_i^2 + \beta_i^2 \left(x_i^2 - x_i^1 \right) \end{aligned} \tag{6-4}$$

with,

$$\beta_i^1 = \begin{cases} \lambda \log \left\{ \exp\left(\dfrac{x_i^L - x_i^1}{\lambda \left(x_i^2 - x_i^1 \right)} \right) + u_i \left(1 - \exp\left(\dfrac{x_i^L - x_i^1}{\lambda \left(x_i^2 - x_i^1 \right)} \right) \right) \right\}, & if \ \ r_i \le 0.5 \\ -\lambda \log \left\{ 1 - u_i \left(1 - \exp\left(\dfrac{x_i^1 - x_i^U}{\lambda \left(x_i^2 - x_i^1 \right)} \right) \right) \right\} & , if \ \ r_i > 0.5 \end{cases} \tag{6-5}$$

$$\beta_i^2 = \begin{cases} \lambda \log \left\{ \exp\left(\dfrac{x_i^L - x_i^2}{\lambda \left(x_i^2 - x_i^1 \right)} \right) + u_i \left(1 - \exp\left(\dfrac{x_i^L - x_i^2}{\lambda \left(x_i^2 - x_i^1 \right)} \right) \right) \right\}, & if \ \ r_i \le 0.5 \\ -\lambda \log \left\{ 1 - u_i \left(1 - \exp\left(\dfrac{x_i^2 - x_i^U}{\lambda \left(x_i^2 - x_i^1 \right)} \right) \right) \right\} & , if \ \ r_i > 0.5 \end{cases} \tag{6-6}$$

where r_i and u_i are uniformly distributed random variable within [0,1]; λ is the scaling parameter, which is always greater than zero. x_i^L and x_i^U are the low bound and upper bound of the variable in the chromosome.

2. Laplace crossover (LX)

Laplace crossover (LX) has recently been introduced by Deep and Thakur [141]. It is a parent centric operator. Using LX, two offspring are generated from a pair of parents in the following way.

First, two uniformly distributed random numbers u_i, $u'_i \in [0,1]$ are generated. Then, a random number β_i is generated which follows the Laplace distribution by simply inverting the distribution function of Laplace distribution as follows:

$$\beta_i = \begin{cases} a - b\log_e(u_i), & u_i' \le 0.5 \\ a + b\log_e(u_i), & u_i' > 0.5 \end{cases} \tag{6-7}$$

The offspring are given by the equation,

$$\begin{aligned} \xi_i &= x_i^1 + \beta_i \left| x_i^1 - x_i^2 \right| \\ \eta_i &= x_i^2 + \beta_i \left| x_i^1 - x_i^2 \right| \end{aligned} \tag{6-8}$$

where a and b are constants.

3. Arithmetical crossover (AC)

The Arithmetical crossover (AC) has been introduced by Michalewicz [232]. Simple arithmetic operators are defined as the combination of two vectors (chromosomes) as follows:

$$\begin{aligned} \xi_i &= \lambda x_i^1 + x_i^2 (1 - \lambda) \\ \eta_i &= x_i^1 (1 - \lambda) + \lambda x_i^2 \end{aligned} \tag{6-9}$$

where λ is a uniformly distributed random variable between 0 and 1.

(II) Brief descriptions of some adopted optimization algorithms

1. MOGA-II (Poles *et al.* [191])

The advanced Multi-Objective Genetic Algorithm (MOGA-II) was presented by Poles et al. [191]. MOGA-II was developed based on standard genetic algorithms and has one-point crossover, directional crossover, mutation and selection as operators for reproduction. It uses a smart multi-search elitism for robustness, and directional crossover for fast convergence. The efficiency of MOGA-II is controlled by its operators (classical crossover, directional crossover, mutation and selection) and by the use of elitism. Each variable is represented as a binary string where the length of the string depends on the base (the number of allowed values for the variable).

2. NSGA-II by [139]

The Non-dominated Sorting Genetic Algorithm NSGA-II [139] was derived from its parent algorithm NSGA [198]. The method uses a genetic algorithm for population evolution, in combination with a fast non-dominated sorting approach to classify solutions according to level of non-domination, and has a crowding distance operator to preserve solution diversity. In NSGA-II, an elitism-preserving approach is used for multi-objective searches. Elitism is introduced, storing all non-dominated solutions discovered so far, beginning with the initial population. Elitism enhances the convergence properties towards the true Pareto-optimal set. A parameter-less diversity preservation mechanism can be adopted. The diversity and spread of solutions are guaranteed without the use of sharing parameters, since NSGA-II adopts a suitable parameter-less niching approach. It uses the crowding distance, which estimates the density of solutions in objective space, and a crowded comparison operator, which guides the selection process towards a uniformly spread Pareto frontier.

3. PSO by Mostaghim [192]

Particle swarm optimization (PSO) is a population-based stochastic global optimization algorithm which was suggested by Kennedy and Eberhart [199] in an attempt to simulate the graceful choreographs of swarms of birds, as part of a socio-cognitive study on the notion of “collective intelligence” in biological populations.

In PSO, a number of simple entities ‘the particles’ are randomly placed in the search space of a

given problem or a given function, and each entity evaluates the objective function at a particular location. Each particle then determines its movement through the search space by combining some aspect of the history of its own actual and best (best-fitness) locations with those of one or more members of the swarm, with some random perturbations. The next iteration takes place after all particles have been moved. Eventually the swarm as a whole, like a flock of birds collectively foraging for food, is likely to move close to an optimum of the fitness function.

As in GA, the particle swarm paradigm has attracted the interest of researchers, due to its ability to solve multi-objective problems. Thus, many advanced versions based on the original PSO have been suggested and applied. Among these advanced versions, a widely used version proposed by Mostaghim [192] has been adopted in this study.

(III) Anisotropic elastic viscoplastic model "ANICREEP"

Based on Yin et al. [199], the main constitutive equations are listed as follows:

$$\dot{\varepsilon}_{ij} = \dot{\varepsilon}_{ij}^{e} + \dot{\varepsilon}_{ij}^{vp} \tag{A1}$$

$$\dot{\varepsilon}_{ij}^{vp} = \mu \left(\frac{p_m^d}{p_m^r} \right)^{\beta} \frac{\partial f_d}{\partial \sigma'_{ij}} \tag{A2}$$

$$f_r = \frac{\frac{3}{2}\left(\sigma_d'^r - p'^r \alpha_d\right) : \left(\sigma_d'^r - p'^r \alpha_d\right)}{\left(M^2 - \frac{3}{2}\alpha_d : \alpha_d\right) p'^r} + p'^r - p_m^r = 0 \tag{A3}$$

$$d\alpha_d = \omega \left[\left(\frac{3\sigma_d}{4p'} - \alpha_d \right) \left\langle d\varepsilon_v^{vp} \right\rangle + \omega_d \left(\frac{\sigma_d}{3p'} - \alpha_d \right) d\varepsilon_d^{vp} \right] \tag{A4}$$

$$p_m^r = (1+\chi)\, p_{mi} \tag{A5}$$

$$dp_{mi} = p_{mi} \left(\frac{1+e_0}{\lambda_i - \kappa} \right) d\varepsilon_v^{vp} \tag{A6}$$

$$d\chi = -\chi\xi \left(\left| d\varepsilon_v^{vp} \right| + \xi_d d\varepsilon_d^{vp} \right) \tag{A7}$$

where $\dot{\varepsilon}_{ij}$ denotes the (*i*,*j*) component of the total strain rate tensor, and the superscripts *e* and *vp* represent, respectively, the elastic and the viscoplastic components. The elastic behavior in the proposed model is assumed to be isotropic, as in the Modified Cam Clay model. The $p_m{}^d$ is the size of the dynamic loading surface. The $p_m{}^r$ and p_{mi} are the size of the reference and the intrinsic yield surfaces respectively. The initial reference preconsolidation pressure $\sigma_{p0}'^r$ obtained from an oedometer test can be used as an input to calculate the initial size p_{m0} using Eq.(A3).

The slope of the critical state line *M* is expressed as follows:

$$M = M_c \left[\frac{2c^4}{1 + c^4 + (1 - c^4)\sin 3\theta} \right]^{\frac{1}{4}} \tag{A8}$$

where $c = (3 - \sin\phi_c)/(3 + \sin\phi_c)$ according to the Mohr-Coulomb yield criterion (ϕ_c is the friction angle); $-\pi/6 \le \theta = (1/3)\sin^{-1}\left(-3\sqrt{3}\bar{J}_3 / 2\bar{J}_2^{3/2}\right) \le \pi/6$ using $\bar{J}_2 = (1/2)\bar{s}_{ij} : \bar{s}_{ij}$, $\bar{J}_3 = (1/3)\bar{s}_{ij}\bar{s}_{jk}\bar{s}_{ki}$ with $\bar{s}_{ij} = \sigma_d - p'\alpha_d$.

The model was implemented as a user-defined model in the 2D Version 9 of PLAXIS for a coupled consolidation analysis based on Biot's theory (see details in Yin et al. [199]).

During consolidation coupled analyses, the permeability k varies with void ratio e:

$$k = k_0 10^{(e-e_0)/c_k} \tag{A9}$$

Soil constants and state variables are summarized in Table A1 with their recommended methods of determination (see details in Yin et al. [199]).

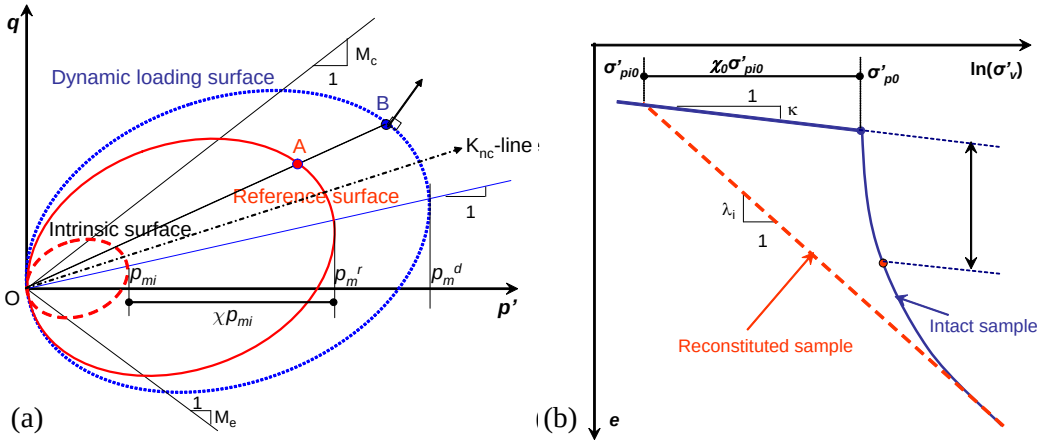

Fig. 1A Definitions for the model in (a) p'- q space; and (b) one-dimensional compression condition.

Table A1. State parameters and soil constants of elastic viscoplastic model

Group	Parameter	Definition	Determination
Modified Cam Clay parameters	σ'^{r}_{p0}	Initial reference preconsolidation pressure	From a selected oedometer test whose loading-rate is used as reference strain-rate
	e_0	Initial void ratio (state parameter)	From oedometer test
	υ'	Poisson's ratio	From initial part of stress-strain curve (Typically varying from 0.15 to 0.35)
	κ	Slope of the swelling line	From 1D or isotropic consolidation test
	λ_i	Intrinsic slope of the compression line	From 1D or isotropic consolidation test
	M	Slope of the critical state line	From triaxial shear test
Anisotropy parameters	α_0	Initial anisotropy (state parameter for calculating initial components of the fabric tensor)	For K_0-consolidated samples by P[1] §
	ω	Absolute rate of yield surface rotation	Calculated by P[2] §
Destructuration parameters	χ_0	Initial bonding ratio	From shear vane test or oedometer test by P[3] §
	ξ	Absolute rate of bond degradation	From consolidation tests with two different stress ratios $\eta=q/p'$, e.g. oedometer test and isotropic consolidation test, calculated by P[4] §
	ξ_d	Relative rate of bond degradation	
Viscosity parameters	$C_{\alpha ei}$	Secondary compression coefficient	From 24h oedometer test on reconstituted sample
Hydraulic parameters	k_{v0}, k_{h0}	Initial vertical and horizontal permeability	From oedometer tests
	c_k	Permeability coefficient	From curve e-log(k)

§ Remark: [P1]: $\alpha_0 = \alpha_{K0} = \eta_{K0} - \frac{M^2 - \eta_{K0}^2}{3}$ with $\eta_{K0} = \frac{3M}{6-M}$ (based on Jacky's formula)

[P2]: $\omega = \frac{1+e_0}{(\lambda_i - \kappa)} \ln \frac{10M_c^2 - 2\alpha_{K0}\omega_d}{M_c^2 - 2\alpha_{K0}\omega_d}$

[P3]: $\chi_0 = S_t - 1$ (from shear vane test), or $\chi_0 = \sigma'_{p0}/\sigma'_{pi0} - 1$ (from oedometer tests)

[P4]: $\xi + \xi \cdot \xi_d \frac{2(\eta - \alpha)}{(M^2 - \eta^2)} = \frac{-(1+e_0)}{e^{vp}} \ln \left[\frac{\sigma'_f}{\chi_0 \exp\left(\frac{e^{vp}}{\lambda_i - \kappa}\right)\sigma'_{vi0}} - \frac{1}{\chi_0} \right]$

References

1. Loukidis D, Salgado R. Effect of relative density and stress level on the bearing capacity of footings on sand. *Géotechnique* 2010; **61**(2): 107-119.
2. Griffiths D, Lane P. Slope stability analysis by finite elements. *Géotechnique* 1999; **49**(3): 387-403.
3. Shen S-L, Ma L, Xu Y-S, Yin Z-Y. Interpretation of increased deformation rate in aquifer IV due to groundwater pumping in Shanghai. *Canadian Geotechnical Journal* 2013; **50**(11): 1129-1142.
4. Karstunen M, Yin ZY. Modeling time-dependent behavior of Murro test embankment. *Geotechnique* 2010; **60**(10): 735-749.
5. Shen S-L, Wu H-N, Cui Y-J, Yin Z-Y. Long-term settlement behavior of metro tunnels in the soft deposits of Shanghai. *Tunnelling and Underground Space Technology* 2014; **40**: 309-323.
6. Ou C-Y, Hsieh P-G, Chiou D-C. Characteristics of ground surface settlement during excavation. *Canadian Geotechnical Journal* 1993; **30**(5): 758-767.
7. Hicher P-Y, Shao J-F. Modèles de comportement des sols et des roches: Lois incrémentales viscoplasticité, endommagememt: Hermès Science, 2002.
8. Gioda G, Maier G. Direct search solution of an inverse problem in elastoplasticity: identification of cohesion, friction angle and in situ stress by pressure tunnel tests. *Int J Numer Methods Eng* 1980; **15**(12): 1823-1848.
9. Wood DM, Mackenzie N, Chan A. Selection of parameters for numerical predictions. Predictive Soil Mechanics: Proceedings of the Wroth Memorial Symposium, Oxford, UK Thomas Telford, London1992. p. 496-512.
10. Simpson AR, Priest SD. The application of genetic algorithms to optimization problems in geotechnics. *Computers and Geotechnics* 1993; **15**(1): 1-19.
11. Pal S, Wije Wathugala G, Kundu S. Calibration of a constitutive model using genetic algorithms. *Computers and Geotechnics* 1996; **19**(4): 325-348.
12. Papon A, Riou Y, Dano C, Hicher PY. Single-and multi-objective genetic algorithm optimization for identifying soil parameters. *Int J Numer Anal Methods Geomech* 2012; **36**(5): 597-618.
13. Levasseur S, Malécot Y, Boulon M, Flavigny E. Soil parameter identification using a genetic algorithm. *Int J Numer Anal Methods Geomech* 2008; **32**(2): 189-213.
14. Levasseur S, Malecot Y, Boulon M, Flavigny E. Statistical inverse analysis based on genetic algorithm and principal component analysis: Method and developments using synthetic data. *Int J Numer Anal Methods Geomech* 2009; **33**(12): 1485-1511.

15. Levasseur S, Malecot Y, Boulon M, Flavigny E. Statistical inverse analysis based on genetic algorithm and principal component analysis: Applications to excavation problems and pressuremeter tests. *Int J Numer Anal Methods Geomech* 2010; **34**(5): 471-491.
16. Rechea C, Levasseur S, Finno R. Inverse analysis techniques for parameter identification in simulation of excavation support systems. *Computers and Geotechnics* 2008; **35**(3): 331-345.
17. Samarajiva P, Macari EJ, Wathugala W. Genetic algorithms for the calibration of constitutive models for soils. *Int J Geomech* 2005; **5**(3): 206-217.
18. Rokonuzzaman M, Sakai T. Calibration of the parameters for a hardening–softening constitutive model using genetic algorithms. *Computers and Geotechnics* 2010; **37**(4): 573-579.
19. Calvello M, Finno RJ. Selecting parameters to optimize in model calibration by inverse analysis. *Computers and Geotechnics* 2004; **31**(5): 410-424.
20. Zentar R, Hicher P, Moulin G. Identification of soil parameters by inverse analysis. *Computers and Geotechnics* 2001; **28**(2): 129-144.
21. Obrzud RF, Vulliet L, Truty A. Optimization framework for calibration of constitutive models enhanced by neural networks. *Int J Numer Anal Methods Geomech* 2009; **33**(1): 71-94.
22. Zhang Y, Gallipoli D, Augarde C. Parameter identification for elasto-plastic modeling of unsaturated soils from pressuremeter tests by parallel modified particle swarm optimization. *Computers and Geotechnics* 2013; **48**: 293-303.
23. Zhao B, Zhang L, Jeng D, Wang J, Chen J. Inverse analysis of deep excavation using differential evolution algorithm. *Int J Numer Anal Methods Geomech* 2015; **39**(2): 115-134.
24. Vardakos S, Gutierrez M, Xia C. Parameter identification in numerical modeling of tunneling using the Differential Evolution Genetic Algorithm (DEGA). *Tunnelling and Underground Space Technology* 2012; **28**(0): 109-123.
25. Jin YF, Yin ZY, Shen SL, Hicher PY. Selection of sand models and identification of parameters using an enhanced genetic algorithm. *Int J Numer Anal Methods Geomech* 2016: 10.1002/nag.2487.
26. Jin Y-F, Yin Z-Y, Shen S-L, Hicher P-Y. Investigation into MOGA for identifying parameters of a critical state based sand model and parameters correlation by factor analysis. *Acta Geotech* 2016. 10.1007/s11440-015-0425-5
27. Ye L, Jin Y-F, Shen S-L, Sun P-P, Zhou C. An efficient parameter identification procedure for soft sensitive clays. *Journal of Zhejiang University SCIENCE A* 2016; **17**(1): 76-88.
28. Sobol IM. On the distribution of points in a cube and the approximate evaluation of integrals. *USSR Computational Mathematics and Mathematical Physics* 1967; **7**(4): 86-112.
29. McKay MD, Beckman RJ, Conover WJ. Comparison of three methods for selecting values of

input variables in the analysis of output from a computer code. *Technometrics* 1979; **21**(2): 239-245.

30. Knabe T, Datcheva M, Lahmer T, Cotecchia F, Schanz T. Identification of constitutive parameters of soil using an optimization strategy and statistical analysis. *Computers and Geotechnics* 2013; **49**: 143-157.
31. Yin ZY, Hicher PY. Identifying parameters controlling soil delayed behavior from laboratory and in situ pressuremeter testing. *Int J Numer Anal Methods Geomech* 2008; **32**(12): 1515-1535.
32. Ardalan H, Eslami A, Nariman-Zadeh N. Piles shaft capacity from CPT and CPTu data by polynomial neural networks and genetic algorithms. *Computers and Geotechnics* 2009; **36**(4): 616-625.
33. Hashash YMA, Levasseur S, Osouli A, Finno R, Malecot Y. Comparison of two inverse analysis techniques for learning deep excavation response. *Computers and Geotechnics* 2010; **37**(3): 323-333.
34. Huang Z, Zhang L, Cheng S, Zhang J, Xia X. Back-Analysis and Parameter Identification for Deep Excavation Based on Pareto Multiobjective Optimization. *Journal of Aerospace Engineering* 2014; **28**(6): A4014007.
35. Gens A, Ledesma A, Alonso E. Estimation of parameters in geotechnical backanalysis—II. Application to a tunnel excavation problem. *Computers and Geotechnics* 1996; **18**(1): 29-46.
36. Gong W, Luo Z, Juang CH, Huang H, Zhang J, Wang L. Optimization of site exploration program for improved prediction of tunneling-induced ground settlement in clays. *Computers and Geotechnics* 2014; **56**: 69-79.
37. Yu H, Li S, Duan H, Liu Y. A procedure of parameter inversion for a nonlinear constitutive model of soils with shield tunneling. *Computers & Mathematics with Applications* 2011; **61**(8): 2005-2009.
38. Beck A, Teboulle M. Gradient-based algorithms with applications to signal recovery. *Convex Optimization in Signal Processing and Communications* 2009: 42-88.
39. Mor é JJ. The Levenberg-Marquardt algorithm: implementation and theory. Numerical analysis: Springer, 1978. p. 105-116.
40. Marquardt DW. An algorithm for least-squares estimation of nonlinear parameters. *Journal of the society for Industrial and Applied Mathematics* 1963; **11**(2): 431-441.
41. Dano C, Hicher PY, Rangeard D, Marchina P. Interpretation of dilatometer tests in a heavy oil reservoir. *Int J Numer Anal Methods Geomech* 2007; **31**(10): 1197-1215.
42. Lecampion B, Constantinescu A, Nguyen Minh D. Parameter identification for lined tunnels in a viscoplastic medium. *Int J Numer Anal Methods Geomech* 2002; **26**(12): 1191-1211.

43. Finno RJ, Calvello M. Supported excavations: observational method and inverse modeling. *Journal of geotechnical and geoenvironmental engineering* 2005; **131**(7): 826-836.
44. Malécot Y, Levasseur S, Boulon M, Flavigny E. Inverse analysis on in situ geotechnical measurement using a genetic algorithm. Ninth International Symposium on Numerical Models in Gemechanics–NUMOG IX2004. p. 223-228.
45. Anandarajah A, Agarwal D. Computer-aided calibration of a soil plasticity model. *Int J Numer Anal Methods Geomech* 1991; **15**(12): 835-856.
46. Rangeard D, Y Hicher P, Zentar R. Determining soil permeability from pressuremeter tests. *Int J Numer Anal Methods Geomech* 2003; **27**(1): 1-24.
47. Chi S-Y, Chern J-C, Lin C-C. Optimized back-analysis for tunneling-induced ground movement using equivalent ground loss model. *Tunnelling and Underground Space Technology* 2001; **16**(3): 159-165.
48. Tang Y-G, Kung GT-C. Application of nonlinear optimization technique to back analyses of deep excavation. *Computers and Geotechnics* 2009; **36**(1): 276-290.
49. Nelder JA, Mead R. A simplex method for function minimization. *The computer journal* 1965; **7**(4): 308-313.
50. Lagarias JC, Reeds JA, Wright MH, Wright PE. Convergence properties of the Nelder--Mead simplex method in low dimensions. *SIAM J Optim* 1998; **9**(1): 112-147.
51. Ritter A, Hupet F, Muñoz-Carpena R, Lambot S, Vanclooster M. Using inverse methods for estimating soil hydraulic properties from field data as an alternative to direct methods. *Agricultural Water Management* 2003; **59**(2): 77-96.
52. John H. Holland, Adaptation in natural and artificial systems. MIT Press, Cambridge, MA, 1992.
53. Golberg DE. Genetic algorithms in search, optimization, and machine learning1989.
54. Goldberg DE. Real-coded genetic algorithms, virtual alphabets, and blocking. *Complex Systems* 1991; **5**(2): 139-168.
55. Janikow CZ, Michalewicz Z. An experimental comparison of binary and floating point representations in genetic algorithms. Proceedings of the Fourth International Conference on Genetic Algorithms (ICGA). Morgan Kaufmann, San Francisco1991. p. 31-36.
56. Feng X-T, Li S, Liao H, Yang C. Identification of non-linear stress-strain-time relationship of soils using genetic algorithm. *Int J Numer Anal Methods Geomech* 2002; **26**(8): 815-830.
57. Yazdani M, Daryabari A, Farshi A, Talatahari S. Application of Taguchi Method and Genetic Algorithm for Calibration of Soil Constitutive Models. *Journal of Applied Mathematics* 2013; **2013**(1-11.
58. Mahbod M, Zand-Parsa S. Prediction of soil hydraulic parameters by inverse method using

genetic algorithm optimization under field conditions. *Archives of Agronomy and Soil Science* 2010; **56**(1): 13-28.

59. Schneider S, Jacques D, Mallants D. Inverse modeling with a genetic algorithm to derive hydraulic properties of a multi-layered forest soil. *Soil Research* 2013; **51**(5): 372-389.
60. Ines AV, Droogers P. Inverse modeling in estimating soil hydraulic functions: a Genetic Algorithm approach. *Hydrology and Earth System Sciences Discussions* 2002; **6**(1): 49-66.
61. Zolfaghari AR, Heath AC, McCombie PF. Simple genetic algorithm search for critical non-circular failure surface in slope stability analysis. *Computers and Geotechnics* 2005; **32**(3): 139-152.
62. Xue J-F, Gavin K. Simultaneous determination of critical slip surface and reliability index for slopes. *Journal of geotechnical and geoenvironmental engineering* 2007; **133**(7): 878-886.
63. McCombie P, Wilkinson P. The use of the simple genetic algorithm in finding the critical factor of safety in slope stability analysis. *Computers and Geotechnics* 2002; **29**(8): 699-714.
64. Goh AT. Genetic algorithm search for critical slip surface in multiple-wedge stability analysis. *Canadian Geotechnical Journal* 1999; **36**(2): 382-391.
65. Sun J, Li J, Liu Q. Search for critical slip surface in slope stability analysis by spline-based GA method. *Journal of geotechnical and geoenvironmental engineering* 2008; **134**(2): 252-256.
66. Park HI, Park B, Kim YT, Hwang DJ. Settlement Prediction in a Vertical Drainage-Installed Soft Clay Deposit Using the Genetic Algorithm (GA) Back-Analysis. *Mar Georesour Geotechnol* 2009; **27**(1): 17-33.
67. Chan C, Zhang L, Ng JT. Optimization of pile groups using hybrid genetic algorithms. *Journal of geotechnical and geoenvironmental engineering* 2009; **135**(4): 497-505.
68. Cui L, Sheng D. Genetic algorithms in probabilistic finite element analysis of geotechnical problems. *Computers and Geotechnics* 2005; **32**(8): 555-563.
69. Chan W, Fwa T, Tan C. Road-maintenance planning using genetic algorithms. I: Formulation. *Journal of Transportation Engineering* 1994; **120**(5): 693-709.
70. Pedroso DM, Williams DJ. Automatic calibration of soil–water characteristic curves using genetic algorithms. *Computers and Geotechnics* 2011; **38**(3): 330-340.
71. Kennedy J. Particle swarm optimization. Encyclopedia of machine learning: Springer, 2011. p. 760-766.
72. Eberhart RC, Shi Y. Comparison between genetic algorithms and particle swarm optimization. Evolutionary Programming VII: Springer, 1998. p. 611-616.
73. Elbeltagi E, Hegazy T, Grierson D. Comparison among five evolutionary-based optimization algorithms. *Advanced Engineering Informatics* 2005; **19**(1): 43-53.

74. Mulia A. Identification of Soil Constitutive Soil Model Parameters Using Multi-Objective Particle Swarming Optimization. Master thesis, 2012.
75. Nguyen-Tuan L, Lahmer T, Datcheva M, Stoimenova E, Schanz T. A novel parameter identification approach for buffer elements involving complex coupled thermo-hydro-mechanical analyses. *Computers and Geotechnics* 2016; **76**: 23-32.
76. Sadoghi Yazdi J, Kalantary F, Sadoghi Yazdi H. Calibration of Soil Model Parameters Using Particle Swarm Optimization. *Int J Geomech* 2011; **12**(3): 229-238.
77. Zhang Y, Gallipoli D, Augarde CE. Simulation-based calibration of geotechnical parameters using parallel hybrid moving boundary particle swarm optimization. *Computers and Geotechnics* 2009; **36**(4): 604-615.
78. Meier J, Schaedler W, Borgatti L, Corsini A, Schanz T. Inverse Parameter Identification Technique Using PSO Algorithm Applied to Geotechnical Modeling. *Journal of Artificial Evolution and Applications* 2008; 1-14.
79. Schanz T, Zimmerer MM, Datcheva M, Meier J. Identification of constitutive parameters for numerical models via inverse approach. *Felsbau* 2006; **24**(2): 11-21.
80. Knabe T, Schweiger HF, Schanz T. Calibration of constitutive parameters by inverse analysis for a geotechnical boundary problem. *Canadian Geotechnical Journal* 2012; **49**(2): 170-183.
81. Zhang Y, Augarde C, Gallipoli D. Identification of hydraulic parameters for unsaturated soils using particle swarm optimization. Proceedings 1st European Conference on Unsaturated Soils2008. p. 765-771.
82. Fontan M, Ndiaye A, Breysse D, Bos F, Fernandez C. Soil–structure interaction: Parameters identification using particle swarm optimization. *Computers & Structures* 2011; **89**(17): 1602-1614.
83. Cheng Y, Li L, Chi S-c, Wei W. Particle swarm optimization algorithm for the location of the critical non-circular failure surface in two-dimensional slope stability analysis. *Computers and Geotechnics* 2007; **34**(2): 92-103.
84. Bharat TV, Sivapullaiah PV, Allam MM. Swarm intelligence-based solver for parameter estimation of laboratory through-diffusion transport of contaminants. *Computers and Geotechnics* 2009; **36**(6): 984-992.
85. Busetti F. Simulated annealing overview. *JP Morgan, Italy* 2003.
86. Kirkpatrick S, Vecchi MP. Optimization by simmulated annealing. *Science* 1983; **220**(4598): 671-680.
87. Xiang Y, Gubian S, Suomela B, Hoeng J. Generalized simulated annealing for global optimization: the GenSA Package. *R Journal* 2013; **5**(1): 13-28.

88. Li S, Liu Y, He X, Liu Y. Global search algorithm of minimum safety factor for slope stability analysis based on annealing simulation. *Chinese Journal of Rock Mechanics and Engineering* 2003; **22**(2): 236-240. (in Chinese)
89. Price K, Storn R. Differential evolution: a simple evolution strategy for fast optimization. *Dr Dobb's journal* 1997; **22**(4): 18-24.
90. Storn R, Price K. Differential evolution–a simple and efficient heuristic for global optimization over continuous spaces. *Journal of global optimization* 1997; **11**(4): 341-359.
91. Qin AK, Huang VL, Suganthan PN. Differential evolution algorithm with strategy adaptation for global numerical optimization. *Evolutionary Computation, IEEE Transactions on* 2009; **13**(2): 398-417.
92. Jia D, Zheng G, Khan MK. An effective memetic differential evolution algorithm based on chaotic local search. *Information Sciences* 2011; **181**(15): 3175-3187.
93. Su G-s, Zhang X-f, Chen G-q, Fu X-y. Identification of structure and parameters of rheological constitutive model for rocks using differential evolution algorithm. *Journal of Central South University of Technology* 2008; **15**(1): 25-28.
94. Zhang Y, Feng X-T, Gallipoli D, Augarde C. Parameter identification in BBM using a parallel asynchronous differential evolution algorithm. In: 5th International Conference on Unsaturated Soils. Barcelona, Spain2010. p. 1001-1007.
95. Karaboga D. An idea based on honey bee swarm for numerical optimization. Technical report-tr06, Erciyes University, Engineering faculty, Computer engineering department, 2005.
96. Karaboga D, Akay B. A comparative study of artificial bee colony algorithm. *Applied Mathematics and Computation* 2009; **214**(1): 108-132.
97. Karaboga D, Basturk B. A powerful and efficient algorithm for numerical function optimization: artificial bee colony (ABC) algorithm. *Journal of global optimization* 2007; **39**(3): 459-471.
98. Gao W, Liu S, Huang L. A global best artificial bee colony algorithm for global optimization. *J Comput Appl Math* 2012; **236**(11): 2741-2753.
99. Kang F, Li J, Ma Z. An artificial bee colony algorithm for locating the critical slip surface in slope stability analysis. *Engineering Optimization* 2013; **45**(2): 207-223.
100. Kang F, Li J, Ma Z, Li H. Artificial bee colony algorithm with local search for numerical optimization. *Journal of Software* 2011; **6**(3): 490-497.
101. Cheng M-Y, Cao M-T, Tran D-H. A hybrid fuzzy inference model based on RBFNN and artificial bee colony for predicting the uplift capacity of suction caissons. *Automation in Construction* 2014; **41**: 60-69.
102. Kang F, Li J. Artificial bee colony algorithm optimized support vector regression for system

reliability analysis of slopes. *Journal of computing in civil engineering* 2015: 04015040.

103. Zhao H, Zhao M, Zhu C. Reliability-based optimization of geotechnical engineering using the artificial bee colony algorithm. *KSCE Journal of Civil Engineering* 2015: 1-9.
104. Dorigo M, Gambardella LM. Ant colony system: a cooperative learning approach to the traveling salesman problem. *Evolutionary Computation, IEEE Transactions on* 1997; **1**(1): 53-66.
105. Dorigo M, Maniezzo V, Colorni A. Ant system: optimization by a colony of cooperating agents. *Systems, Man, and Cybernetics, Part B: Cybernetics, IEEE Transactions on* 1996; **26**(1): 29-41.
106. Dorigo M, Birattari M, Stützle T. Ant colony optimization. *Computational Intelligence Magazine, IEEE* 2006; **1**(4): 28-39.
107. Abbaspour K, Schulin R, Van Genuchten MT. Estimating unsaturated soil hydraulic parameters using ant colony optimization. *Adv Water Res* 2001; **24**(8): 827-841.
108. Kahatadeniya KS, Nanakorn P, Neaupane KM. Determination of the critical failure surface for slope stability analysis using ant colony optimization. *Eng Geol* 2009; **108**(1): 133-141.
109. Afshar A, Haddad OB, Mariño MA, Adams B. Honey-bee mating optimization (HBMO) algorithm for optimal reservoir operation. *J Franklin Inst* 2007; **344**(5): 452-462.
110. Ali E, Abd-Elazim S. Bacteria foraging optimization algorithm based load frequency controller for interconnected power system. *Int J Electr Power Energy Syst* 2011; **33**(3): 633-638.
111. Gandomi AH, Alavi AH. Krill herd: a new bio-inspired optimization algorithm. *Communications in Nonlinear Science and Numerical Simulation* 2012; **17**(12): 4831-4845.
112. Tsai J-T, Liu T-K, Chou J-H. Hybrid Taguchi-genetic algorithm for global numerical optimization. *Evolutionary Computation, IEEE Transactions on* 2004; **8**(4): 365-377.
113. Shi X, Liang Y, Lee H, Lu C, Wang L. An improved GA and a novel PSO-GA-based hybrid algorithm. *Information Processing Letters* 2005; **93**(5): 255-261.
114. Herrera F, Lozano M, Sánchez AM. Hybrid crossover operators for real-coded genetic algorithms: an experimental study. *Soft Computing* 2005; **9**(4): 280-298.
115. Fan S-KS, Liang Y-C, Zahara E. A genetic algorithm and a particle swarm optimizer hybridized with Nelder–Mead simplex search. *Computers & Industrial Engineering* 2006; **50**(4): 401-425.
116. Liu B, Wang L, Jin Y-H, Tang F, Huang D-X. Improved particle swarm optimization combined with chaos. *Chaos, Solitons Fractals* 2005; **25**(5): 1261-1271.
117. Cheng C-T, Wang W-C, Xu D-M, Chau K. Optimizing hydropower reservoir operation using hybrid genetic algorithm and chaos. *Water Resour Manage* 2008; **22**(7): 895-909.
118. Kao Y-T, Zahara E. A hybrid genetic algorithm and particle swarm optimization for multimodal functions. *Applied Soft Computing* 2008; **8**(2): 849-857.

119. Juang C-F. A hybrid of genetic algorithm and particle swarm optimization for recurrent network design. *Systems, Man, and Cybernetics, Part B: Cybernetics, IEEE Transactions on* 2004; **34**(2): 997-1006.
120. El-Abd M. A hybrid ABC-SPSO algorithm for continuous function optimization. Swarm Intelligence (SIS), 2011 IEEE Symposium on: IEEE, 2011. p. 1-6.
121. Shelokar P, Siarry P, Jayaraman VK, Kulkarni BD. Particle swarm and ant colony algorithms hybridized for improved continuous optimization. *Applied Mathematics and Computation* 2007; **188**(1): 129-142.
122. Jiang A, Wang S, Tang S. Feedback analysis of tunnel construction using a hybrid arithmetic based on Support Vector Machine and Particle Swarm Optimization. *Automation in Construction* 2011; **20**(4): 482-489.
123. Khajehzadeh M, Taha MR, El-Shafie A. Reliability analysis of earth slopes using hybrid chaotic particle swarm optimization. *Journal of Central South University of Technology* 2011; **18**(5): 1626-1637.
124. Calvello M, Finno R. Calibration of soil models by inverse analysis. Proc International Symposium on Numerical Models in Geomechanics, NUMOG VIII2002. p. 107-116.
125. Zhang ZF, Ward AL, Gee GW. Estimating soil hydraulic parameters of a field drainage experiment using inverse techniques. *Vadose Zone Journal* 2003; **2**(2): 201-211.
126. Hill MC. Methods and guidelines for effective model calibration: US Geological Survey Denver, CO, USA, 1998.
127. Bäck T. Evolutionary algorithms in theory and practice: evolution strategies, evolutionary programming, genetic algorithms: Oxford university press, 1996.
128. Van Laarhoven PJ, Aarts EH. Simulated annealing: theory and applications: Springer Science & Business Media, 1987.
129. Kennedy J. Particle swarm optimization. Encyclopedia of Machine Learning: Springer, 2010. p. 760-766.
130. Bäck T, Schwefel H-P. An overview of evolutionary algorithms for parameter optimization. *Evolutionary computation* 1993; **1**(1): 1-23.
131. Javadi A, Farmani R, Toropov V, Snee C. Identification of parameters for air permeability of shotcrete tunnel lining using a genetic algorithm. *Computers and Geotechnics* 1999; **25**(1): 1-24.
132. GOH AT. Search for critical slip circle using genetic algorithms. *Civil Engineering Systems* 2000; **17**(3): 181-211.
133. Vahdati P, Levasseur S, Mattsson H, Knutsson S. Inverse Mohr-Coulomb soil parameter

identification of an earth and rockfill dam by genetic algorithm optimization. *Electron J Geotech Eng* 2013; **18**: 5419-5440.

134. Arumugam MS, Rao M, Palaniappan R. New hybrid genetic operators for real coded genetic algorithm to compute optimal control of a class of hybrid systems. *Applied Soft Computing* 2005; **6**(1): 38-52.
135. Mokhade AS, Kakde OG. Overview of selection schemes in real-coded genetic algorithms and their applications. *Journal of Industrial and Intelligent Information Vol* 2014; **2**(1): 71-77.
136. Deb K, Agrawal RB. Simulated binary crossover for continuous search space. *Complex systems* 1995; **9**(2): 115-148.
137. Da Ronco CC, Benini E. GeDEA-II: A simplex crossover based evolutionary algorithm including the genetic diversity as objective. *Engineering Letters* 2013; **21**(1): 23-35.
138. Chuang Y-C, Chen C-T, Hwang C. A real-coded genetic algorithm with a direction-based crossover operator. *Information Sciences* 2015; **305**(1): 320-348.
139. Deb K, Pratap A, Agarwal S, Meyarivan T. A fast and elitist multiobjective genetic algorithm: NSGA-II. *Evolutionary Computation, IEEE Transactions on* 2002; **6**(2): 182-197.
140. Zitzler E, Thiele L. Multiobjective optimization using evolutionary algorithms—a comparative case study. Parallel problem solving from nature—PPSN V: Springer, 1998. p. 292-301.
141. Deep K, Thakur M. A new crossover operator for real coded genetic algorithms. *Applied Mathematics and Computation* 2007; **188**(1): 895-911.
142. Deep K, Thakur M. A new mutation operator for real coded genetic algorithms. *Applied Mathematics and Computation* 2007; **193**(1): 211-230.
143. Poles S, Fu Y, Rigoni E. The effect of initial population sampling on the convergence of multi-objective genetic algorithms. Multiobjective Programming and Goal Programming: Springer, 2009. p. 123-133.
144. Schanz T, Vermeer P, Bonnier P. The hardening soil model: formulation and verification. *Beyond 2000 in computational geotechnics* 1999: 281-296.
145. Richart F, Hall J, Woods R. Vibrations of soils and foundations. International Series in Theoretical and Applied Mechanics. Englewood Cliffs, NJ: Prentice-Hall, 1970.
146. Andria-Ntoanina I, Canou J, Dupla J. Caractérisation mécanique du sable de Fontainebleau NE34 à l'appareil triaxial sous cisaillement monotone. *Laboratoire Navier-Géotechnique (CERMES, ENPC/LCPC)* 2010.
147. Gaudin C, Schnaid F, Garnier J. Sand characterization by combined centrifuge and laboratory tests. *International Journal of Physical Modeling in Geotechnics* 2005; **5**(1): 42-56.
148. Yin ZY, Chang CS. Stress–dilatancy behavior for sand under loading and unloading conditions.

Int J Numer Anal Methods Geomech 2013; **37**(8): 855-870.

149. Yin ZY, Chang CS, Hicher PY. Micromechanical modeling for effect of inherent anisotropy on cyclic behavior of sand. *Int J Solids Struct* 2010; **47**(14-15): 1933-1951.
150. Yin Z-Y, Zhao J, Hicher P-Y. A micromechanics-based model for sand-silt mixtures. *Int J Solids Struct* 2014; **51**(6): 1350-1363.
151. Chang CS, Yin ZY. Micromechanical modeling for behavior of silty sand with influence of fine content. *Int J Solids Struct* 2011; **48**(19): 2655-2667.
152. Roscoe KH, Burland J. On the generalized stress-strain behavior of wet clay. *Engineering Plasticity* 1968: 535-609.
153. Sheng J. Laboratory tests and constitutive modeling on the mechanical behavior of Shanghai clays: Shanghai: Shanghai Jiaotong University, 2012. (in Chinese)
154. Yin Z-Y, Xu Q, Hicher P-Y. A simple critical-state-based double-yield-surface model for clay behavior under complex loading. *Acta Geotech* 2013; **8**(5): 509-523.
155. Yin ZY, Chang CS, Hicher PY, Karstunen M. Micromechanical analysis of kinematic hardening in natural clay. *Int J Plast* 2009; **25**(8): 1413-1435.
156. Yin ZY, Chang CS, Karstunen M, Hicher PY. An anisotropic elastic-viscoplastic model for soft clays. *Int J Solids Struct* 2010; **47**(5): 665-677.
157. Yin ZY, Hattab M, Hicher PY. Multiscale modeling of a sensitive marine clay. *Int J Numer Anal Methods Geomech* 2011; **35**(15): 1682-1702.
158. Yin ZY, Xu Q, Chang CS. Modeling Cyclic Behavior of Clay by Micromechanical Approach. *Journal of engineering mechanics* 2013; **139**(9): 1305-1309.
159. Yin Z-Y, Yin J-H, Huang H-W. Rate-Dependent and Long-Term Yield Stress and Strength of Soft Wenzhou Marine Clay: Experiments and Modeling. *Marine Georesources & Geotechnology* 2015; **33**(1): 79-91.
160. Yin Z-Y, Zhu Q-Y, Yin J-H, Ni Q. Stress relaxation coefficient and formulation for soft soils. *Géotechnique Letters* 2014; **4**(January-March): 45-51.
161. Rezania M, Javadi AA, Giustolisi O. An evolutionary-based data mining technique for assessment of civil engineering systems. *Engineering computations* 2008; **25**(6): 500-517.
162. Shahin MA. State-of-the-art review of some artificial intelligence applications in pile foundations. *Geoscience Frontiers* 2014; **7**(1): 33-44.
163. Adeli H. Neural networks in civil engineering: 1989–2000. *Computer-Aided Civil and Infrastructure Engineering* 2001; **16**(2): 126-142.
164. Rezania M, Javadi AA. A new genetic programming model for predicting settlement of shallow foundations. *Canadian Geotechnical Journal* 2007; **44**(12): 1462-1473.

165. Alemdag S, Gurocak Z, Cevik A, Cabalar A, Gokceoglu C. Modeling deformation modulus of a stratified sedimentary rock mass using neural network, fuzzy inference and genetic programming. *Eng Geol* 2015; **203**: 70-82.
166. Gurocak Z, Solanki P, Alemdag S, Zaman MM. New considerations for empirical estimation of tensile strength of rocks. *Eng Geol* 2012; **145**: 1-8.
167. Rezania M, Javadi AA, Giustolisi O. Evaluation of liquefaction potential based on CPT results using evolutionary polynomial regression. *Computers and Geotechnics* 2010; **37**(1): 82-92.
168. Rezania M, Faramarzi A, Javadi AA. An evolutionary based approach for assessment of earthquake-induced soil liquefaction and lateral displacement. *Eng Appl Artif Intell* 2011; **24**(1): 142-153.
169. Adilah N, Ghani AA, Mohamed AS, Hamid RN. Use of evolutionary polynomial regression (EPR) for prediction of total sediment load of Malaysian rivers. *Int J Eng* 2012; **6**(5): 265-277.
170. Ahangar-Asr A, Faramarzi A, Mottaghifard N, Javadi AA. Modeling of permeability and compaction characteristics of soils using evolutionary polynomial regression. *Comput Geosci* 2011; **37**(11): 1860-1869.
171. Alemdag S. Assessment of bearing capacity and permeability of foundation rocks at the Gumustas Waste Dam Site (NE Turkey) using empirical and numerical analysis. *Arabian Journal of Geosciences* 2015; **8**(2): 1099-1110.
172. Gurocak Z, Alemdag S. Assessment of permeability and injection depth at the Atasu dam site (Turkey) based on experimental and numerical analyses. *Bull Eng Geol Environ* 2012; **71**(2): 221-229.
173. Ebrahimian B, Movahed V. Evaluation of Axial Bearing Capacity of Piles in Sandy Soils by CPT Results. The 15th Marine Industries Conference (MIC2013) October 2013-Kish Island: 1-6.
174. Alemdag S, Gurocak Z, Solanki P, Zaman M. Estimation of bearing capacity of basalts at the Atasu dam site, Turkey. *Bull Eng Geol Environ* 2008; **67**(1): 79-85.
175. Faramarzi A, Javadi AA, Ahangar-Asr A. Numerical implementation of EPR-based material models in finite element analysis. *Computers & Structures* 2013; **118**(100-108.
176. Faramarzi A, Javadi AA, Alani AM. EPR-based material modeling of soils considering volume changes. *Comput Geosci* 2012; **48**: 73-85.
177. Javadi AA, Faramarzi A, Ahangar-Asr A. Analysis of behavior of soils under cyclic loading using EPR-based finite element method. *Finite Elem Anal Des* 2012; **58**: 53-65.
178. Ahangar-Asr A, Faramarzi A, Javadi AA. A new approach for prediction of the stability of soil and rock slopes. *Engineering computations* 2010; **27**(7): 878-893.

179. Alemdag S, Akgun A, Kaya A, Gokceoglu C. A large and rapid planar failure: causes, mechanism, and consequences (Mordut, Gumushane, Turkey). *Arabian Journal of Geosciences* 2014; **7**(3): 1205-1221.
180. Gurocak Z, Alemdag S, Zaman MM. Rock slope stability and excavatability assessment of rocks at the Kapikaya dam site, Turkey. *Eng Geol* 2008; **96**(1): 17-27.
181. Giustolisi O, Savic D. A symbolic data-driven technique based on evolutionary polynomial regression. *Journal of Hydroinformatics* 2006; **8**(3): 207-222.
182. Yamamoto K, Inoue O. New evolutionary direction operator for genetic algorithms. *AIAA journal* 1995; **33**(10): 1990-1993.
183. Skempton AW, Jones O. Notes on the compressibility of clays. *Quarterly Journal of the Geological Society* 1944; **100**(1-4): 119-135.
184. Wroth C, Wood D. The correlation of index properties with some basic engineering properties of soils. *Canadian Geotechnical Journal* 1978; **15**(2): 137-145.
185. Nagaraj T, Murthy BS. Rationalization of Skempton's compressibility equation. *Geotechnique* 1983; **33**(4): 433-443.
186. Carrier III N. Consolidation parameters derived from index tests. *Geotechnique* 1985; **35**(2): 211-213.
187. Nagaraj T, Murthy BS. A critical reappraisal of compression index equations. *Geotechnique* 1986; **36**(1): 27-32.
188. Burland J. On the compressibility and shear strength of natural clays. *Geotechnique* 1990; **40**(3): 329-378.
189. Sridharan A, Nagaraj H. Compressibility behavior of remolded , fine-grained soils and correlation with index properties. *Canadian Geotechnical Journal* 2000; **37**(3): 712-722.
190. Nath A, DeDalal S. The role of plasticity index in predicting compression behavior of clays. *Electron J Geotech Eng* 2004; **9**: 1-7.
191. Poles S, Rigoni E, Robic T. MOGA-II performance on noisy optimization problems. International Conference on Bioinspired Optimization Methods and their applications BIOMA Ljubljana, Slovena (Oct 2004)2004. p. 51-62.
192. Mostaghim S. Multi-Objective Evolutionary Algorithms: Data Structures, Convergence, and Diversity. Germany: University of Karlsruhe, 2004.
193. Hong Z, Yin J, Cui Y-J. Compression behavior of reconstituted soils at high initial water contents. *Geotechnique* 2010; **60**(9): 691-700.
194. Hong Z-S, Zeng L-L, Cui Y-J, Cai Y-Q, Lin C. Compression behavior of natural and reconstituted clays. *Geotechnique* 2012; **62**(4): 291-301.

195. Zhu Q-Y, Yin Z-Y, Wang J-H, Xia X-H. One Dimension Compression Model for Natural Clays Considering Structure Disturbance. *Journal of Civil, Architectural & Environmental Engineering* 2012; **34**(3): 28-34.
196. Yin J-H. Properties and behavior of Hong Kong marine deposits with different clay contents. *Canadian Geotechnical Journal* 1999; **36**(6): 1085-1095.
197. Yin Z, Xu Q, Yu C. Elastic-Viscoplastic Modeling for Natural Soft Clays Considering Nonlinear Creep. *Int J Geomech* 2014; **15**(5): A6014001.
198. Kimoto S, Oka F. An elasto-viscoplastic model for clay considering destructuralization and consolidation analysis of unstable behavior. *Soils and Foundations* 2005; **45**(2): 29-42.
199. Yin ZY, Karstunen M, Chang CS, Koskinen M, Lojander M. Modeling Time-Dependent Behavior of Soft Sensitive Clay. *Journal of geotechnical and geoenvironmental engineering* 2011; **137**(11): 1103-1113.
200. Moreira N, Miranda T, Pinheiro M, Fernandes P, Dias D, Costa L, et al. Back analysis of geomechanical parameters in underground works using an Evolution Strategy algorithm. *Tunnelling and Underground Space Technology* 2013; **33**(143-158.
201. Yepes V, Alcala J, Perea C, González-Vidosa F. A parametric study of optimum earth-retaining walls by simulated annealing. *Eng Struct* 2008; **30**(3): 821-830.
202. Deb K. Multi-objective optimization using evolutionary algorithms: John Wiley & Sons, 2001.
203. Herrera F, Lozano M, Verdegay JL. Tackling real-coded genetic algorithms: Operators and tools for behavioral analysis. *Artificial intelligence review* 1998; **12**(4): 265-319.
204. Leroueil S, Kabbaj M, Tavenas F, Bouchard R. STRESS-STRAIN-STRAIN RELATION FOR THE COMPRESSIBILITY OF SENSITIVE NATURAL CLAYS. *Geotechnique* 1985; **35**(2): 159-180.
205. Rocchi G, Fontana M, Da Prat M. Modeling of natural soft clay destruction processes using viscoplasticity theory. *Geotechnique* 2003; **53**(8): 729-745.
206. Yin ZY, Karstunen M. Modeling strain-rate-dependency of natural soft clays combined with anisotropy and destructuration. *Acta Mech Solida Sin* 2011; **24**(3): 216-230.
207. Yin ZY, Wang JH. A one-dimensional strain-rate based model for soft structured clays. *Science China-Technological Sciences* 2012; **55**(1): 90-100.
208. Zhu Q-Y, Yin Z-Y, Hicher P-Y, Shen S-L. Nonlinearity of one-dimensional creep characteristics of soft clays. *Acta Geotech* 2015: 1-14.
209. Gens A, Nova R. Conceptual bases for a constitutive model for bonded soils and weak rocks. *Geotechnical engineering of hard soils-soft rocks* 1993; **1**(1): 485-494.
210. Yin ZY, Chang CS. Microstructural modeling of stress-dependent behavior of clay. *Int J Solids*

Struct 2009; **46**(6): 1373-1388.

211. Chang CS, Yin ZY. Micromechanical Modeling for Inherent Anisotropy in Granular Materials. *Journal of Engineering Mechanics-Asce* 2010; **136**(7): 830-839.
212. Yin Z, Hicher PY. Micromechanics-based model for cement-treated clays. *Theoretical and Applied Mechanics Letters* 2013; **3**(2): 021006.
213. Graham J, Houlsby G. Anisotropic elasticity of a natural clay. *Geotechnique* 1983; **33**(2): 165-180.
214. Biarez J, Hicher P-Y. Elementary mechanics of soil behavior: saturated remolded soils: AA Balkema, 1994.
215. Yao Y, Hou W, Zhou A. UH model: three-dimensional unified hardening model for overconsolidated clays. *Geotechnique* 2009; **59**(5): 451.
216. Yao YP, Sun DA. Application of Lade's criterion to Cam-clay model. *Journal of engineering mechanics* 2000; **126**(1): 112-119.
217. Yao Y-P, Kong L-M, Zhou A-N, Yin J-H. Time-dependent unified hardening model: Three-dimensional elastoviscoplastic constitutive model for clays. *Journal of engineering mechanics* 2014; **141**(6): 04014162.
218. Zeng L. Deformation Mechanism and Compression Model of Natural Clays. Nanjing, China: Southeast University, 2010. (in Chinese)
219. Wang L-Z, Yin Z-Y. Stress Dilatancy of Natural Soft Clay under an Undrained Creep Condition. *Int J Geomech* 2012; **0**(0): A4014002.
220. DAN H-B, WANG L-Z. Rotational hardening law based on elastoviscoplastic constitutive model. *Chinese Journal of Rock Mechanics and Engineering* 2010; 29(1): 184-92. (in Chinese)
221. Duncan JM, Chang C-Y. Nonlinear analysis of stress and strain in soils. *Journal of the Soil Mechanics and Foundations Division* 1970; **96**(5): 1629-1653.
222. Jefferies M. Nor-Sand: a simple critical state model for sand. *Geotechnique* 1993; **43**(1): 91-103.
223. Gajo A, Wood M. Severn–Trent sand: a kinematic-hardening constitutive model: the q–p formulation. *Geotechnique* 1999; **49**(5): 595-614.
224. Taiebat M, Dafalias YF. SANISAND: Simple anisotropic sand plasticity model. *Int J Numer Anal Methods Geomech* 2008; **32**(8): 915-948.
225. Yin ZY, Chang CS, Hicher PY, Wang JH. Micromechanical analysis of the behavior of stiff clay. *Acta Mechanica Sinica* 2011; 27(6): 1013-22.
226. Ghaboussi J, Sidarta D. New nested adaptive neural networks (NANN) for constitutive modeling. *Computers and Geotechnics* 1998; **22**(1): 29-52.

227. Wöhling T, Vrugt JA, Barkle GF. Comparison of Three Multiobjective Optimization Algorithms for Inverse Modeling of Vadose Zone Hydraulic Properties. *Soil Sci Soc Am J* 2008; **72**(2): 305.
228. Liu Y-J, Li G, Yin Z-Y, Dano C, Hicher P-Y, Xia X-H, et al. Influence of grading on the undrained behavior of granular materials. *CR Mec* 2014; **342**(2): 85-95.
229. Li G, Liu Y-J, Dano C, Hicher P-Y. Grading-Dependent Behavior of Granular Materials: From Discrete to Continuous Modeling. *Journal of engineering mechanics* 2014. 0(0): 04014172.
230. Manzari MT, Dafalias YF. A critical state two-surface plasticity model for sands. *Geotechnique* 1997; **47**(2): 255-272.
231. Thakur M, Meghwani SS, Jalota H. A modified real coded genetic algorithm for constrained optimization. *Applied Mathematics and Computation* 2014; **235**(292-317.
232. Michalewicz Z. Genetic algorithms+data structures=evolution programs: Springer-Verlag, New York, 1992.